PATHOGENESIS OF EBOLA HEMORRHAGIC FEVER IN PRIMATE MODELS *IN VIVO* AND *IN VITRO*

by

Thomas W. Geisbert

Dissertation submitted to the Faculty of the Program in Molecular Pathobiology of the Uniformed Services University of the Health Sciences in partial fulfillment of the requirements for the degree of Doctor of Philosophy, 2003.

The author hereby certifies that the use of any copyrighted material in this thesis manuscript entitled:

"Pathogenesis of Ebola Hemorrhagic Fever in Cynomolgus Macaques: Evidence that Dendritic Cells Are Early and Sustained Targets of Infection"

and

"Pathogenesis of Ebola Hemorrhagic Fever in Primate Models: Evidence that Hemorrhage Is Not a Direct Effect of Virus-Induced Cytolysis of Endothelial Cells"

and

"Mechanisms Underlying Coagulation Abnormalities in Ebola Hemorrhagic Fever: Overexpression of Tissue Factor in Primate Monocytes/Macrophages is a Key Event"

beyond brief excerpts is with the permission of copyright of owner, and will save and hold harmless the Uniformed Services University of the Health Sciences from any damage which may arise from such copyright violations.

Thomas W. Geisbert
Department of Pathology
Uniformed Services University of the Health Sciences

ABSTRACT

Title of Dissertation: Pathogenesis of Ebola Hemorrhagic Fever in Primate Models *In Vivo* and *In Vitro*

Thomas W. Geisbert,

Doctor of Philosophy, 2003

Dissertation directed by:

Dr. Elliott Kagan, M.D., F.R.C.Path.

Professor of Pathology, Professor of Emerging Infectious Diseases, and Professor of Preventive Medicine & Biometrics

Ebola virus (EBOV) causes severe hemorrhagic fever (HF) with high mortality in humans and nonhuman primates. Despite progress made during the last decade to identify key modulators of EBOV pathogenesis, cultural mores, and a range of logistical problems, have hindered the systematic pathogenetic analysis of human EBOV infections. Nonhuman primate models of EBOV HF were developed, but with few exceptions, previous investigations examined animals naturally infected or killed when moribund, and shed little light on the pathogenesis of infection during times before death. In this study, we investigated the process(es) triggering the coagulation abnormalities characteristic of primate EBOV infections and attempted to identify the sequence of key

morphologic, virologic, and inflammatory events. This study examined tissues of 21 nonhuman primates over time and also temporally evaluated EBOV infection of primary human monocytes/macrophages (PHM) and endothelial cells *in vitro*. Results showed that tissue factor plays an important role in triggering the hemorrhagic complications that characterize EBOV infections, and dysregulation of protein C exacerbates disease. Increased levels of TF were associated with lymphoid macrophages, while analysis of peripheral blood mononuclear cell RNA showed increased tissue factor transcripts by day 3. Analysis of PHM RNA at 1, 24, and 48 hours showed increased tissue factor transcripts while levels of tissue factor protein were dramatically increased by day 2. A rapid drop in plasma protein C levels was evident in all monkeys by day 2. Moreover, replication of EBOV in endothelial cells was not consistently observed until the latter stages of disease, well after the onset of disseminated intravascular coagulation, suggesting that the characteristic coagulation abnormalities are not the direct result of EBOV-induced cytolysis of endothelial cells. Dendritic cells in lymphoid tissues were identified as early and sustained targets of EBOV implicating their role in the immunosuppression characteristic of EBOV infections. Bystander apoptosis and loss of NK cells was a prominent finding suggesting the importance of innate immunity in determining the fate of the host. Accordingly, primate models have been invaluable in identifying several new targets for chemotherapeutic interventions that may ameliorate the effects of EBOV HF.

PATHOGENESIS OF EBOLA HEMORRHAGIC FEVER IN CYNOMOLGUS MONKEYS: EVIDENCE THAT DENDRITIC CELLS ARE EARLY AND SUSTAINED TARGETS OF INFECTION

and

PATHOGENESIS OF EBOLA HEMORRHAGIC FEVER IN PRIMATE MODELS: EVIDENCE THAT HEMORRHAGE IS NOT A DIRECT EFFECT OF VIRUS-INDUCED CYTOLYSIS OF ENDOTHELIAL CELLS

and

MECHANISMS UNDERLYING COAGULATION ABNORMALITIES IN EBOLA HEMORRHAGIC FEVER: OVEREXPRESSION OF TISSUE FACTOR IN PRIMATE MONOCYTES/MACROPHAGES IS A KEY EVENT

by

Thomas W. Geisbert

Dissertation submitted to the Faculty of the Department of Pathology Graduate Program of the Uniformed Services University of the Health Sciences in partial fulfillment of the requirements for the degree of Doctor of Philosophy, 2003.

ACKNOWLEDGEMENTS

I am very grateful to the Department of Pathology for giving me the opportunity to pursue my goals, particularly Dr. Friedman for allowing me to be a small part of this program. I express my thanks to all USUHS faculty who have guided me through this learning experience. Thanks to Dr. Helke and Janet Anastasi for overseeing and managing a highly successful and dynamic graduate program.

I especially thank the committee members of this dissertation: Dr. Kagan, I am especially grateful to you for being my advisor, mentor, and friend. Thank you so much for giving me this opportunity, jumping through so many hoops to help me, and always encouraging me. Dr. Marty, you are awesome! You are the eternal optimist and it is contagious. You have provided a wealth of knowledge and I will continue to call on you for help. Dr. Dvekser, thank you for being a fantastic instructor/Course Director and teaching me about molecular biology. I truly appreciate how you provided mentorship and assistance without reservation. Dr. Maheshwari, thank you for teaching me about interferons. Your door was always open and I really appreciated that. Dr. Giam, I will never forget how you bailed me out by agreeing to serve on this committee at the 11th hour. I have learned so much from you, and I have especially enjoyed working with you on all of the virology projects. Dr. Jahrling, "Pete," thank you for believing in me, taking a chance on me, and teaching me to be a scientist. You are my mentor, my role model, and my one of my very best friends. I thank you so much for being tough when you had to be tough, but always being there to pick me up when I fell down. There is not enough space to list everything you have done for me, and what it means to me. Most importantly, I know that you will be on the ship with me if it ever goes down.

I also thank my USAMRIID support group. COL Kelly Davis, this is an emotional moment realizing that you will be retiring this year. I am forever indebted to you for allowing me to pursue my goals. You have always been there for me whether times were good or bad. I guess it has been around 12 years, hundreds of BSL-4 necropsies and EM support, and frankly it's been one heck of a ride! I will miss you tremendously. You have taught me your motto of "Do What's Right" and I will never forget. Dr. Lisa Hensley, "Leese," first and most of all, thank you for being the kid sister I never had. At end of the day, when it is all said and done, that means more to me than anything else. Thanks for everything you have taught me and thanks for tolerating me. There is no way that I would have been able to do this without you. Pete, Lisa, and Joan, you are my rock and my foundation. From Reston through Amerithrax and Corvas, we have traveled this road together.

Most of all, I thank my family. Thanks to my wife Joan, who has given up her husband for the last 3+ years, and to my sons, Todd and Torey, who have given up their dad. Thanks to my mom and dad for being the greatest parents a son could ask for.

TABLE OF CONTENTS

LIST OF FIGURES

LIST OF ABBREVIATIONS

cIAP	Cellular inhibitor of apoptosis protein
COX	Cyclooxygenase
DC	Dendritic cell
DC-SIGN	DC-specific ICAM-3 grabbing non-integrin CD209
DIC	Disseminated intravascular coagulation
EBOV	Ebola virus
FRC	Fibroblastic reticular cell
GP	Glycoprotein
HF	Hemorrhagic fever
ICAM-1	intercellular adhesion molecule-1
IFN	Interferon
IL	Interleukin
LD_{50}	Median lethal dose
MBGV	Marburg virus
MCP	Monocyte chemotactic protein
MHC	Major histocompatibility complex
MIP	Macrophage inflammatory protein
NAIP	Neuronal apoptosis inhibitory protein
NFκB	Nuclear factor kappaB
NO	Nitric oxide
ORF	Open reading frame
PFU	Plaque forming unit
PHM	Primary human monocytes/macophages
sGP	Soluble glycoprotein
TNF	Tumor necrosis factor
TRAIL	Tumor necrosis factor-related apoptosis-inducing ligand
TUNEL	terminal deoxynucleotidyl transferase mediated deoxyuridine triphosphate nick-end labeling
VCAM-1	vascular cell adhesion molecule-1

INTRODUCTION

Among viruses causing hemorrhagic fever (HF), and among emerging infectious diseases with global impact in general, Ebola virus (EBOV) and Marburg virus (MBGV) stand out for their impressive lethality. Along with MBGV, the four species of EBOV (Zaire, Sudan, Reston, Ivory Coast) make up the negative-stranded, enveloped RNA virus family *Filoviridae* in the order *Mononegavirales*. Acute mortality caused by the Zaire species of EBOV is approximately 80% in human outbreaks (Bowen *et al*., 1977; Johnson *et al*., 1977; Khan *et al*., 1999) and greater than 90% in monkey models of the genus *Macaca* (Bowen *et al*., 1978; Fisher-Hoch *et al*., 1992; Jaax *et al*., 1996; Geisbert *et al*., 2002b). Effective EBOV vaccines and treatments are not available and development of countermeasures is an immediate concern because EBOV has potential as a biological terrorism and warfare threat (Alibek and Handelman, 1999; Miller *et al*., 2001). Progress in understanding the origins of the pathophysiological changes that make EBOV infections of humans so devastating have been slow; a primary reason is the status of filoviruses as biosafety level 4 pathogens necessitating study in high-containment settings.

EBOVs were first recognized during near-simultaneous explosive outbreaks in 1976 in small communities in the former Zaire (now the Democratic Republic of the Congo) (WHO, 1978a) and Sudan (WHO, 1978b). There was significant secondary transmission through reuse of unsterilized needles and syringes and nosocomial contacts. These independent outbreaks involved serologically distinct viral species. The EBOV-Zaire outbreak involved 318 cases and 280 deaths (88% mortality), while the EBOV-Sudan outbreak involved 280 cases and 148 deaths (53% mortality). Since 1976, EBOV has

appeared sporadically in Africa, causing several small- to mid-size outbreaks between 1976 and 1979. In 1995, there was a large epidemic of EBOV-Zaire HF involving 315 cases, with an 81% case fatality rate, in Kikwit, a community in the former Zaire (Khan *et al*., 1999). Meanwhile, between 1994 and 1996, there were smaller outbreaks caused by the EBOV-Zaire virus in Gabon (Georges-Courbot *et al*., 1997). Most recently, in 2000, Gulu, Uganda suffered a large epidemic of viral hemorrhagic fever attributed to the Sudan species of EBOV (CDC, 2001).

In 1989, a third species of EBOV appeared in Reston, Virginia, in association with an outbreak of viral HF among cynomolgus monkeys (*Macaca fascicularis*) imported to the United States from the Philippine Islands (Jahrling *et al*., 1990). Hundreds of monkeys were infected (with high mortality) in this episode, but no human cases occurred, although four animal caretakers seroconverted without overt disease. Epizootics in cynomolgus monkeys recurred at other facilities in the U.S. and Europe through 1992, and again in 1996. A fourth species of EBOV, Ivory Coast, was identified in Côte d'Ivoire in 1994; this species was associated with chimpanzees and only one nonfatal human infection was identified (Le Guenno *et al*., 1995). Very little is known about the natural history of filoviruses. Animal reservoirs and arthropod vectors have been aggressively sought without success (Leirs *et al*., 1999).

EBOV particles have an exotic, thread-like appearance (Figure 1). The basic structure of EBOV particles is long and filamentous although virions take on a variety of forms including "U" and "6" shapes (Geisbert and Jahrling, 1995). EBOV particles average around 1000 nm in length and are uniformly 80 nm in diameter. The virus consists of a nucleocapsid, surrounded by a cross-striated helical capsid. There is an

axial channel in the nucleocapsid, and the whole virion is surrounded by a lipoprotein envelope derived from the host cell.

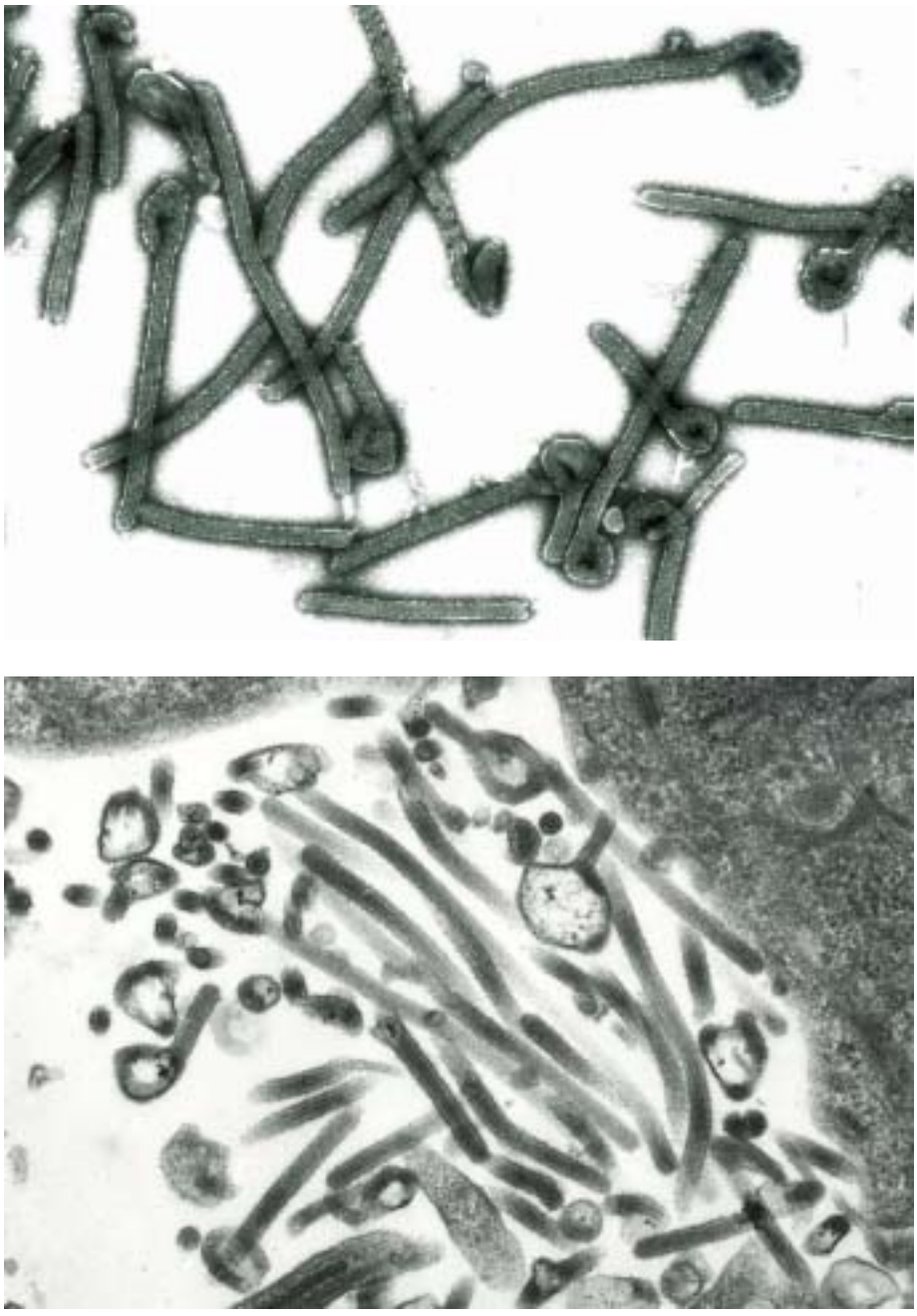

Figure 1. Electron micrographs. Top, Negative contrast of Ebola virus preparation from Vero cell culture fluid. Magnification = X31,500. Bottom, Thin section through Vero cells infected with Ebola virus showing extracellular virions. Magnification = X37,500.

EBOV particles contain a nonsegmented RNA genome of negative polarity (reviewed in Feldmann and Kiley, 1999; Sanchez *et al*. 2001). Briefly, the genome is 18.9 kb in length and is transcribed into eight major subgenomic RNAs that encode seven structural proteins and one nonstructural protein. Four proteins, NP, VP30, VP35, and the catalytic subunit L of the RNA polymerase, are associated with the viral genomic RNA in the ribonucleoprotein complex. The three remaining structural proteins are membrane-associated; VP24 and VP40 are matrix proteins, while GP is a membrane glycoprotein that is located at the surface of EBOV-infected cells and forms the virion spikes. In contrast to the MBGV GP, which encodes a single product, the GP, in a conventional open reading frame (ORF), the EBOV GP gene is encoded in two ORFs. Studies by Volchkov et al. (1995) and Sanchez et al. (1996) showed that approximately 80% of mRNA transcribed from the EBOV GP gene is unedited and encodes a single ORF, ORFI. Unedited transcription from ORF1 directs synthesis of a 364-residue soluble GP, sGP, which is rapidly secreted from infected cells as a disulfide-linked homodimer (Sanchez *et al*., 1998). A transcriptional editing event that connects ORFI and ORFII is required to produce full-length, membrane-anchored GP, from the remaining 20% of mRNA.

The GPs of both EBOV and MBGV are posttranslationally cleaved by furin into an extracellular protein (GP_1) and a membrane-anchored protein (GP_2), which are covalently linked by disulfide bonds (Volchkov *et al*., 1998a). GP_1 presumably mediates receptor binding and subsequent fusion with susceptible cells. The virions spikes are formed by trimers of the GP_1-GP_2 heterodimer, however, much of the GP_1 is released from the complex with GP_2 during posttranslational processing yielding a soluble form of GP_1.

Volchkkov et al. (1998b) reported that this soluble form of GP_1 is also released from infected cells.

The pathogenic significance of the soluble glycoproteins from filovirus-infected cells is largely unknown. High levels of sGP were detected in sera of acutely infected patients (Sanchez *et al*., 1999), and it is tempting to speculate that sGP plays an important role in EBOV disease pathogenesis. However, MBGV, which causes a nearly identical disease in primates, does not express sGP. Yang et al. (1998) reported that EBOV sGP binds to human neutrophils and inhibits early neutrophil activation. This study concluded that sGP diminished innate immunity through its specific binding to CD16b. This report has been particularly controversial, as several other groups were unable to reproduce these results (Maruyama *et al*., 1998). Most recently, Sui and Marasco (2002) demonstrated that the initial observations of Yang et al. (1998) were erroneous and showed by flow cytometric analysis that limited washing conditions led to the nonspecific formation of immune complexes on the neutrophil surface proving that neutrophils do not express a specific receptor for EBOV sGP.

The EBOV sGP-neutrophil binding studies were the first of a number of *in vitro* studies focusing on EBOV glycoproteins that resulted in misleading conclusions. As other examples, it was reported that murine antisera produced after vaccination with a plasmid encoding EBOV GP enhanced the infectivity of vesicular stomatitis virus pseudotyped with the GP in human embryonic kidney 293T cells (Takada *et al*., 2001). The authors suggested that antibody-dependent enhancement plays an important role in EBOV pathogenesis and raised concerns regarding the use of passive immunotherapies in treating EBOV infections. Subsequent studies failed to show evidence of antibody-

dependent enhancement using a battery of EBOV GP-specific antibodies tested against wild-type EBOV *in vitro* (Geisbert *et al*., 2002a), and more importantly failed to show evidence of antibody-dependent enhancement in EBOV infections *in vivo* (Geisbert *et al*., 2002a; Parren *et al*., 2002). As a final example, several studies have reported that the EBOV GP is the primary determinant of EBOV pathogenicity (Chan *et al*., 2000; Yang *et al*., 2000); these studies showed that expression of EBOV transmembrane glycoproteins in 293T cells and endothelial cells caused cytotoxicity and cell detachment. However, Volchkov et al. (2001), using a reverse genetics system, attributed these results to *in vitro* artifacts induced by overexpression of GP, and provided data suggesting that cytotoxicity caused by GP is controlled through transcriptional editing and expression of sGP.

While recent advances in the development of pseudotyped viruses and other *in vitro* systems have facilitated efforts to elucidate the pathogenetic mechanisms of EBOV, there are intrinsic problems with these systems. Issues that cause concern include the potential alteration of host range; proper processing and presentation of viral proteins; and accurate reproduction of the concomitant expression of, and interactions with, other viral proteins. This may be a more important consideration for filoviruses than viruses of other families given the unique morphology of filoviral particles. Virulence is determined by a delicate balance of viral invasive properties for target tissues, immunologic responses (both protective and deleterious), and secondary responses such as triggering of the complement and coagulation cascades. While critical virus:cell interactions can be isolated *in vitro*, there is no substitute for measuring virologic, immunologic, and pathogenic processes in an animal to further understand the disease progression. In this

thesis, we focused our studies on a nonhuman primate model of EBOV HF, and used *in vitro* systems to further explore specific aspects of EBOV infection.

The use of animal models has been invaluable for studying the pathogenesis of numerous infectious diseases as well as for testing the efficacy of experimental prophylactic and therapeutic vaccine and/or drug regimens. Animal models that adequately reproduce human EBOV HF are needed to gain further insight into the pathogenesis of these diseases and to test the efficacy of promising interventions. Guinea pigs, mice, and hamsters have been employed to study filoviral HF (Ryabchikova *et al*., 1996; Bray *et al*., 1998; Connolly *et al*., 1999). While rodents clearly have utility as models of filoviral disease, we recently showed that rodent models of EBOV HF are not ideal for studying human EBOV HF (Geisbert *et al*., 2002b); others have suggested that guinea pigs are inadequate for analyzing the pathogenesis of human EBOV HF (Ryabchikova *et al*., 1996). More specifically, neither mice nor guinea pigs exhibit the hemorrhagic manifestations that characterize primate EBOV infections. Also, bystander lymphocyte apoptosis, which is associated with human and nonhuman primate EBOV infections (Geisbert *et al*., 2000), was not a prominent feature of EBOV infection in mice or guinea pigs (Bray *et al*., 1998; Connolly *et al*., 1999). As expected, clinical disease and related pathology in nonhuman primates infected with EBOV appear to more closely resemble features described in human EBOV HF.

EBOV HF in humans and nonhuman primates is characterized by hypotension, generalized fluid distribution problems, coagulative disorders, and hemorrhages. The pathophysiology of human EBOV HF is largely unknown because of the limited number of cases being managed in a medical setting equipped for both safe and exhaustive

clinical laboratory evaluations. Moreover, there has been a paucity of information regarding the pathology and pathogenesis of EBOV infection in humans. Despite over 1,000 known fatal cases of EBOV infection, only a very limited number of tissues from two cases of EBOV-Sudan in 1976, three cases of EBOV-Zaire in 1976, and 18 of cases of EBOV-Zaire in 1996 have been examined (Dietrich *et al*., 1978; Ellis *et al*., 1978; Murphy, 1978; Zaki and Goldsmith, 1999a). Recent studies of EBOV-Zaire outbreaks in Kikwit and Gabon have provided valuable information on the inflammatory responses during EBOV infections (Baize *et al*., 1999; Villinger *et al*., 1999; Baize *et al*., 2002) and many of the reported findings are consistent with those of experimentally infected nonhuman primates (Hensley *et al*., 2002).

During the last decade, nonhuman primate models of EBOV HF have proved valuable in providing new information regarding EBOV pathogenesis. For example, the importance of monocytes/macrophages as primary cellular targets was shown in a number of studies (Geisbert *et al*., 1992; Jaax *et al*., 1996; Davis *et al*., 1997; Ryabchikova *et al*., 1999a). However, with few exceptions, previous investigations examined animals killed when moribund and shed little light on the pathogenesis of EBOV infection during the period before death. In fact, the temporal sequence of events in EBOV-infected nonhuman primates has not been established and it is uncertain what cell types represent the early cellular targets of EBOV in primates. While dendritic cells play particularly important roles in initiating and regulating the host immune response, there is no information on the predilection of EBOV for dendritic cells *in vivo*, and only one study has shown that dendritic cells are permissive to EBOV *in vitro* (Hensley *et al*., 2002).

Immunosuppression and profound lymphopenia and lymphoid depletion are also characteristic features of EBOV HF in primates. A number of viruses are thought to induce immunosuppression by infecting and impairing the function of dendritic cells, thereby enhancing their chance to escape immune surveillance (Kruse *et al*., 2000; Sevilla *et al*., 2000; Raftery *et al*., 2001). Moreover, extensive lymphocyte apoptosis appears to be critical to the pathogenesis of EBOV in humans and nonhuman primates (Baize *et al*., 1999; Geisbert *et al*., 2000). The mechanism(s) underlying such apoptosis have been unclear. It is not due to direct viral infection; lymphocytes are not productively infected, and infected mononuclear phagocyte system cells are not apoptotic. While bystander lymphocyte apoptosis was demonstrated in tissues of moribund nonhuman primates (Geisbert *et al*., 2000), there is no data available to show whether this is an early versus a late event in the disease course. Therefore, the first project outlined in this thesis was to determine whether dendritic cells were early cellular targets of EBOV *in vivo* and to determine whether bystander lymphocyte apoptosis is an early or late event in EBOV HF.

EBOV replication was demonstrated in endothelial cells in one of the four studies evaluating human EBOV-infected tissues (Zaki and Goldsmith, 1999a), and has also been reported in tissues of moribund nonhuman primates (Baskerville *et al*., 1985;Geisbert *et al*., 1992; Jaax *et al*., 1996; Davis *et al*., 1997). These limited *in vivo* observations have been cited by several recent *in vitro* studies suggesting that the EBOV GP is the main determinant of vascular cell injury and therefore it is direct infection of endothelial cells that causes the hemorrhagic diathesis (Yang *et al*., 1998; Yang *et al*., 2000). Clearly, viral infections can exert changes in the vascular endothelium by directly inducing

changes in endothelial cell expression of cytokines, chemokines, and cellular adhesion molecules or by inducing necrosis or apoptosis. However, viral infections can also exert changes in vascular endothelia indirectly, for example, by infecting and activating leukocytes and triggering the synthesis and local production of proinflammatory soluble factors.

The second project outlined in this thesis has been to determine whether EBOV directly induces the activation/cytopathic disruption of primate endothelial cells *in vitro* and to determine the course of infection and detectable cytopathic disruption of endothelium in nonhuman primates, i.e., to determine whether EBOV infection of endothelial cells is an early event or a terminal event in the disease course relative to the first signs of any disruption/degeneration of the endothelium and or evidence of coagulation abnormalities. The importance of this project is that it cannot be concluded that EBOV-induced damage to the endothelium is due exclusively to immune-mediated mechanisms without first examining the direct effects of EBOV infection on endothelial cell activation and vascular permeability.

Virus-induced dysregulation of immune mediator production can clearly influence disease pathogenesis. For example, increased levels of IFN-α and the overproduction of reactive oxygen species have been associated with bystander lymphocyte apoptosis (Kayagaki et al., 1999; Takabayashi, 2000). Overproduction of TNF-α and other immune mediators can damage vascular endothelia (Mantovani *et al*., 1992; Worall *et al*., 1997). The symptoms of EBOV HF are comparable to those of the cytokine-induced systemic inflammatory response syndrome that is a surplus reaction of the host triggered by pathogens or their products, and also includes development of coagulation abnormalities.

The inflammatory and procoagulant host responses to infection are inextricably intertwined. Inflammatory cytokines (e.g., TNFα, IL-1β, and IL-6) and cytokine receptors (e.g., tissue factor) are capable of activating coagulation and inhibiting fibrinolysis, whereas the procoagulant thrombin is capable of stimulating multiple inflammatory pathways (Grignani and Maiolo, 2000; Levi *et al*., 2001). Previous studies have shown increased production of proinflammatory cytokines (IL-6, TNF-α, and IFN-α) during EBOV infection of humans and nonhuman primates (Baize *et al*., 1999; Villinger *et al*., 1999; Hensley *et al*., 2002).

While disseminated intravascular coagulation (DIC) is often viewed to be a prominent manifestation of EBOV infection in primates, the presence of DIC in human EBOV infections has been a controversial topic; cultural mores and logistical problems have hampered systematic studies. No single laboratory test is sufficient to permit a definitive diagnosis of DIC. In most instances, a diagnosis of DIC can be made by taking into consideration the underlying disease in conjunction with a combination of laboratory findings (Levi *et al*., 1999; Mammen, 2000; Levi, 2001). In human EBOV cases, fibrin deposition has been documented at autopsy (Murphy, 1978); furthermore, clinical laboratory data suggest that DIC is likely to be a prominent feature of human disease (Isaacson *et al*., 1978; WHO, 1978a,b). The coagulation picture is clearer for nonhuman primates. Numerous studies showed histologic and biochemical evidence of DIC syndrome in EBOV infection in a variety of nonhuman primate species (Bowen *et al*., 1978; Fisher-Hoch *et al*., 1983; Fisher-Hoch *et al*., 1985; Fisher-Hoch *et al*., 1992; Geisbert *et al*., 1992; Jaax *et al*., 1996; Ryabchikova *et al*., 1999a; Bray *et al*., 2001; Geisbert *et al*., 2002).

Consumptive coagulopathy was described in several studies of EBOV-Zaire-infected nonhuman primates (Fisher-Hoch *et al*., 1983; Fisher-Hoch *et al*., 1985; Bray *et al*., 2001), and is postulated to be a result of extensive virus-induced tissue injury, and the dysfunction or damage of platelets and endothelial cells. As noted in these and other studies, the increase in the activated partial thromboplastin time was more marked than that of the prothrombin time, consistent with a greater disturbance of the intrinsic than the extrinsic pathway (Fisher-Hoch *et al*., 1983; Bray *et al*., 2001). Traditionally, blood coagulation pathways are divided into extrinsic and intrinsic pathways, converging at the point where factor X is activated. The intrinsic pathway is initiated by activation of factor XII, while the extrinsic pathway is activated by tissue factor, a cellular lipoprotein exposed at sites of tissue injury (Semeraro and Colucci, 1997). Such a division, however, is only an artifact of *in vitro* testing; there are, in fact interconnections between the two pathways. For example, a tissue factor-factor VIIa complex also activates factor IX in the intrinsic pathway. Despite progress made during the last decade to identify key modulators of EBOV pathogenesis, there is no universal concept on the triggering mechanism of the hemorrhagic diathesis of EBOV infection. Involvement of tissue factor in EBOV infections has not been reported.

Therefore, the third project outlined in this thesis has been to determine whether EBOV infection of primate monocytes/macrophages induces tissue factor gene transcription and tissue factor expression. If our hypotheses that EBOV infection of endothelial cells does not directly induce the activation/cytopathic disruption of vascular endothelia and that EBOV infection of monocytes/macrophages leads to increased tissue factor expression, are correct, the prevailing dogma that direct and rapid destruction of

the endothelial cell by uncontrolled viral replication is the primary trigger for the systemic intravascular coagulation that characterizes EBOV infections, will be strongly countered by an alternative theory that will provide new targets for the rational development of chemotherapeutic interventions.

Before beginning any pathogenesis studies using animal models, nonhuman primates in the case of this thesis, careful consideration must be given to the choice of species, sex, age, route of infection, dose administered, and the nature of the challenge virus itself. It is very difficult to compare results among the various published studies of EBOV HF in nonhuman primates because of differences among these factors. Several nonhuman primate species have been employed to model EBOV-Zaire HF including African green monkeys (*Chlorocebus aethiops*) (Bowen *et al*., 1978; Fisher-Hoch *et al*., 1992; Davis *et al*., 1997; Ryabchikova *et al*., 1999a,b), cynomolgus macaques (*Macaca fascicularis*) (Fisher-Hoch *et al*., 1992; Jahrling *et al*., 1996a; Jahrling *et al*., 1999; Sullivan *et al*., 2000; Geisbert *et al*., 2002), rhesus macaques (Bowen *et al*., 1978; Fisher-Hoch *et al*., 1985; Johnson *et al*., 1995; P'yankov *et al*., 1995; Jaax *et al*., 1996; Geisbert *et al*., 2002), and hamadryad baboons (*Papio hamadryas*) (Mikhailov *et al*., 1994; Borisevich *et al*., 1995; Chepurnov *et al*., 1995a; Markin *et al*., 1997; Kudoyarova-Zubavichene *et al*., 1999; Ryabchikova *et al*., 1999a,b). Similar pathologic features of EBOV-Zaire infection have been documented among these species; however, a few pathologic features differ. Most notably, African green monkeys do not present with the maculopapular rash that is characteristic of disease in macaques and baboons (Bowen *et al*., 1978; Fisher-Hoch *et al*.; 1985, Fisher-Hoch *et al*., 1992; Mikhailov *et al*., 1994; Johnson *et al*., 1995; P'yankov *et al*., 1995; Jaax *et al*., 1996; Jahrling *et al*., 1996a);

importantly, this rash is also a prominent feature of human disease (Bowen *et al*., 1978; Davis *et al*., 1997).

Few studies have evaluated the pathogenesis of EBOV-Sudan in nonhuman primates (Ellis *et al*., 1978; Bowen *et al*., 1980; Fisher-Hoch *et al*., 1992). The disease course in experimentally-infected rhesus and cynomolgus macaques appears much slower than that seen in EBOV-Zaire infections (Ellis *et al*., 1978; Fisher-Hoch *et al*., 1992) and rates of survival appear consistent with human disease. EBOV-Sudan infection was not lethal in a small cohort of African green monkeys nor was EBOV-Reston (Fisher-Hoch *et al*., 1992). Similar to EBOV-Sudan, and unlike EBOV-Zaire, the disease course in EBOV-Reston-infected cynomolgus monkeys is protracted (Jahrling *et al*., 1996b). As with MBGV, bystander lymphocyte apoptosis is proposed to be the mechanism of lymphoid depletion in nonhuman primates experimentally infected with EBOV-Reston as well as EBOV-Zaire (Geisbert *et al*., 2000) (Fig. 3). Little is known about the pathogenesis of EBOV-Ivory Coast in nonhuman primates, apart from its high lethality in chimpanzees (*Pan troglodytes verus*) (Formenty *et al*., 1999; Wyers *et al*., 1999). The single chimpanzee examined had multifocal necrosis in the liver, diffuse fibrinoid necrosis in splenic red pulp, and increased numbers of immunopositive macrophages (Wyers *et al*., 1999).

The nature of the challenge virus is also an important consideration in pathogenesis studies, and has been inconsistent in previous EBOV efforts. For example, some studies used organ homogenates to challenge naïve animals (Bowen *et al*., 1978; Ellis *et al*., 1978; Bowen *et al*., 1980; Fisher-Hoch *et al*., 1983; Fisher-Hoch *et al*., 1985; Mikhailov *et al*., 1994; P'yankov *et al*., 1995; Ryabchikova *et al*., 1999a,b), while other studies

employed fluids collected from EBOV-infected cell cultures (Fisher-Hoch *et al*., 1992; Johnson *et al*., 1995; Jahrling *et al*., 1996a,b; Jaax *et al*., 1996; Davis *et al*., 1997; Jahrling *et al*., 1999; Sullivan *et al*., 2000; Geisbert *et al*., 2002). Some challenge viruses used were passed multiple times in animals and/or cell cultures while other challenge viruses are low passage and closer to the original isolate. To more fully characterize the isolates employed for our nonhuman primate studies, we recently certified that our viral stocks were not contaminated with endotoxins (Hensley *et al*., 2002). Previously, EBOV isolates used in animal studies were not screened for endotoxins, a confounding variable if present at biologically relevant levels.

The wide range of challenge doses used in EBOV nonhuman primate studies has been a particularly controversial topic. The goal of any nonhuman primate model is to accurately reproduce human disease; however, little is known regarding what constitutes a typical dose and route of exposure in human EBOV infections. Most cases that propagate outbreaks are thought to occur by direct contact with infected patients and/or cadavers (WHO, 1978a,b; Dowell *et al*., 1999; Khan *et al*., 1999). Infectious EBOV and/or RNA have been isolated from semen and genital secretions (Rodriguez *et al*., 1999; Rowe *et al*., 1999) and detected in skin (Zaki *et al*., 1999b) in human cases; and have also been experimentally demonstrated in body fluids and nasal secretions of nonhuman primates (Jahrling *et al*., 1996b). Moreover, rhesus macaques were lethally infected with EBOV-Zaire by conjunctival exposure (Jaax *et al*., 1996). Laboratory exposure through needlestick and EBOV-infected blood has been reported (Breman *et al*., 1978); these exposures would likely entail doses of at least 1000 plaque forming units (PFU) if viremias associated with terminal patients are comparable to viremias in EBOV-

Zaire-infected nonhuman primates, which often reach levels as high as 10^7 PFU/ml (Jahrling *et al*., 1999). Human viremia data have been notoriously difficult to generate (Ksizaek *et al*., 1999), yet the fact that circulating EBOV particles are readily detected by direct electron microscopic examination of postmortem tissues (Dietrich *et al*., 1978; Ellis *et al*., 1978; Murphy 1978; Zaki and Goldsmith, 1999a) suggest comparable levels considering the threshold for ultrastructural detection. Butchering of a chimpanzee for consumption was linked to an outbreak of EBOV-Zaire in Gabon (Georges-Courbot *et al.*, 1997). Contact exposure was the likely route of transmission in this episode, but ingestion of filovirus-contaminated foods cannot be ruled out as a potential route of exposure in natural infections. Organ infectivity titers in EBOV-infected nonhuman primates are frequently in the 10^7 to 10^8 PFU/gram range (Jahrling *et al*., 1999); thus, it is likely that exposure through the oral route would invariably be associated with very high infectious doses. In fact, EBOV-Zaire is highly lethal when orally administered to rhesus macaques (Jaax *et al*., 1996).

The role of aerogenic transmission in outbreaks is unknown, but is thought to be uncommon (Peters and LeDuc, 1999). Aerosol transmission in nonhuman primates was implicated in the 1989-1990 epizootic of EBOV-Reston (Jahrling *et al*., 1996); high concentrations of virus in nasal secretions and ultrastructural visualization of abundant viral particles in alveoli were reported (Jahrling *et al*., 1996). Filoviruses are moderately stable in aerosol (Bazhutin *et al*., 1992; Chepurnov *et al*., 1995b), and intercage transmission, suggesting mediation by small-particle aerosols, was documented for EBOV-Zaire (Jaax *et al*., 1995). Moreover, EBOV-Zaire is highly infectious by aerosol exposure in rhesus macaques (Johnson *et al*., 1995; P'yankov *et al*., 1995).

Consideration of challenge dose demands some explanation of infectious units, a subject of debate when comparing various studies. For mouse-adapted EBOV, the murine median lethal dose (LD_{50}) was reported to be within the range of 0.025-.04 Vero PFU (i.e., the dose of 1 Vero PFU was equivalent to ~ 30 mouse LD_{50}) (Bray *et al*., 1998). Direct counting of virions mixed with a known concentration of microspheres revealed that 1 PFU was equivalent to 25-30 virions (Bray *et al*., 1998). Therefore, 1 LD_{50} equaled roughly 1 virion in this system. Titration of the 1995 isolate of EBOV-Zaire, used in nonhuman primate studies, by electron microscopy gave a similar ratio of virions to PFU (Bray *et al*., 1998). While a systematic titration has not been performed, the LD_{50} of this isolate in cynomolgus monkeys is less than 10 Vero PFU (T.W. Geisbert, unpublished).

The dose of challenge virus clearly affects the disease course as has been suggested in data collected during outbreaks. In the 1976 EBOV-Zaire outbreak in Yambuku, the incubation period reported for person-to-person transmission exceeded the incubation period for injections or needlestick accidents (Breman *et al*., 1978), which would presumably be associated with higher exposure levels. We observed similar dosing results in our nonhuman primate models. For example, exposure of cynomolgus monkeys (n = 15) to 1000 PFU of EBOV-Zaire by intramuscular injection produces a 100 percent lethal infection with deaths occurring 6-7 days postinfection (Geisbert *et al*., 2002). When the challenge dose was lowered to 10 PFU (n = 4), uniform lethality was still achieved, but deaths occurred 9-12 days postinfection (T.W. Geisbert, unpublished). Others have also noted a protracted disease course concomitant with serial dilution of EBOV-Zaire (Rassadkin *et al*., 2000). It is not surprising that developing viremia levels

appear to be affected by challenge dose. Viremia has been reported as early as 24 hours after subcutaneous infection of rhesus macaques with a high infectious dose (10^5 PFU) of EBOV-Zaire (Fisher-Hoch *et al*., 1985). In rhesus and cynomolgus macaques infected with 1000 PFU of EBOV-Zaire, viremia is first detected 3 days after infection (Geisbert *et al*., 2002), while viremia occurred 4-5 days after infection in baboons exposed to 20-50 newborn mouse LD_{50} of EBOV-Zaire (Ryabchikova *et al*., 1999a).

In this thesis, we have chosen to use the EBOV-Zaire species, as it is the most important EBOV as a human pathogen and also as a potential bioweapon. The isolate employed is of low passage and has been shown to be free of endotoxin. Our studies have focused primarily on cynomolgus macaques because this is the species most frequently used for EBOV vaccine studies (Sullivan *et al*., 2000; Geisbert *et al*., 2002). We have selected a challenge dose (1000 PFU), and route of infection (intramuscular injection), that reflects a likely laboratory exposure and has been uniformly lethal with animals dying 6-7 days after exposure (Geisbert *et al*., 2002). We also evaluated EBOV infection of primary human monocytes/macrophages and endothelial cells over time to further clarify the role of these cells in the disease pathogenesis. Together, the studies outlined in this thesis attempt to more definitively characterize the pathogenesis of EBOV HF in primate models. Understanding the kinetics of host-pathogen relationships and identifying critical pathogenetic processes should aid in the rational development of vaccines and antiviral therapeutics.

Pathogenesis of Ebola Hemorrhagic Fever in Cynomolgus Macaques: Evidence that Dendritic Cells Are Early and Sustained Targets of Infection

Thomas W. Geisbert,[*,‡] Lisa E. Hensley,[*] Tom Larsen,[*] Howard A. Young,[†] Douglas S. Reed,[*] Joan B. Geisbert,[*] Dana P. Scott,[*] Elliott Kagan,[‡] Peter B. Jahrling,[*] and Kelly J. Davis[*]

From the United States Army Medical Institute of Infectious Diseases,[*] Fort Detrick, Maryland; Laboratory of Experimental Immunology, Center for Cancer Research, NCI-Frederick,[†] Frederick, MD; and the Uniformed Services University of the Health Sciences,[‡] Bethesda, MD

Running Head: Ebola Pathogenesis in Cynomolgus Monkeys

Corresponding author:

Thomas W. Geisbert
USAMRIID
Attn: MCMR-UIV
1425 Porter Street
Fort Detrick, MD 21702-5011

E-mail: tom.geisbert@amedd.army.mil
Phone: 301-619-4803
Fax: 301-619-4627

Abstract

Ebola virus (EBOV) infection causes a severe and fatal hemorrhagic disease that in many ways appears to be similar in humans and nonhuman primates; however, little is known about the pathogenesis of EBOV hemorrhagic fever. In this study, 21 cynomolgus monkeys were experimentally infected with EBOV and examined sequentially over 6 days to investigate the pathologic events of EBOV infection that lead to death. Importantly, dendritic cells in lymphoid tissues were identified as early and sustained targets of EBOV implicating their importance in the immunosuppression characteristic of EBOV infections. Bystander lymphocyte apoptosis, previously described in end-stage tissues, occurred early in the disease course in intravascular and extravascular locations. Of note, apoptosis and loss of NK cells was a prominent finding suggesting the importance of innate immunity in determining the fate of the host. Analysis of peripheral blood mononuclear cell (PBMC) gene expression showed temporal increases in TRAIL and Fas transcripts revealing a possible mechanism for the observed bystander apoptosis, while upregulation of NAIP and cIAP2 mRNA suggest that EBOV has evolved additional mechanisms to resist host defenses by inducing protective transcripts in cells that it infects. The sequence of pathogenetic events identified in this study should provide new targets for rational prophylactic and chemotherapeutic interventions.

Introduction

Among viruses causing hemorrhagic fever (HF), and among emerging infectious diseases with global impact in general, Ebola virus (EBOV) stands out for its impressive lethality. Along with Marburg virus (MBGV), the four species of EBOV (Zaire, Sudan, Reston, Ivory Coast) make up the negative-stranded, enveloped RNA virus family *Filoviridae*. Acute mortality caused by the Zaire species of EBOV is approximately 80% in human outbreaks[1-3] and greater than 90% in monkey models of the genus *Macaca*.[4-7] There is currently no vaccine or therapy for EBOV or MBGV hemorrhagic fever approved for human use. Progress in understanding the origins of the pathophysiologic changes that make EBOV infections of humans so devastating have been slow; a primary reason is the status of filoviruses as biosafety level 4 pathogens necessitating study in high-containment settings.

Animal models that adequately reproduce human EBOV HF are clearly needed to gain further insight into the pathogenesis of this disease. Previous vaccine and drug intervention strategies in rodents, with few exceptions, have failed to predict protection of nonhuman primates against infection with Ebola virus (EBOV). We recently showed that two rodent models of EBOV infection are not ideal for studying human EBOV HF; neither mice nor guinea pigs exhibit the hemorrhagic manifestations that characterize human EBOV infections.[7] Others have also noted differences in coagulopathy between the nonhuman primate and rodent models.[8,9] Furthermore, lymphocyte apoptosis, which is associated with human EBOV HF, was not a prominent feature of EBOV infection in mice or guinea pigs.[10,11] Clinical disease and related pathology in nonhuman primates

infected with EBOV appear to more closely resemble features described in human EBOV hemorrhagic fever.[12,13] However, with few exceptions, previous investigations examined naturally infected monkeys or animals killed when moribund, and shed little light on the pathogenesis of EBOV infection during times before death. The requirements to demonstrate efficacy of vaccines and/or various chemotherapeutic regimens intended for use in humans, demands that the pathogenesis of the disease and correlates of immunity be understood in nonhuman primates.

Several nonhuman primate species have been employed to model EBOV (Zaire) HF including African green monkeys (*Chlorocebus aethiops*, formerly *Cercopithecus aethiops*)[4,5,14], cynomolgus macaques (*Macaca fascicularis*)[5,7,15-17], rhesus macaques (*Macaca mulatta*)[4-7,18-20], and hamadryad baboons (*Papio hamadryas*).[21-26] Similar pathologic features of EBOV infection have been documented among these species; however, African green monkeys do not present with a macular cutaneous rash that is a characteristic feature of disease in macaques and baboons.[4-6,15,18-21] Importantly, this rash is also a prominent feature of human disease.[4,14] We focused much of our recent work on cynomolgus macaques, the species most frequently used for filoviral vaccine studies.[7,17] Our cynomolgus monkey model uses a challenge dose and route that reflects a likely laboratory exposure and has been uniformly lethal with animals dying 6-7 days after exposure.[7]

Modern virological methods have made it possible to investigate the genetic basis of virulence and to identify the genes and their expression products affecting the severity of

the course of disease. While various clinical pathology parameters have provided valuable information regarding filoviral disease, paradigms concerning the intricate pathogenetic mechanisms of EBOV HF require a more thorough understanding of the cells that maintain viral replication and functional changes in infected cells. The aim of this study was to characterize the early stages of EBOV HF in a relevant nonhuman primate model of human disease. Understanding the kinetics of host-pathogen relationships, and identifying critical pathogenetic processes are important for the rational development of vaccines and antiviral therapeutics. In the study described here, cynomolgus monkeys were experimentally inoculated with EBOV, and virological and host parameters of infection were longitudinally analyzed.

Materials and Methods

Animals and Inoculations

Healthy, filovirus-seronegative, adult male cynomolgus (*Macaca fascicularis*) macaques (n = 21, 4 to 6.5 kg) were used for these studies. Animals were inoculated in the left or right caudal thigh with 1 ml of viral stock that contained 1000 plaque forming units (PFU) of EBOV (Zaire species). The EBOV used in this study was originally obtained from a fatally infected human from the former Zaire in 1995.[15] Inoculated animals were monitored twice each day for signs of illness. Scheduled necropsies were performed at 1 (n = 3), 2 (n = 3), 3 (n = 4), 4 (n = 4), 5 (n = 4), and 6 (n = 3) days postinfection. Longitudinal blood samples were analyzed by complete blood counts, clinical chemistry, and fluorescence-activated cells sorter analysis of various cell populations (described below). In addition to animals euthanized and exsanguinated for necropsy each day,

blood was also collected from 9 of the monkeys at day 1, 12 at day 2, 6 at day 3, and 3 at day 4 postinfection.

Clinical Evaluation

Monkeys were observed twice daily for clinical signs of illness, and signs were recorded on an individual clinical data record maintained for each animal. Each monkey was specifically evaluated for anorexia, diarrhea, nasal exudates, vomiting, conjunctivitis, cutaneous rash, dehydration, central nervous system disturbances, reduced activity, and hemorrhage using a subjective scoring system.

Hematology

Total white blood cell counts, white blood cell differentials, red blood cell counts, platelet counts, hematocrit values, total hemoglobin, mean cell volume, mean corpuscular volume, and mean corpuscular hemoglobin concentration were determined from blood samples collected in tubes containing EDTA, using a laser-based hematologic Analyzer (Coulter Electronics, Hialeah, FL). The white blood cell differentials were performed manually on Wright-stained blood smears.

Coagulation Tests and Serum Biochemistry

Plasma levels of fibrin degradation products (D-dimers) were measured by an enzyme-linked immunosorbent assay (ELISA) according to manufacturer's directions ("Asserachrom D-D", Diagnostica Stago, Inc., Parsippany, NJ). Serum samples were tested for sodium, potassium, chloride, calcium, phosphorus, partial pressure of oxygen

(PO_2), partial pressure of carbon dioxide (PCO_2), bicarbonate as total CO_2 content (TCO_2), and pH using an i-STAT Portable Clinical Analyzer (i-STAT Corportation, Princeton, NJ). Concentrations of albumin (ALB), amylase (AMY), alanine aminotransferase (ALT), aspartate aminotransferase (AST), alkaline phosphatase (ALP), gamma-glutamyltransferase (GGT), glucose (GLU), cholesterol (CHOL), total protein (TP), total bilirubin (TBIL), urea nitrogen (BUN), and creatinine (Cr) were measured using a Piccolo Point-Of-Care Blood Analyzer (Abaxis, Sunnyvale, CA).

Detection of Endotoxin

Levels of gram-negative bacterial endotoxin in frozen plasma samples were measured with a commercially available chromogenic limulus amebocyte assay (BioWhittaker, Walkersville, MD). The absorbance of each microplate well was read at 405 to 410 nm, and endotoxin concentrations were calculated by linear regression. To control for nonspecific background, baseline absorbance levels were collected immediately after adding chromagen (before development) and subtracted from the absorbance measured after development. This corrected value was then used to calculate endotoxin concentration. The viral inoculum used in this study was assayed and shown to be free of endotoxin (< 0.1 EU/ml).

Cytokine/Chemokine and Nitrate Production

Cytokine/chemokine levels in monkey sera/plasma were assayed using commercially available ELISA kits according to manufacturer's directions. Cytokines/chemokines assayed included monkey IL-2, IL-4, IL-10, IL-12, IFN-γ, and TNF-α (BioSource

International, Inc., Camarillo, CA). ELISAs for human proteins known to be compatible with cynomolgus macaques included IL-6, IFN-α, IFN-ß, MIP-1α, and MIP-1ß (BioSource); and human IL-1ß, IL-8, IL-18, and MCP-1 (R & D Systems, Minneapolis, MN). Nitrate levels were determined using a colorimetric assay according to manufacturer's directions (R&D Systems).

Necropsy

A complete necropsy was performed on all animals. Tissue samples of all major organs were collected from each monkey for histopathologic, immunohistochemical, and *in situ* hybridization examination and were immersion-fixed in 10% neutral buffered formalin. Select tissues for ultrastructural examination were immersion-fixed in 4% formaldehyde plus 1% glutaraldehyde in 0.1 mol/L Millonig's phosphate buffer for transmission electron microscopy (TEM) or 2% formaldehyde plus 0.1% glutaraldehyde in the Millonig's buffer for immunoelectron microscopy.

Histology

Formalin-fixed tissues for histology, immunohistochemistry, and in situ hybridization were processed and embedded in paraffin according to conventional methods.[27] Histology sections were cut at 5 to 6 µm on a rotary microtome, mounted on glass slides, and stained with hemotoxylin and eosin. Replicate sections of all tissues were mounted on positively charged glass slides (Superfrost Plus, Fisher Scientific, Pittsburgh, PA) and immunohistochemically stained for detection of viral antigen by an immunoperoxidase

method according to kit procedures (Envision System, DAKO Corporation, Carpinteria, CA), or by a fluorescence-based method.

Immunohistochemistry

Immunoenzymatic methodology. Sections were deparaffinized and rehydrated through a series of graded ethanols, pretreated with DAKO Ready to Use Proteinase K (DAKO) for 6 minutes at room temperature, and blocked with DAKO's Serum Free Protein Block for 20 minutes before exposure to antibody. Tissue sections were incubated with primary antibody overnight a 4°C using an anti-EBOV rabbit polyclonal (kindly provided by Cindy Rossi) (1:500) or an equal mixture of mouse monoclonal antibodies to EBOV GP and VP40 (1:5000).[6] An alkaline phosphatase-labeled polymer (DAKO Envision® System, Alkaline phosphatase) was added for 30 minutes and color development was achieved by exposing tissue to the substrate 6-bromo-2-hydroxyl-3-naphtholic acid (Histomark Red®, Kirkegaard and Perry, Gaithersburg, MD) for 50 minutes in the dark. Sections were counterstained with hematoxylin. Negative controls included replicate sections exposed to anti-Marburg virus antibodies and unexposed cynomolgus monkey tissue; archived EBOV-infected cynomolgus tissue served as positive controls.

Immunofluorescence methodology. Tissue sections were deparafinized, rehydrated, and incubated in 20 µg/ml of proteinase K for 30 minutes at room temperature. Sections were subsequently rinsed, placed in normal goat serum for 20 minutes and transferred to a mixture of the anti-EBOV monoclonal antibodies as described above for 30 minutes at room temperature. After incubation, sections were rinsed and stained with goat anti-

mouse alexa 594 (Molecular Probes, Eugene OR), incubated with a pan T cell marker, CD3 (DAKO), for 30 minutes at room temperature, rinsed, and incubated in goat anti-mouse alexa 488 (Molecular Probes).

For co-localization of macrophage and/or dendritic cell markers and EBOV antigens, two different techniques were performed. Briefly, deparaffinized tissue sections were pretreated with proteinase K (20 μg/ml) for 30 minutes at room temperature and incubated in normal goat serum for 20 minutes. Sections were then incubated in either a macrophage marker (Ab-1, Oncogene Research Products, San Diego, CA), or a marker for dendritic cells (DC-SIGN, kindly provided by Dr. Vineet KewalRamani, NCI-Frederick), for 30 minutes at room temperature. After incubation, sections were placed in goat anti-mouse alexa 594 (Molecular Probes) for 30 minutes at room temperature and rinsed. Sections were transferred to a blocking solution consisting of a cocktail of mouse IgGs and irrelevant mouse anti-Marburg virus antibodies, and incubated for 20 minutes at room temperature. The excess blocking cocktail was removed and sections were incubated in a fluorescein isothiocyanate (FITC)-conjugated EBOV for 30 minutes at room temperature. The FITC-conjugated anti-EBOV pool was produced by diluting the purified, concentrated anti-EBOV murine monoclonal antibodies (described above) to 1 mg/ml and dialyzing overnight at 4ºC in 0.1 M sodium bicarbonate buffer, pH 8.5. The antibodies were recovered and mixed with FITC on celite (Sigma-Aldrich, St. Louis, MO) and incubated, rotating, for 2 hours at room temperature. FITC-conjugated antibodies were then separated from unbound FITC by passage over a Sephadex G-25 (Amersham Biosciences, Piscataway, NJ) column. To increase the sensitivity of the

staining, sections were incubated in an anti-FITC alexa 488 (Molecular Probes) for 30 minutes at room temperature. After rinsing in PBS, sections were mounted in an aqueous mounting medium containing 4',6'-diamidino-2-phenylindole (DAPI) (Vector Laboratories, Burlingame, CA) and examined with a Nikon E600 fluorescence microscope (Nikon Instech Co., Ltd., Kanagawa, Japan).

To confirm co-localization patterns, double stains were also performed using a rabbit anti-EBOV polyclonal antibody. Briefly, after the proteinase K digestion, blocking in normal goat serum, and incubation in either the anti-macrophage marker or DC-SIGN antibody, sections were incubated in goat anti-mouse alexa 488 for 30 minutes at room temperature. Sections were rinsed, incubated in rabbit anti-EBOV antibody for 30 minutes at room temperature, rinsed and incubated in goat anti-rabbit alexa 594 (Molecular Probes). After rinsing in PBS, sections were mounted in an aqueous mounting medium containing DAPI (Vector Laboratories) and examined with a Nikon E600 fluorescence microscope (Nikon Instech Co.) and/or a Bio-Rad Radiance2000MP confocal microscope (Bio-Rad, Hercules, CA).

In Situ Hybridization

EBOV GP and VP40 RNA were localized in tissues using digoxigenin-labeled DNA probes. Probe constructs were plasmids (pCR2.1, Invitrogen, San Diego, CA) containing complementary DNA sequences for EBOV GP or VP40. Probes were labeled by nick translation with digoxigenin-11-UTP (Boehringer Mannheim, Indianapolis, IN) according to the manufacturer's recommendations. Before hybridization, tissue sections

were incubated with 40 µg/ml of nuclease-free proteinase K (Boehringer Mannheim) in Tris-buffered saline, pH 7.6, for 30 minutes at 37ºC. For hybridization, probes were denatured at 95ºC for 5 minutes, placed on ice, and then applied to tissue sections and incubated overnight at 42ºC. After hybridization, sections were washed in buffer, and incubated in alkaline phophatase-conjugated, antidigoxigenin antibody (Boehringer Mannheim), diluted 1:600, for 1 hour at 37ºC. Sections were washed and the color was developed with 5-bromo-4-chloro-3-indolyl phosphate (NBT/BCIP, Life Technologies, Gaithersburg, MD) as the substrate and nitro blue tetrazolium salt (NBT) as the chromagen for 1 hour at 37ºC. Sections were counterstained with nuclear fast red (Vector Laboratories). Tissue sections incubated in the pCR2.1 plasmid lacking the EBOV gene inserts served as negative controls.

TUNEL Staining

Spleen and various lymph nodes were evaluated for apoptosis using both a chromagen-based in situ terminal deoxynucleotidyl transferase mediated deoxyuridine triphosphate nick-end labeling (TUNEL) assay (In Situ Cell Death Detection Kit, Roche, Indianapolis, IN) or a fluoroscence-based TUNEL assay (ApopTag assay, Intergen, Purchase, NY) as previously described.[28] A pan B cell marker, CD20 (DAKO); a pan T cell marker, CD3 (DAKO); a plasma cell marker, NCL-PC (Vector Laboratories); and a macrophage marker, Ab-1 (Oncogene Research Products) were employed to aid in identifying architectural landmarks within the lymphoid tissues and identify apoptotic cell types. Briefly, 5-µm replicate sections of routinely processed, paraffin-embedded tissues were collected on Superfrost/plus slides (Fisher), deparaffinized, and rehydrated through

graded ethanols to diethyl procarbonate-treated water (Sigma-Aldrich). Sections were treated with 20 µg/ml of proteinase K for 30 minutes at 37°C, and washed in PBS. For chromagen-based assays, sections were treated with 50 µl of the TUNEL reaction mixture and incubated for 1 hour at 37°C. Sections were then rinsed in TBS containing 0.1% Triton and 0.1% bovine serum albumin (BSA) to stop the reaction. Slides were placed in the anti-fluorescein-alkaline phosphatase conjugate (Roche) diluted 1:3 in 100 mM Tris-HCL containing 1% BSA for 30 minutes at 37°C. Sections were rinsed in TBS, the reaction developed in 5-bromo-4-chloro-3-indolyl phosphate (X-phosphate/BCIP) and nitro blue tetrazolium salt, and sections counterstained with nuclear fast red. For the florescence-based TUNEL assay, sections were placed in an equilibration buffer for 5 to 10 minutes after the proteinase K pretreatment. Excess equilibration buffer was removed, and sections were treated with reaction buffer containing deoxynucleotidyl transferase-mediated enzyme for 1 hour at 37°C. Sections were rinsed and incubated in a stop solution at room temperature for 10 minutes and washed in PBS. Sections were then incubated in anti-digoxigenin-rhodamine diluted in blocking buffer for 30 minutes at 37°C. Sections were rinsed in PBS and incubated in normal goat serum for 20 minutes at room temperature. Serum was removed and the sections were incubated with the individual cell markers for 1 hour at 37°C and rinsed in PBS. Sections stained with CD3 were treated with goat anti-rabbit alexa 488 (Molecular Probes) for 30 minutes at 37°C. Sections labeled with CD20, or NCL-PC, were incubated in goat anti-rabbit FITC (Sigma-Aldrich) for 30 minutes at 37°C. After rinsing in PBS, sections were mounted in an aqueous mounting medium containing DAPI and examined on a Nikon E600 fluorescence microscope (Nikon Instech Co.) using a wide-

band green filter or a blue-band filter for visualization of TUNEL or cell marker labeling, respectively.

Electron Microscopy

Paraformaldehyde/glutaraldehyde-fixed tissues and peripheral blood mononuclear cells for transmission electron microscopy were postfixed in 1% osmium tetroxide in 0.1 mol/L Millonig's phosphate buffer, rinsed, stained with 0.5% uranyl acetate in ethanol, dehydrated in graded ethanol and propylene oxide, and embedded in Poly/Bed 812 resin (Polysciences, Warrington, PA). Areas to be examined by electron microscopy were selected from 1-µm sections stained with toluidine blue. Ultrathin sections were cut, placed on 200-mesh copper electron microscopy grids, stained with uranyl acetate and lead citrate, and examined using a JEOL 1200 EX transmission electron microscope (JEOL Ltd., Peabody, MA) at 80 kV.

Postembedment immunoelectron microscopy was performed on portions of aldehyde-fixed inguinal lymph node and spleen, embedded in LR White resin (Polysciences). Briefly, ultrathin sections were floated on drops of 4% normal goat serum in 0.1% BSA plus 0.05% Tween 20 in 0.2 mol/L TRIS (BTT), then incubated with the primary antibodies (either the DC-SIGN marker for dendritic cells described above or irrelevant isotype control). Sections were then incubated with goat-anti mouse IgG conjugated to 10 nm colloidal gold, rinsed, stained with uranyl acetate and lead citrate and examined with a JEOL 1200 EX transmission electron microscope (JEOL) at 80 kV.

Virus Isolation from Plasma and Tissues

Infectious virus in EDTA plasma was assayed by counting plaques on Vero cells maintained as monolayers in 6-well plates under agarose, as previously described.[29] Portions of liver, spleen, lung, kidney, adrenal gland, pancreas, heart, testis, brain, femoral bone marrow, and mandibular, axillary, and left and right inguinal lymph nodes were aseptically collected during necropsy and stored at -70°C until assayed for virus. After thawing, tissues were weighed and ground by mortar and pestle with alundum in 5 ml of EMEM with Earl's salts with 10% fetal calf serum. Tissue homogenates were centrifuged at 10,000 x g for 15 minutes and viral titers were determined as detailed above.

RNAse Protection Assays

Peripheral blood mononuclear cells were separated from EDTA-treated peripheral blood collected from monkeys before and after exposure to EBOV by centrifugation on Histopaque (Sigma-Aldrich) at 250 x g for 30 minutes. Cells at the interface were harvested, washed in RPMI 1640, and treated with TriZol. The Multiprobe RNAse Protection assay was performed according to the manufacturer's directions (Pharmingen, San Diego, CA) with the following modifications: for hybridization, probes were synthesized with 33P UTP (70-80 mC/full reaction) by using the Pharmingen In Vitro Transcription kit. After incubation, yeast tRNA and EDTA were added as described by the manufacturer (Pharmingen), the reaction was placed on Amersham-Pharmacia G25 Microspin columns (Amersham-Pharmacia, Piscataway, NJ) and the probe was purified by centrifugation for 2 minutes at 3,000 rpm. 33P UTP (0.5-1.0 x 106 cpm) was added to

each RNA in a final hybridization volume of 10-20 µl (at least 50% Pharmingen hybridization buffer). For RNAse inactivation, a master cocktail, containing 200 µl of Ambion RNAse inactivation reagent (Ambion Inc., Austin, TX), 50 µl of ethanol, 5 mg of yeast tRNA and 1µl of Ambion GycoBlue co-precipitate per RNA sample was used to precipitate the protected RNA. After adding the RNAse-treated samples to 250 µl of the inactivation/precipitation cocktail, we mixed the samples, placed them at -70°C for 30 minutes, and centrifuged them at 14,000 rpm for 15 minutes. The supernatants were decanted, a sterile cotton swap was used to remove excess liquid, and the pellet was resuspended in 3 µl of Pharmingen sample buffer.

Flow Cytometric Analysis of PBMC

For flow cytometry analysis, the following monoclonal antibodies were obtained from Pharmingen (San Diego, CA) and used in this study: anti-human CD3-FITC (SP34), CD4-PE (RPA-T4), and CD8-APC (RPA-T8). PBMC isolated from EBOV-infected macaques were washed in RPMI containing 10% fetal calf serum and then frozen at -70^{o}C in medium containing 10% dimethylsulfoxide. For flow cytometry analysis, PBMC were thawed and washed twice with PBS, pH 7.4, containing 0.5% BSA and 0.1% sodium azide (PBA). The cells were resuspended with 100 µl of diluted monoclonal antibody specific for surface antigens followed by incubation at 4^{o}C for 20 minutes. Cells were washed twice with PBA, fixed by resuspension in 3% paraformaldehyde buffer and stored at 4^{o}C overnight. Flow cytometry analysis of the samples was then conducted using a FACSCalibur (Becton Dickinson, San Jose, CA). Data were analyzed using WinMDI software (The Scripps Research Institute, La Jolla, CA).

Results

Clinical Illness

At 24 hours, no evidence of clinical illness was detected in any of the animals physically examined. By 48 hours, one monkey had a cutaneous rash involving a small area on the left shoulder. By day 3, three of ten (3/10) animals given physical examinations had fevers (defined as temperature over 102°F) with temperatures ranging from 103.3°F to 104.1°F; one of these animals, and two afebrile animals, had cutaneous rashes involving the axilla and/or groin. By day 4, six of seven monkeys given physical examinations were febrile, with temperatures ranging from 103.2°F to 104.5°F; three of these animals had macular cutaneous rashes on the arms (Figure 1A) and groins, and on two of these animals, the rash also involved the thorax, proximal limbs, and face, particularly on the periorbital area and forehead. Mild dehydration (approximately 5% as evaluated subjectively by skin-fold retraction) and anorexia were noted in two animals and diarrhea was seen in a single animal. By day 5, all seven remaining animals were febrile and had characteristic macular cutaneous rashes (Figure 1B); six of the seven animals were anorexic, two showed 10% dehydration; all showed signs of moderate to severe depression. At day 6, one animal, which had been monitored late the previous evening, was found dead early in the morning. The remaining two animals were recumbent and had depressed body temperatures. In fact, the temperature of one of these animals had fallen from 103.8°F to 96.6°F within 48 hours. Both animals had macular cutaneous rashes and showed evidence of capillary hemorrhage/leakage. One animal exhibited frank blood originating from the nares and one from the rectum.

Hematology, Flow Cytometry, and Clinical Chemistry

Total and differential white blood cell counts revealed developing leukocytosis due to an increased neutrophilia (Figure 2). By day 6, the mean white blood cell counts were 2.5 times baseline values. Neutrophils ranged from approximately 58% of the leukocyte population on day 1 to 79% on day 4 (an approximate 1.4-fold increase), while monocytes declined from approximately 4% on day 1 to 0.75% on day 5. There was a concomitant lymphopenia as lymphocytes dropped from approximately 33% of the leukocyte population on day 1 to less than 9% on day 4, and then appeared to slightly rebound to just less than 15% on day 6 (Figure 2). Thrombocytopenia developed as platelets declined from a preinfection mean of 412 x $10^3/mm^3$ to 174 x $10^3/mm^3$ on day 6 (Figure 2). A slight decline in platelets began on day 2 with a significant drop occurring between days 3 and 4. Development of fibrin degradation products (D-dimers) showed rapid increases of 45-fold by day 4 and 55-fold by day 5 (Figure 2). Hemoglobin, hematocrit, and erythrocyte counts dropped between preinfection levels and day 6 with the most notable drop occurring between days 4 and 5. Nucleated red blood cells were detected in peripheral blood smears of all animals at days 5 and 6. Döhle bodies were seen in neutrophils of all animals by day 4, and marked increases in immature neutrophils (band cells) were also noted in all monkeys by day 4.

Flow cytometry was employed on peripheral blood mononuclear cells (PBMC) to better understand changes in these cells during the course of lethal EBOV infection. Depletion of CD4 and CD8 lymphocytes developed as the disease progressed while the number of

circulating B lymphocytes remained constant. Separation of the CD8 subset into NK cells and T lymphocytes showed a dramatic decline in the NK population with nearly 75% decrease in numbers by day 4 (Figure 3). This pattern of NK and CD8 lymphocyte depletion was consistent for all macaque samples examined during this study. Examination of other surface antigens (CD69, CD25, CD44) suggested that little if any T or B lymphocyte activation occurred after EBOV exposure (D.S. Reed, in preparation).

Early serum enzyme levels were unremarkable, but all were elevated during the late stages of disease (Figure 4). On day 6, AST rose sharply (range, 1287-1671 IU/L) as did ALT (range, 237-511 IU/L). AP levels were increased nearly fourfold over baseline values, while GGT levels increased approximately 2.5-fold over baseline. BUN levels remained generally within normal limits through day 4, after which, on day 5 and 6 there were marked elevations (2.5- and 5.5-fold over baseline, respectively). Serum creatinine levels increased nearly sixfold over baseline by day 6. Total serum proteins did not fluctuate during the course of infection; however, decreases in serum albumin levels were seen by day 4 indicating a loss of only small molecular weight proteins.

Necropsy Findings

Necropsy findings were unremarkable in the animals euthanized at 24 and 48 hours. By day 3 and continuing through day 6, inguinal lymph nodes of all EBOV-infected monkeys were enlarged (1.5 to 3 times normal size) and reddened. Similar changes (lymphadenopathy) of the axillary lymph nodes appeared by day 3 (3/4) and were a consistent finding through day 6 (Figure 1C). Lymphadenopathy of mandibular and

mesenteric lymph nodes was seen in one of four animals by day 4 and was present in all animals thereafter. The liver was slightly enlarged with rounded friable capsular borders and had a reticulated pattern visible from the capsular surface at days 4 through 6. Other findings at day 4 included bilateral enlargement (two times normal size) and reddening of the tonsils (2/4), and mild congestion of the small intestine (1/4). The presence of gross lesions increased dramatically between days 4 and 5. Findings at days 5 and 6 were similar and included urinary bladder petechiae (4/7) (Figure 1D), a sharply demarcated zone of congestion at the junction of the pylorus and the duodenum (5/7) (Figure 1, E and F), a reddening of the ileocecal valve interpreted as congestion in the gut-associated lymphoid tissue (GALT) (6/7) (Figure 1, G and H), congestion of the proximal colon GALT (3/7), congestion of adrenal glands (6/7), petechiae and congestion of the rectum (1/7), bilateral testicular petechiae and ecchymoses (3/7), hemorrhage of gums (1/7), presence of petechiae on gums and buccal membranes (1/7), bilateral reddening and enlargement of tonsils (2/7), ulceration of glandular mucosa of stomach (1/7), and multifocal epicardial petechiae (1/7).

Viral Titers in Blood and Tissues

Onset of plasma viremia was rapid, occurring within 3 days, and ranged from 1.4 to 4.2 $\log_{10}$ PFU/ml (mean, 2.5). Peak viremia (mean 6.9 $\log_{10}$ PFU/ml) occurred on day 6 (Figure 5). While virus was associated with peripheral blood leukocytes, this interaction was not assayed. In tissues, infectious virus was first detected on day 2 in spleen, inguinal lymph node, and mesenteric lymph node, suggesting these organs are early sites of viral replication; and on day 3 in axillary lymph node, mandibular lymph node, liver,

lung, and bone marrow (Figure 5). Mean organ titers increased progressively and reached their highest levels (5.5-8.6 $\log_{10}$ PFU/g) on day 6. The highest titers were documented in the spleen, followed by liver, the various lymph nodes, and adrenal gland.

Analysis of Cytokines/Chemokines, Nitrate, and Endotoxin in Circulation

In order to evaluate the immune response to EBOV challenge, total RNA from extracted circulating peripheral blood mononuclear cells (PBMC) was analyzed for an array of immunoregulatory transcripts. Plasma and/or sera were also analyzed for levels of cytokines/chemokines. Increased mRNA transcripts for MIP-1α (Figure 6A) and M-CSF were detected in some of the animals (3/4 and 2/4, respectively) by day 2, and were observed in all animals by day 3. Transcripts for IL-6 (Figure 6B), IL-8 (Figure 6A), IL-15, MCP-1 (Figure 6A), MIP-1β (Figure 6A), and common cytokine receptor γ chain were observed by day 4 in all monkeys, while increased transcripts for TNF-α were noted in some animals at day 4 (2/4), but were not consistently seen until days 5 and 6 (Figure 6C). Transcripts for IP-10 (Figure 6D) and RANTES were unchanged through day 3 and then appeared to decline at days 4-6. Transcripts for TGFβ1 increased slightly at day 2 and returned to baseline levels by day 4. Changes in levels of transcripts for IL-1α, IL-1β, IL-10, IL-13, GM-CSF, leukotriene B4, and TNF-β were not detected in any of the monkeys.

No detectable increases in plasma/serum levels of cytokines/chemokines were observed early (days 1 or 2) in the disease course. Results were recorded as positive if OD values were greater than twice the OD of pre-EBOV challenge controls. At day 3, very high

levels MIP-1α (> 2000 pg/ml) were detected in three of three monkeys (Figure 7), while elevated levels of IL-6 were also observed (3/3). At day 4, levels of IL-6 (> 500 pg/ml) had markedly increased (3/3) and these highly elevated levels were maintained through the course of infection (Figure 7). Increased levels of IFN-α (3/3) (Figure 7) and IL-2 (1/4) were also detected at day 4. By days 5 and 6, levels of IFN-α were highly elevated (> 5000 pg/ml) in sera of all monkeys; increased levels of TNF-α (> 25 pg/ml) were also observed in all animals, as were levels of IFN-β (> 1000 IU/ml), IL-18 (> 2500 pg/ml), MCP-1 (> 4000 pg/ml), and MIP-1β (> 300 pg/ml) (Figure 7). Increases in levels of IL-2 were detected in one of three monkeys at day 5 and one of two animals at day 6, while increased levels of IFN-γ were only observed at day 6 (2/2). Increased levels of IL-1β, IL-4, IL-8, IL-10 and IL-12 were not detected in any animal at any time point.

In order to assess the potential involvement of nitric oxide in EBOV pathogenesis, nitrate levels in plasma were measured as a marker for nitric oxide synthase (NOS). Analysis of the macaque samples demonstrated increased levels of nitrate (> 200 mmol/L) by day 3 (3/3) (Figure 7). At day 5, levels of nitrate (> 550 mmol/L) had further increased (3/3) (Figure 7). Endotoxin levels were also measured in these animals, but increased levels were not detected in serum or plasma of any monkey tested any time point during the study.

Histology, Immunohistochemistry, In Situ Hybridization, and Ultrastructure

Lymphoid Tissues

Lymph Nodes. By *in situ* hybridization (ISH), EBOV RNA was detected within 48 hours in a single sinus macrophage in the mesenteric lymph node of one of three monkeys. At day 3, immunohistochemistry (IHC) showed foci of immunopositive macrophages (Figure 8A and Figure 9A) and dendritiform cells in the cortical sinuses of the left inguinal lymph node of one of four animals. Rare immunopositive macrophages and dendritiform cells were seen in cortical sinuses of the right inguinal node, and axillary and mesenteric nodes of this animal. Although no single marker thus far uniquely identifies dendritic cells (DC), a C-type lectin, DC-specific ICAM-3 grabbing non-integrin CD209 (DC-SIGN), is highly expressed on primate DC, and is only found on specialized macrophages in the alveoli and decidua.[30] Immunofluorescence analysis (IFA) showed that the EBOV-positive dendritiform cells in these lymph nodes were also positive for DC-SIGN (Figure 8B).

In axillary, inguinal, mandibular, mediastinal, and mesenteric lymph nodes, the first histological changes were noted at day 4. The subcapsular, cortical, and medullary sinuses contained extravasated red blood cells with evidence of erythrophagocytosis (3/4) and hemosiderosis (1/4); areas of multifocal congestion (2/4) and small numbers of neutrophils were present in the sinuses of the mediastinal lymph node (1/4); and apoptotic bodies and tingible body macrophages were multifocally present in follicles of mesenteric and inguinal lymph nodes (2/4). Immunoreactive macrophages were present in subcapsular, cortical, and medullary sinuses of all nodes (3/4) at day 4 (Figure 8C).

EBOV-positive DC (Figure 8, D and E; and Figure 9B) and spindle-shaped cells interpreted as fibroblastic reticular cells (FRC) were multifocally present in the paracortex (sparing the follicles) of all nodes (3/4); these immunoreactive cells were most frequently present in paravascular regions adjacent to high endothelial venules (HEV). EBOV-positive fibrocytes were noted in the mandibular lymph node capsule of one animal. ISH corroborated the IHC findings at day 4. Ultrastructurally, characteristic EBOV inclusion material[31] was detected in sinus macrophages and in cells morphologically consistent with DC.[32,33] Immunoelectron microscopy demonstrated that these EBOV-infected DC were positive for DC-SIGN.

At day 5, depletion of germinal centers was a prominent and consistent finding in all lymph nodes (4/4) and varying numbers of apoptotic bodies and tingible body macrophages were noted in follicles of all animals; two of four animals had apoptotic-like bodies present within HEV of the mandibular lymph nodes. The number of previously described RNA- and EBOV antigen-positive cells increased considerably between days 4 and 5. Numerous EBOV-positive DC and sinus macrophages were detected in all lymph nodes of all four animals. EBOV-positive endothelial cells lining HEV were observed in all lymph nodes at day 5 (4/4). At day 6, apoptotic-like bodies were frequently seen in all lymph nodes and were observed in sinuses as well as follicles (4/4), and numbers of EBOV-positive cells increased, particularly of endothelial cells lining HEV (3/3).

Spleen. At day 2, EBOV RNA was seen in rare macrophages in the red pulp's cords of Bilroth in two of three animals and in monocytes in red pulp sinusoids in the remaining animal. By day 3, multiple small foci of antigen- and RNA-positive macrophages and DC were detected in red pulp cords of Bilroth and in marginal zones (4/4); adjacent FRC-like cells, were also antigen-positive in one animal. On day 4, there were increased numbers of neutrophils and monocytes in the red pulp sinusoids and marginal zones (4/4). In two of four monkeys, basophilic nuclear debris was present in the red pulp sinusoids. Multifocally, macrophages in the red pulp and marginal zone were positive for viral RNA and antigen (4/4); monocytes in the red pulp were occasionally EBOV-positive (4/4); as were red pulp and marginal zone DC (4/4); and spindle-shaped cells, interpreted as FRC in the red pulp, marginal zones, and very infrequently in white pulp (in the periarteriolar lymphoid sheaths [PALS]) but sparing follicles (4/4). By TEM, tissue macrophages in red pulp and marginal zone occasionally contained intracytoplasmic EBOV inclusions and/or budding virions (4/4); EBOV inclusions and/or budding virions were sporadically seen in marginal zone cells morphologically consistent with DC (3/4) (Figure 10A). Immunoelectron microscopy showed positive gold-sphere labeling of these EBOV-infected DC for DC-SIGN. Of note, DC-SIGN-positive DC that contained EBOV inclusions and/or budding virions were occasionally detected in marginal zone of one monkey at day 3 (Figure 10B). Two morphologically distinct populations of EBOV-infected, DC-SIGN-positive cells were seen in marginal zones at days 3 and 4. One population had typical dendritic-like processes with an electron-dense cytoplasm and few organelles (Figure 10A). The other population did not show the obvious dendritic-like processes and had a pale cytoplasm with few organelles, but were

more consistently positive for DC-SIGN (Figure 10B). This population was not as easily identifiable by conventional TEM, but was evident when fields were compared in parallel with DC-SIGN-positive cells shown by immunoelectron microscopy (Figure 10C).

At day 5, there were considerable histologic changes in the spleen of all four monkeys. White pulp was characterized by diffuse, mild to moderate, lymphoid depletion and numerous apoptotic-like bodies present in follicular center remnants. Large fibrin deposits and histiocyte necrosis/loss were prominent histologic features in cords of Bilroth and marginal zones (4/4); multifocal hemorrhage and/or congestion were also noted in marginal zones (4/4). Numerous apoptotic-like bodies were present in the red pulp (4/4) and nucleated red blood cells were occasionally observed in red pulp sinusoids and marginal zones (4/4). The number of viral RNA- and antigen-positive macrophages, DC, and FRC in the red pulp and marginal zone (4/4) was markedly increased, but continued to be infrequent in the PALS of the white pulp, between days 4 and 5; endothelial cells were very infrequently immunoreactive (4/4) at day 5. Ultrastructurally, EBOV inclusions were frequently seen in tissue macrophages in red pulp and marginal zone (4/4) and occasionally seen in marginal zone cells that were morphologically consistent with DC (4/4). Free virions were abundant in extracellular spaces and were often enmeshed among fibrin and fibrinocellular debris. Viral antigen and RNA persisted in macrophages and DC at day 6 as did the histologic abnormalities. Additional histologic changes included the appearance of lymphoblasts in periarteriolar sheaths and marginal zones (3/4).

Mucosal-Associated Lymphoid Tissue. We noted no histologic lesions in the tonsils at day 4; however, EBOV-positive macrophages, DC, and FRC, were occasionally observed in paravascular patterns involving the interfollicular areas of the tonsil (3/4). At day 5, apoptotic-like bodies were scattered throughout follicular centers of the tonsils; the distribution of RNA and antigen increased to include foci of EBOV-positive endothelial cells lining HEV (3/4), and rare foci of EBOV-positive tonsillar epithelium (1/4). Follicular center lymphoid depletion was prominent at day 6 (2/3), and increased numbers of EBOV-positive HEV endothelial cells (3/3) and tonsillar epithelium (2/3) were observed. Histologic lesions, EBOV RNA, and antigen distribution patterns in the gut-associated lymphoid tissues were consistent with observations described for lymph nodes.

Thymus. Because our monkeys were adults, the thymus was involuted in all animals. At day 5 and day 6, small foci of EBOV-positive macrophage-like cells, dendritiform cells, and spindle-shaped cells were present in the medulla and at the corticomedullary junction of the thymus (3/4 and 3/3, respectively); these cells were often seen in paravascular areas. EBOV antigen and RNA were infrequently present in endothelial cells of the thymus at day 5 and day 6 in two of four and three of three monkeys, respectively.

Gastrointestinal Tract. No significant lesions were seen at day 4; however, immunoreactive circulating monocytes were occasionally seen in all tissues of three of four monkeys. Small foci of antigen-positive macrophages and fibrocyte-like cells were detected in lamina propria of the stomach (1/4), ileum (1/4), ileocecal valve (3/4), cecum

(1/4), and proximal colon (1/4). At day 5, foci of congestion were observed in the submucosa and lamina propria of the duodenum in four of four monkeys; and in the duodenum, jejunum, ileum, cecum, and colon of one monkey; mild hemorrhage was also noted in the submucosa of the cecum of this animal. EBOV-positive circulating monocytes were seen in tissue sections of all monkeys at day 5. Antigen-positive macrophages and fibrocyte-like cells, and infrequently endothelial cells, were seen in lamina propria of stomach (4/4), duodenum (4/4), jejunum (4/4), ileum (4/4), cecum (4/4), and proximal colon (4/4). Gastrointestinal tract changes at day 6 also included scattered apoptotic-like bodies in intestinal lamina propria with mutifocal intraepithelial apoptotic bodies interpreted to be apoptosis of intraepithelial lymphocytes (2/3); occasional presence of immunopositive fibrocytes and endothelial cells in the tunica submucosa, tunica muscularis, and tunica serosa (3/3); and fibrin thrombi in submucosal vessels of the duodenum with associated degeneration/necrosis of Brunner's glands (1/3).

Liver. No significant hepatic lesions were present at days 2 or 3; however, viral RNA was detected in rare circulating monocytes at day 2 (1/3) (Figure 9C). Viral antigen and RNA were detected in infrequent Kupffer cells of all four monkeys by day 3 (Figure 9D). At day 4, increased numbers of neutrophils and monocytes were seen in sinusoids and central veins (4/4). The number of immunoreactive Kupffer cells increased considerably between days 3 and 4 (3/4). Of note, small strands of fibrillar material, interpreted to be fibrin, were co-localized with these immunopositive Kupffer cells; the strands appeared to extend from the cell surface into the lumen of the sinusoid. Monocytes in the portal veins and sinusoids were occasionally immunoreactive (3/4), and very rare antigen-

positive hepatocytes were observed. Ultrastructurally, sinusoids occasionally contained fibrin deposits, fibrinocellular debris, and free virions; the association of fibrin with EBOV-infected Kupffer cells was confirmed. Hepatocytes with intracytoplasmic filoviral inclusions were detected in rare fields of two of four monkeys.

By day 5, the histologic changes also included small foci of hepatocellular degeneration and necrosis (4/4), degeneration/necrosis and hypertrophy of Kupffer cells (4/4), and multifocal pleomorphic eosinophilic intracytoplasmic inclusions in Kupffer cells and hepatocytes (4/4) (Figure 9E). EBOV antigen and RNA were detected in Kupffer cells (Figure 9F) and circulating mononuclear cells and less frequently in hepatocytes (Figure 9F); endothelial-like sinusoidal lining cells were rarely EBOV-positive. Occasional intrasinusoidal fibrin deposits were seen in all four animals. PTAH and electron microscopy confirmed the presence of intrasinusoidal fibrin and again showed that the fibrin was primarily associated with Kupffer cells. Ultrastructural examination also revealed that many degenerate and necrotic Kupffer cells and lesser hepatocytes contained viral inclusion material. Free virions were observed in association with Kupffer cell debris and in foci of hepatocellular necrosis. Sinusoids and Disse's spaces were expanded, and there was focal disruption of sinusoidal endothelium in areas where EBOV was present. Day 6 findings mirrored those described above for day 5; a slight increase in the number of EBOV-positive endothelial-like sinusoidal lining cells was noted and ultrastructurally, hepatocytes contained numerous lipid droplets.

Endocrine System. The adrenal glands were unremarkable until day 4, when increased numbers of intravascular neutrophils and monocytes were noted in the cortex of two of four monkeys. EBOV antigen and RNA were detected in circulating monocytes (3/4) and in macrophage and spindle-to-dendritiform cells (interpreted as stromal/stellate cells and DC, respectively) (3/4) adjacent to cortical cells in the zona glomerulosa, zona fasciculata, and zona reticularis. Rare EBOV-positive sinusoidal lining cells were seen in the cortex of two of four monkeys. In addition, EBOV RNA was detected in adrenal cortical cells in the zona fasciculata (2/4) and zona reticularis (1/4), stromal cells in the cortex (2/4), and fibrocytes in the capsule (1/4). Histopathology at day 5 included mild, multifocal congestion of the adrenal cortex (4/4) and multifocal degeneration and necrosis of adrenal cortical cells with rare eosinophilic intracytoplasmic inclusions and acute inflammation (2/4). In addition to the nonendocrine cells described above, individual and small foci of antigen-positive adrenal cortical cells were present in the zona glomerulosa, zona fasciculata, and zona reticularis of the cortex at day 5 (4/4); in multiple foci, a thin line of immunoreactivity appeared to separate cortical cells (4/4); this staining was interpreted to represent free intercellular virions, and was subsequently confirmed by electron microscopy. Day 6 histopathology and antigen distribution were similar to those on day 5 (3/3). EBOV was not detected in pituitary gland, thyroid gland, or pancreatic islets of any animal by either IHC or ISH.

Kidneys and Urinary Bladder. The kidneys were unremarkable until day 4 when mild, multifocal congestion was noted in three of four monkeys and fibrin thrombi, confirmed by PTAH staining, were infrequently present in medullary vessels (2/4). Circulating

monocytes contained EBOV antigen and RNA (3/4). Multifocally, proximal convoluted tubular epithelial cells were antigen-positive but viral RNA-negative (2/4); previous studies showed that this staining is likely a result of secretion or reabsorption of VP40 by tubular epithelium and not due to viral infection of these cells.[34] The urinary bladder was histologically normal at day 4; however, immunopositive circulating monocytes were detected in three of four monkeys. At day 5, fibrin thrombi, confirmed by PTAH staining, were multifocally present in renal medullary vessels (3/4). Viral antigen was detected in rare endothelial cells of the capillaries of the renal medulla (1/4), and as described above, viral antigen but not viral RNA, was observed in proximal convoluted tubular epithelial cells (4/4). Small hemorrhages were noted in the urinary bladder lamina propria of one of four monkeys at day 5. RNA- and antigen-positive macrophages (1/4) in the urinary bladder lamina propria and infrequent positive fibrocytes (3/4) and endothelial cells (1/4) in the lamina propria, tunica mucosa, and tunica serosa were present at day 5. By day 6, kidneys were mildly congested (3/3); small foci of intraluminal mineral deposits were seen in cortical tubules (3/3), fibrin thrombi were observed in glomerular (1/3) and medullary (2/3) capillaries. EBOV RNA and antigen were present in fibrocytes and macrophage-like cells in the interstitium of the renal cortex and medulla and in the connective tissue of the renal pelvis (3/3). As described above, the proximal convoluted tubular epithelial cells were antigen-positive but RNA-negative (3/3). Endothelial cells lining capillaries in the medulla and cortex were infrequently EBOV-positive in three of three monkeys; one of three animals showed small hemorrhages in the lamina propria of urinary bladder. The distribution of viral RNA and antigen intensified in the urinary bladder at day 6 in two of three animals.

Multiple foci of EBOV-positive macrophages, fibrocytes, and endothelial cells were observed in the connective tissue of the lamina propria, tunica muscularis, and tunica serosa. There was no viral RNA or antigen detected in the urothelium of any animal.

Respiratory System. The lungs were unremarkable until day 4, when increased numbers of intravascular neutrophils and monocytes were noted in alveolar capillaries and pulmonary veins (3/4). Viral antigen and RNA were frequently detected in circulating monocytes in alveolar capillaries and pulmonary veins (3/4), and rarely seen in alveolar macrophages (3/4). No further changes in lesions or distribution of EBOV were noted in the lungs until day 6 when small deposits of fibrin were observed in alveoli of one of three animals, and increased numbers of EBOV-positive alveolar macrophages were present. No significant lesions were seen in the nares, larynx, or trachea at day 4; monocytes in blood vessels were infrequently immunoreactive. By day 5, individual and small foci of EBOV RNA- and antigen-positive macrophages, DC, and fibrocyte-like cells (often adjacent to capillaries and small venules) were occasionally observed in the superficial dermis of the nares (4/4), lamina propria of the larynx (4/4), and lamina propria of the trachea (3/4). EBOV-positive endothelial cells lining capillaries and venules in these foci were infrequently seen in all four animals. Increased numbers of EBOV-positive endothelial cells were detected at day 6 (3/3).

Reproductive System. Testis, epididymis, and prostate gland were unremarkable at day 4; however, circulating monocytes contained EBOV antigen in three of four animals. At day 5, mild multifocal hemorrhages (2/4) and congestion (4/4) was observed in the

parenchyma of the testis. EBOV antigen was detected in circulating monocytes of testis and epididymis of all four animals; endothelial cells and interstitial fibrocytes were infrequently immunoreactive (4/4). No changes, compared to day 5, in the reproductive system were noted at day 6. By day 5, EBOV-positive macrophages and fibrocytes (1/4), and endothelial cells (2/4) were infrequently detected in the prostate. At day 6, increased numbers of these EBOV-positive cells were noted in all three animals.

Skin and Adnexa. Sections of skin from the mucocutaneous junctions of the nares, lip, and sections of haired skin from the chest were examined. No lesions were observed at day 4; however, immunoreactive circulating monocytes were detected in three of four monkeys. By day 5, individual and small foci of RNA- and antigen-positive fibrocytes, macrophages, and DC, often adjacent to capillaries and venules, and infrequently endothelial cells were present in the superficial dermis and lamina propria of the nares and lip (4/4), but not in the dermis of the haired skin of the chest. Similar immunoreactive and RNA-positive cells were present in the haired skin collected from rash sites. At day 6, similar EBOV-positive cells were present in increased numbers in the superficial dermis and lamina propria of the nares and lip (3/3), and were also present in the superficial dermis of the haired skin of the chest (3/3). Additionally, one of three day 6 monkeys also had small foci of EBOV-positive germinal epithelial cells present in the mucous membrane of the lip.

Central and Peripheral Nervous System. No lesions were detected in central nervous system tissues of any monkey examined. EBOV antigen in the central and peripheral

nervous system was limited to circulating monocytes seen in three of four animals at day 4 and all monkeys at day 5 and 6; infrequent endothelial cells of capillaries and venules at day 5 (1/3) and day 6 (3/3); and infrequent fibrocyte-like cells in the chorid plexus and meninges at day 6 (2/3).

Other Tissues. Bone marrow was unremarkable until day 4 when a decreased ratio of nonproliferating maturation storage pool to proliferating pool was observed in the myeloid series cells (3/4). This histologic finding, interpreted as a depletion of the storage pool, was consistent in all monkeys at days 5 and 6. Multifocally, bone marrow macrophages and stromal cells contained EBOV antigen and RNA in three of four monkeys at day 4 and in all animals at days 5 and 6.

Tongue was unremarkable until day 5, when individual and small foci of EBOV-positive macrophages, DC, and fibrocyte-like cells were present in the lamina propria (3/4), and infrequent positive endothelial cells lining capillaries and venules were observed in the lamina propria (3/4). Germinal epithelium of the tongue was multifocally EBOV-positive in one of four animals and this animal also had positive fibrocytes in the deeper tissues of the tongue. Day 6 observations of the EBOV-positive cell types in the tongue (3/3) were consistent with animals at day 5, and one of three day 6 monkeys had small foci of positive germinal epithelial cells.

In the esophagus, individual and small foci of EBOV RNA- and antigen-positive macrophages, DC, fibrocyte-like cells, and endothelial cells, were first noted in the

lamina propria and submucosa of the esophagus at day 5 in two of four animals; this observation was a consistent finding in all animals by day 6. Multiple foci of EBOV RNA- and antigen-positive germinal epithelial cells were detected in one of three day 6 monkeys.

We noted no histologic lesions of the heart on H & E-stained sections, with the exception of one day 6 animal, which had multiple small foci of epicardial hemorrhage. Multifocal immunoreactivity was present in endothelial cells and interstitial cells of the epicardium, endocardium, and myocardium of one of four animals at day 5 and in all three monkeys at day 6.

Evaluation of Apoptosis

Blood. Peripheral blood mononuclear cells (PBMC) were evaluated for evidence of apoptosis by TEM and RNA analysis. Evidence of increased apoptosis was not detected in the PBMC by TEM of any of the day 1 or 2 monkeys compared to the prechallenge PBMC of the 21 animals. By day 3, TEM evidence of morphological apoptosis[35,36] in lymphocytes was observed in nearly every field surveyed (4/4). It appeared that the highest proportion of these apoptotic lymphocytes represented the large granular lymphocyte fraction and, furthermore, had ultrastructural characteristics of NK cells[37,38] (Figure 11A). Specifically, these cells were larger in cross-section (6 to 8 μm) and had abundant cytoplasm that contained granules not seen in other lymphoid cells, and an abundance of mitochondria and polyribosomes. TEM of day 4 PBMC showed increased numbers of apoptotic small lymphocytes (4 to 6 μm in cross-section) and markedly

elevated numbers of neutrophils (Figure 11B), which is consistent with the differential white blood cell counts. By days 5 and 6, increased numbers of apoptotic bodies were present in all fields surveyed, and many of these bodies appeared to be phagocytosed by monocytes/macrophages and neutrophils.

RNA analysis of PBMC showed several gene expression changes in apoptosis-associated signaling molecules. Increased mRNA levels of the pro-apoptotic genes tumor necrosis factor (TNF)-related apoptosis-inducing ligand (TRAIL) (Figure 11C), Fas/CD95 (Figure 11C), and receptor interacting protein (RIP) were observed by day 3 postinfection; Fas-associated death domain protein (FADD), Requiem, and Bcl-2 family proteins bik and bak were noted at later stages of disease. Transcripts for anti-apoptotic genes, cellular inhibitor of apoptosis protein 2 (cIAP-2) and neuronal apoptosis inhibitory protein (NAIP) were increased by days 2 and 3 (Figure 11D), while transcripts of Bcl-2 family proteins bfl-1, bcl-2, and mcl-1 were increased by day 4.

Tissues. No significant findings were observed at 24 hours. At day 2, there was TUNEL-labeling of apoptotic bodies in scattered Kupffer cells and infrequently in circulating monocytes in the liver of one of three monkeys. This same animal also had infrequent TUNEL-positive apoptotic bodies in splenic macrophages and DC in the follicles and paracortex of the axillary lymph node; rare TUNEL-positive lymphocytes were seen in spleen, and in follicles and sinuses of the axillary lymph node. By day 3, TUNEL-positive apoptotic bodies were multifocally detected in Kupffer cells and circulating monocytes in liver and spleen, tissue macrophages in splenic red pulp (3/4),

DC and macrophages in splenic white pulp (3/4), and macrophages in sinus and paracortex of peripheral lymph nodes (3/4). TUNEL-positive circulating lymphocytes were seen in multiple foci of liver (Figure 11E) and spleen, and infrequently noted in follicular centers as would be expected of peripheral lymph nodes. Ultrastructurally, macrophages containing apoptotic bodies were infrequently detected in red pulp of spleen (3 /4) and in sinuses of inguinal lymph nodes (2/4); apoptotic lymphocytes were infrequently seen in sinuses of inguinal lymph nodes (2/4) and occasionally observed within the HEV of inguinal node of one of four animals.

By day 4, Kupffer cells and tissue macrophages in red pulp of spleen with TUNEL-positive apoptotic bodies were numerous in all four monkeys. TUNEL-positive apoptotic bodies were multifocally detected in circulating monocytes in liver and spleen (4/4), DC and macrophages in splenic white pulp (3/4), macrophages in sinuses and paracortex of peripheral lymph nodes (4/4), and macrophages and DC in follicular centers of peripheral lymph nodes (4/4) (Figure 11F). TUNEL-positive circulating lymphocytes were seen in multiple foci of liver and spleen, and peripheral lymph node sinuses (4/4), and less frequently noted in follicular centers of peripheral lymph nodes (4/4). TEM confirmed TUNEL findings and also showed infrequent apoptotic plasma cells in spleen of two of four animals. TUNEL findings were similar at days 5 and 6; increased numbers of apoptotic lymphocytes, and macrophages and DC with TUNEL-positive apoptotic bodies, being detected in all monkeys. The most notable difference by TEM was the abundance of apoptotic lymphocytes, which were readily detected in lymph node sinuses and paracortex.

Discussion

Histologic lesions, IHC, and ISH demonstrated a similar pattern of EBOV infection starting with monocytes/macrophages and DC in the lymphoid tissues and Kupffer cells in liver, progressing to infection of parenchymal cells in liver and adrenal gland, endothelial cells lining sinusoids in liver and adrenal gland as well as HEV in lymphoid tissues, fibrocytes and endothelial cells of connective tissue, and finally to infection of the epithelium. The role of endothelial cells in EBOV pathogenesis is detailed in a companion paper.[39] Our study demonstrates, for the first time, that DC are early and sustained cellular targets of EBOV in nonhuman primates; that lymphocyte apoptosis is a relatively early event in disease progression; and furthermore, it is the NK cell fraction that is likely lost through increased apoptosis early in the course of infection. Previous studies of moribund monkeys demonstrated that EBOV has a predilection for monocytes/macrophages,[6,14,40] and these cells were shown to be early and sustained targets of EBOV in guinea pigs.[11] We also observed early and sustained infection of monocytes/macrophages in our study, with EBOV RNA initially detected in lymphoid monocytes/macrophages at day 2 postinfection. As monocytes/macrophages are usually the cells that elicit the response cascade in the acute phase of inflammation,[41] their early infection represents an effective strategy for evasion of the host defense system as well as facilitating dissemination of the virus.

While the importance of monocytes/macrophages in EBOV pathogenesis have been well-documented,[28,40,42-44] few studies have addressed the importance of DC in EBOV pathogenesis; these cells also play important roles in initiation and regulation of the host

immune response. DC are a family of professional antigen-presenting cells, derived from bone marrow, that have the ability to initiate and modulate cell-mediated immune responses.[45,46] Immature DC function as sentinels of the adaptive immune system; they are located in the peripheral tissues where they capture and process exogenous antigens and migrate to regional lymph nodes where they undergo maturation. A wide variety of stimuli including infectious virus, bacterial antigens, or inflammatory cytokines, can trigger maturation of DC, which is characterized by phenotypic changes including up-regulation of MHC and co-stimulatory molecules and production of IL-12. Presentation of acquired antigen by mature DC leads to T-cell activation.[47,48] Monocytes circulating in the blood could be equally important in the DC response as circulating monocytes counter infection by crossing the endothelial barrier, infiltrating the focus of infection, and developing either into macrophages or DC.

Regarding the importance of EBOV predilection for DC in disease pathogenesis, we speculate that EBOV acts in a manner similar to other viruses that are known to disable the host immune response by attacking and manipulating the very cells that play the most critical roles in initiating the antiviral immune response. DC-tropic viruses such as human immunodeficiency virus,[49,50] measles virus,[51-53] lymphocytic choriomeningitis virus,[54] dengue,[55] cytomegalovirus,[56] and Herpes simplex 1 virus[57] have evolved mechanisms to impair the function of DC, thereby enhancing their chance to escape immune surveillance. Raftery et al. proposed that infection of DC by human cytomegalovirus induces immunosuppression through a multilayered defense strategy that includes partially downregulating MHC molecules, upregulating apoptosis-inducing

ligands CD95L and tumor necrosis factor (TNF)-related apoptosis-inducing ligand (TRAIL) to delete activated T lymphocytes, complemented by a nondeletional mechanism involving undefined viral proteins that suppresses surviving T lymphocytes.[56] Of note, increased TRAIL expression and partial suppression of MHC II were associated with EBOV infection of immature DC *in vitro*;[44] apoptosis of bystander lymphocytes is a characteristic feature of EBOV infections;[28] and furthermore, the well-chronicled discovery of an immunosuppressive motif in the C-terminal region of filoviral glycoproteins[58-60] lends some additional credence to this comparison. Thus, it is evident that the result of interactions between viruses and DC is critical for the outcomes of EBOV infections.

Profound lymphopenia and lymphoid depletion are characteristic features of EBOV HF. Extensive lymphocyte apoptosis appears to be critical to the pathogenesis of EBOV in humans and nonhuman primates.[28,61] In fatalities, widespread lymphocyte apoptosis occurs before the development of an adequate adaptive (B- and T-lymphocyte-mediated) immune response. In survivors, the adaptive immune response, arising in the absence of such pathological lymphocyte apoptosis, controls viral replication and leads to disease resolution. Of note, fatalities have markedly increased serum levels of nuclear mitotic apparatus protein (NuMA), a protein that is efficiently cleaved by caspases during classical and granzyme B-mediated caspase-independent apoptosis.[62,63] In this study, as in a previous study,[28] we clearly show that massive lymphocyte apoptosis is recapitulated in macaques experimentally infected with EBOV. In rhesus and cynomolgus monkeys, there is lymphopenia and lymphocyte depletion/loss in lymphoid tissues. Apoptosis is

evident in lymphocytes, both in the vasculature as well as in lymphoid tissue. Both classical morphology and evidence of DNA fragmentation are seen. The mechanism(s) underlying such apoptosis have been unclear. It is not due to direct viral infection; lymphocytes are not productively infected, and infected mononuclear phagocyte system cells are not apoptotic. In this study, we found evidence of abnormal lymphocyte apoptosis in PBMC, in the vasculature, and in lymphoid tissues as early as day 3 postinfection. By days 4 to 6, a consistent increase in bystander lymphocyte apoptosis was noted in all animals.

We previously showed increased TRAIL expression in EBOV-infected adherent human monocytes/macrophages *in vitro*, and suggested that TRAIL is involved in apoptosis of host lymphocytes.[44] Analysis of apoptotic genes in this study showed increased TRAIL transcripts by day 3 postinfection in PBMC. Type I IFNs are known to enhance TRAIL expression on human lymphocytes making them susceptible to TRAIL-induced apoptosis,[64] and we demonstrated highly elevated plasma levels of Type I IFNs in this study. Measles virus can induce Type I IFN expression in monocytes,[65] and IFN-α treatment induced functional TRAIL expression in monocytes[66] and DC.[67] Functional TRAIL is produced by measles virus-infected DC and mediates their cytotoxic activity.[67] Killer activity is also induced by HIV infection. In fact, HIV infection of human DC leads to release of an as yet unidentified soluble factor(s), which induces apoptosis of thymocytes and activated PBMC.[68] TRAIL involvement in this killer activity has not been tested yet, but increased sensitivity of T cells from HIV patients to TRAIL-induced apoptosis has been described.[69,70] Cytotoxic activity of either measles virus- or HIV-

infected DC results in lymphocyte apoptosis and may be TRAIL mediated. Other studies have reported that IFN-α production upregulates TRAIL production and downregulates TRAIL receptor 2 expression[66] thus protecting monocytes from apoptosis. Furthermore, upregulation of NAIP and cIAP2 mRNA in the macaque PBMC of this study, and in EBOV-infected primary human monocytes/macrophages *in vitro* (TW Geisbert, unpublished observation), suggests that EBOV has evolved an additional mechanism to resist host defenses by inducing these protective transcripts in cells that it infects. In fact, regulation of apoptosis may be part of the pathogenesis of EBOV. Current studies are ongoing to evaluate the role of these genes in promoting/resisting apoptosis of specific lymphocyte populations.

There was no evidence of apoptosis in any EBOV-infected DC. This finding is consistent with previous studies showing that dsRNA infection of DC exerts anti-cytopathic effects.[71,72] For example, Cella et al. demonstrated that DC activation by viruses such as influenza results in the induction of Type I IFN, which triggers a cellular resistance to cytopathic effects via upregulation of MxA protein.[72] This increased resistance allows infected DC to present corresponding antigens and to induce protective immune responses. Similarly, TNF-α can protect DC from cell death by upregulating anti-apoptotic factors such as Bcl-xl.[73,74] Furthermore, the virus-induced production of TNF-α and IFN-α is thought to contribute to the lesser cell death in dengue virus-infected DC in the late phase of virus infection.[55]

There is recent evidence that increased levels of NO at inflammatory sites may affect the biological activity of lymphoid cells. Specifically, recent studies showed that dissipation of mitochondrial membrane potential is an early event in apoptotic cell death, and that a high concentration of NO depressed the mitochondrial membrane potential in human peripheral blood lymphocytes inducing apoptosis.[75] Moreover, Takabayashi et al. showed that apoptosis and the production of reactive oxygen species was highest in NK cells.[75] As we were able to demonstrate elevated plasma levels of nitrate (as marker for NO synthetase) in our EBOV-infected monkeys, we speculate that high concentrations of NO may trigger the bystander apoptosis and loss of NK cells as seen in the animals in this study. In addition, peroxynitrite alone, or with NO, can mediate direct toxicity as well as activated inflammatory cascades via NFκB. Combined, these events may lead to organ injury and contribute to the multiple organ failure that is characteristic of EBOV infections.

Primate EBOV infections are characterized by a dysregulation of normal host immune responses. In this study, we showed increased circulating levels of IFN-α, IL-6, MCP-1, MIP-1α, and MIP-1β at the early- to mid-stages of disease, and IFN-β IL-18, and TNF-α at later stages of disease. We failed to detect increased levels of IFN-γ, IL-4, IL-8, IL-10, or IL-12. Increased levels of IL-10 were associated with fatality in previous EBOV outbreaks.[61,76] One of these studies associated increased levels of IFN-α with fatalities,[76] while the other study did not detect IFN-α, IL-1β, IL-8, or IL-12.[61] Moderate levels of IL-6 and TNF-α were associated with fatal infection in the days before death in the Gabon study,[61] and high levels of TNF-α, but not IL-6, were associated with fatality in

the Kikwit investigation.[76] Increased levels of IL-2 were noted in two of seven fatal cases in the Kikwit study; we noted slightly increased levels of IL-2 in two of five late-stage (days 5 and 6) monkeys. Our results are as comparable to those of these previous human studies as each of the human studies is to each other. There are some notable differences, particularly with regard to increased levels of IL-10, which were associated with fatal cases of EBOV in both human studies, while changes in IL-10 were not detected in any of our EBOV-infected cynomolgus monkeys.

Notwithstanding issues of unknown routes and doses of exposure, and preexisting medical conditions, there are other concerns when comparing information obtained from patients during EBOV outbreaks with information gathered from nonhuman primates under experimental conditions. Clinical identification of EBOV infection, particularly in tropical settings, is problematic as initial symptoms are nonspecific and similar to those of more common infections including malaria, salmonellosis, typhoid fever, and shigellosis. A typical course of action in these cases is intervention with broad-spectrum antibiotics. However, the use of antibiotics, while clearly warranted, may confound interpretation of the immunological response to EBOV, thus, making it difficult to fully evaluate human immunopathogenesis and compare it with what is known about nonhuman primate models, where animals are not usually treated with antibiotics or given any supportive care. It is known that antibacterial agents can modify acute-phase inflammatory responses through their effects on cytokine synthesis by monocytes.[77-80] It has also been shown that antibiotic-induced changes in the gut microflora can modulate the gut cytokine production after tissue injury with or without hemorrhagic shock.[81,82]

In summary, the paradigm that we propose for EBOV pathogenesis in primates, based on results of the current study, is as follows: EBOV spreads from the initial infection site via monocytes and DC to regional lymph nodes, likely via lymphatics, and to liver and spleen via blood. At these sites, EBOV infects tissue macrophages (including Kupffer cells) and DC. EBOV activates DC early in the course of infection by upregulating expression of TRAIL. Such overexpression of TRAIL, which is sustained as the disease progresses by overexpression of IFN-α, participates in T lymphocyte deletion via bystander apoptosis, and establishment of virus-induced immunosuppression. Concomitantly, EBOV-infected monocytes/macrophages release a variety of soluble factors including proinflammatory cytokines such as MIP-1α and MCP-1 that recruit additional macrophages to areas of infection making more target cells available for viral exploitation, and further amplifying an already dysregulated host response. As disease progresses, increased levels of oxygen free radicals (e.g., NO), released by EBOV-infected macrophages at inflammatory sites, trigger apoptosis of NK cells thwarting the innate immune response and leaving the host little time to mount an adaptive response. Left unchecked, extensive viral replication leads to increased levels of additional proinflammatory cytokines, notably IL-6, which then trigger the coagulation cascade. Activation of the coagulation cascade, in turn, activates the fibrinogenic and fibrinolytic pathways leading to DIC. Inhibitors of the clotting system are consumed at a rate that exceeds synthesis by liver parenchymal cells, which by this point have been rendered dysfunctional by the viral assault. Left unchecked, the fibrinogenic and/or fibrinolytic

coagulopathy could result in rapid progression of fibrin thrombi, and/or hemorrhagic shock, multiple organ failure, and finally death of the host.

This sequence of morphologic, cytologic, virologic, serologic, and inflammatory change after an EBOV infection creates a useful model in the study of experimentally induced EBOV HF and the sequence of pathogenetic events identified should provide new targets for rational prophylactic and chemotherapeutic interventions. Because of massive synergism and redundancy in the pathways of apoptosis, inflammation and the development of hemorrhagic shock, it is likely that combined or appropriate sequential targeting of the above-listed pathways for treatment modalities will be more effective than targeting a single pathway.

Acknowledgements

Opinions, interpretations, conclusions, and recommendations are those of the authors and are not necessarily endorsed by the U.S. Army. Research was conducted in compliance with the Animal Welfare Act and other Federal statutes and regulations relating to animals and experiments involving animals and adheres to principles stated in the *Guide for the Care and Use of Laboratory Animals*, National Research Council, 1996. The facility where this research was conducted is fully accredited by the Association for Assessment and Accreditation of Laboratory Animal Care International. The research described herein was sponsored by the Medical Chemical/Biological Defense Research Program, U.S. Army Medical Research and Material Command (Project No. 02-4-4J-081).

The authors thank Denise Braun, Lynda Miller, Roswita Moxley, Jeff Brubaker, Steve Moon, Neil Davis, and Larry Ostby for their expert technical assistance. The authors also express thanks to Gabriela Dveksler, Aileen Marty, Rahda Maheshwari, and Chou-Zen Giam for helpful discussions and comments and to Gordon Ruthel for skillful assistance with confocal microscopy.

References

1. Bowen ETW, Lloyd G, Harris WJ, Platt GS, Baskerville A, Vella EE: Viral haemorrhagic fever in southern Sudan and northern Zaire. Lancet 1977, 1:571-573.
2. Johnson KM, Lange JV, Webb PA, Murphy FA. Isolation and partial characterization of a new virus causing acute haemorrhagic fever in Zaire. Lancet 1977, 1:569-571.
3. Khan AS, Tshioko K, Heymann DL, Le Guenno B, Nabreth P, Kerstiens B, Fleerackers Y, Kilmarx PH, Rodier GR, Nkuku O, Rollin PE, Sanchez A, Zaki SR, Swanepoel R, Tomori O, Nichol ST, Peters CJ, Muyembe-Tamfum JJ, Ksiazek TG. The reemergence of Ebola hemorrhagic fever, Democratic Republic of the Congo, 1995. J Infect Dis 1999, 179(Suppl 1):S76-S86
4. Bowen ETW, Platt GS, Simpson DIH, McArdell LB, Raymond RT: Ebola haemorrhagic fever: experimental infection of monkeys. Trans R Soc Trop Med Hyg 1978, 72:188-191
5. Fisher-Hoch SP, Brammer LT, Trappier SG, Hutwagner LC, Farrar BB, Ruo SL, Brown BG, Hermann LM, Perez-Oronoz GI, Goldsmith CS, Hanes MA, McCormick JB: Pathogenic potential of filoviruses: role of geographic origin of primate host and virus strain. J Infect Dis 1992, 166:753-763
6. Jaax NK, Davis KJ, Geisbert TW, Vogel P, Jaax GP, Topper M, Jahrling PB: Lethal experimental infection of rhesus monkeys with Ebola-Zaire (Mayinga) virus by the oral and conjunctival route of exposure. Arch Pathol Lab Med 1996, 120:140-155

7. Geisbert TW, Pushko P, Anderson K, Smith J, Davis KJ, Jahrling PB: Evaluation in nonhuman primates of vaccines against Ebola virus. Emerg Infect Dis 2002, 8:503-507
8. Ryabchikova E, Kolesnikova L, Smolina M, Tkachev V, Pereboeva L, Baranova S, Grazhdantseva A, Rassadkin Y: Ebola virus infection in guinea pigs: presumable role of granulomatous inflammation in pathogenesis. Arch Virol 1996, 141:909-921
9. Bray M, Hatfill S, Hensley L, Huggins JW: Haematological, biochemical and coagulation changes in mice, guinea-pigs and monkeys infected with a mouse-adapted variant of Ebola Zaire virus. J Comp Pathol 2001, 125:243-253
10. Bray M, Davis K, Geisbert T, Schmaljohn C, Huggins J: A mouse model for evaluation of prophylaxis and therapy of Ebola hemorrhagic fever. J Infect Dis 1998, 178:651-661
11. Connolly BM, Steele KE, Davis KJ, Geisbert TW, Kell WM, Jaax NK, Jahrling PB: Pathogenesis of experimental Ebola virus infection in guinea pigs. J Infect Dis 1999, 179(Suppl 1):S203-S217
12. Murphy FA: Pathology of Ebola virus infection. Ebola Virus Haemorrhagic Fever. Edited by SR Pattyn. New York, Elsevier/North-Holland Biomedical Press, 1978, pp 43-60
13. Zaki SR, Goldsmith CS: Pathologic features of filovirus infections in humans. Curr Top Microbiol Immunol 1999, 235:97-116
14. Davis KJ, Anderson AO, Geisbert TW, Steele KE, Geisbert JB, Vogel P, Connolly BM, Huggins JW, Jahrling PB, Jaax NK: Pathology of experimental

Ebola virus infection in African green monkeys. Arch Pathol Lab Med 1997, 121:805-819

15. Jahrling PB, Geisbert J, Swearengen JR, Jaax GP, Lewis T, Huggins JW, Schmidt JJ, LeDuc JW, Peters CJ: Passive immunization of Ebola virus-infected cynomolgus monkeys with immunoglobulin from hyperimmune horses. Arch Virol 1996, 11(Suppl):135-140
16. Jahrling PB, Geisbert TW, Geisbert JB, Swearengen JR, Bray M, Jaax NK, Huggins JW, LeDuc JW, Peters CJ: Evaluation of immune globulin and recombinant interferon-α2b for treatment of experimental Ebola virus infections. J Infect Dis 1999, 179(Suppl 1):S224-S234
17. Sullivan NJ, Sanchez A, Rollin PE, Yang Z-Y, Nabel GJ: Development of a preventative vaccine for Ebola virus infection in primates. Nature 2000, 408:605-609
18. Fisher-Hoch SP, Platt GS, Neild GH, Southee T, Baskerville A, Raymond RT, Lloyd G, Simpson DIH: Pathophysiology of shock and hemorrhage in a fulminating viral infection (Ebola). J Infect Dis 1985, 152:887-894
19. Johnson E, Jaax N, White J, Jahrling P: Lethal experimental infections in rhesus monkeys by aerosolized Ebola virus. Int J Exp Pathol 1995, 76:227-236
20. P'yankov OV, Sergeev AN, P'ankova OG, Chepurnov AA: Experimental Ebola fever in macaca rhesus. Vopr Virusol 1995, 40:113-115
21. Mikhailov VV, Borisevich IV, Chernikova NK, Potryvaeva NV, Krasnyanskii VP: An evaluation of the possibility of Ebola fever specific prophylaxis in baboons (*Papio hamadryas*). Vopr Virusol 1994, 39:82-84

22. Borisevich IV, Mikhailov VV, Krasnyanskii VP, Gradoboev VN, Lebedinskaya YV, Potryvaeva NV, Timan'kova GD: Creation and study of immunoglobulin to Ebola fever. Vopr Virusol 1995, 40:270-273

23. Chepurnov AA, Chernukhin IV, Ternovoi VA, Kudoiarova NM, Makhova NM, Azaev MSh, Smolina MP: Attempts to develop a vaccine against Ebola fever. Vopr Virusol 1995, 40:257-260

24. Markin VA, Mikhailov VV, Krasnyanskii VP, Borisevich IV, Firsova IV: Development of emergency prophylaxis and treatment of Ebola fever. Vopr Virusol 1997, 42:31-34

25. Kudoyarova-Zubavichene NM, Sergeyev NN, Chepurnov AA, Netesov SV: Preparation and use of hyperimmune serum for prophylaxis and therapy of Ebola virus infections. J Infect Dis 1999, 179(Suppl 1):S218-S223

26. Ryabchikova EI, Kolesnikova LV, Luchko SV: An analysis of features of pathogenesis in two animal models of Ebola virus infection. J Infect Dis 1999, 179(Suppl 1):S199-S202

27. Prophet EB, Mills B, Arrington JB, Sobin LH, editors: Laboratory Methods in Histotechnology. Washington, DC, Armed Forces Institute of Pathology, 1992, pp 25-59

28. Geisbert TW, Hensley LE, Gibb TR, Steele KE, Jaax NK, Jahrling PB: Apoptosis induced in vitro and in vivo during infection by Ebola and Marburg viruses. Lab Invest 2000, 80:171-186

29. Jahrling PB: Filoviruses and Arenaviruses. Manual of Clinical Microbiology. Edited by PR Murray, EJ Baron, M Pfaller, FC Tenover, RH Yolken. Washington, DC, ASM Press, 1999, pp 1125-1136

30. Soilleux EJ, Morris LS, Leslie G, Chehimi J, Luo Q, Levroney E, Trowsdale J, Montaner LJ, Doms RW, Weissman D, Coleman N, Lee B: Constitutive and induced expression of DC-SIGN on dendritic cell and macrophage subpopulations in situ and in vitro. J Leukoc Biol 2002, 41:445-457

31. Geisbert TW, Jahrling PB: Differentiation of filoviruses by electron microscopy. Virus Res 1995, 39:129-150

32. Moschella SL, Cropley TG: Mononuclear phagocytic and dendritic cell systems. J Am Acad Dermatol 1990, 22:1091-1097

33. Wacker HH, Radzun HJ, Parwaresch MR: Accessory cells in normal human and rodent lymph nodes: morphology, phenotype, and functional implications. Curr Top Pathol 1990, 84:193-218

34. Steele K, Crise B, Kuehne A, Kell W: Ebola virus glycoprotein demonstrates differential cellular localization in infected cell types of nonhuman primates and guinea pigs. Arch Pathol Lab Med 2001, 125:625-30

35. Majno G, Joris I: Apoptosis, oncosis, and necrosis: an overview of cell death. Am J Pathol 1995, 146:3-15

36. Granville DJ, Carthy CM, Hunt DWC, McManus BM: Apoptosis: molecular aspects of cell death and disease. Lab Invest 1998, 78:893-913

37. Ferrarini M, Grossi CE: Ultrastructure and cytochemistry of the human large granular lymphocytes. Immunobiology of Natural Killer Cells. Edited by E Lotzova, RB Herberman. Boca Raton, CRC Press, 1986, pp 34-50
38. Neighbour PA, Huberman HS, Kress Y: Human large granular lymphocytes and natural killing: ultrastuctural studies of strontium-induced degranulation. Eur J Immunol 1982, 588-595
39. Geisbert TW, Young HA, Jahrling PB, Davis KJ, Larsen T, Kagan E, Hensley LE: Pathogenesis of Ebola hemorrhagic fever in primate models: evidence that hemorrhage is not the direct result of virus-induced cytolysis of endothelial cells, submitted
40. Geisbert TW, Jahrling PB, Hanes MA, Zack PM: Association of Ebola related Reston virus particles and antigen with tissue lesions of monkeys imported to the United States. J Comp Pathol 1992, 106:137-152
41. Baumann H, Gauldie J: The acute phase response. Immunol Today 1994, 15:74-89
42. Feldmann H, Bugany H, Mahner F, Klenk H-D, Drenckhahn D, Schnittler H-J: Filovirus-induced endothelial leakage triggered by infected monocytes/macrophages. J Virol 1996, 70:2208-2214
43. Stroher U, West E, Bugany H, Klenk HD, Schnittler HJ, Feldmann H: Infection and activation of monocytes by Marburg and Ebola viruses. J Virol 2001, 75:11025-33

44. Hensley LE, Young HA, Jahrling PB, Geisbert TW: Proinflammatory response during Ebola virus infection of primate models: possible involvement of the tumor necrosis factor receptor superfamily. Immunol Lett 2002, 80:169-179

45. Banchereau J, Briere F, Caux C, Davoust J, Lebecque S, Liu YJ, Pulendran B, Palucka K: Immunobiology of dendritic cells. Annu Rev Immunol 2000, 18:767-811

46. Stingl G, Bergstresser PR: Dendritic cells: a major story unfolds. Immunol Today 1995, 16:330-333

47. Larsen CP, Steinman RM, Witmer-Pack M, Hankins DF, Morris PJ, Austyn JM: Migration and maturation of Langerhans cells in skin transplants and explants. J Exp Med 1990, 172:1483-1493

48. Inaba K, Metlay JP, Crowley MT, Steinman RM: Dendritic cells pulsed with protein antigens in vitro can prime antigen-specific, MHC-restricted T cells in situ. J Exp Med 1990, 172:631-640

49. Macatonia SE, Gompels M, Pinching AJ, Patterson S, Knight SC: Antigen-presentation by macrophages but not by dendritic cells in human immunodeficiency virus (HIV) infection. Immunology 1992, 75:576-581

50. Blauvelt A, Clerici M, Lucey DR, Streinberg SM, Yarchoan R, Walker R, Shearer GM, Katz SI: Functional studies of epidermal Langerhans cells and blood monocytes in HIV-infected persons. J Immunol 1995, 154:3506-3515

51. Grosjean I, Caux C, Bella C, Berger I, Wild F, Banchereau J, Kaiserlian D: Measles virus infects human dendritic cells and blocks their allostimulatory properties for $CD4^+$ T Cells. J Exp Med 1997, 186:801-812

52. Fugier-Vivier I, Servet-Delprat C, Rivailler P, Rissoan M-C, Liu Y-J, Rabourdin-Combe C: Measles virus suppresses cell-mediated immunity by interfering with the survival and function of dendritic and T cells. 1997, J Exp Med 186, 813-823

53. Schnorr J-J, Xanthakos S, Keikavoussi P, Kampgen E, ter Meulen V, Schneider-Schaulies S: Induction of maturation of human blood dendritic cell precursors by measles virus is associated with immunosuppression. Proc Natl Acad Sci 1997, 94:5326-5331

54. Sevilla N, Kunz S, Holz A, Lewicki H, Homann D, Yamada H, Campbell KP, de la Torre JC, Oldstone MB: Immunosuppression and resultant viral persistence by specific viral targeting of dendritic cells. J Exp Med 2000, 192:1249-1260

55. Ho L-J, Wang J-J, Shaio M-F, Kao C-L, Chang D-H, Han S-W, Lai J-H: Infection of human dendritic cells by dengue viruses causes cell maturation and cytokine production. J Immunol 2001, 166:1499-1506

56. Raftery MJ, Schwab M, Eibert SM, Samstag Y, Walczak H, Schonrich G: Targeting the function of mature dendritic cells by human cytomegalovirus: a multilayered viral defense strategy. Immunity 2001, 15:997-1009

57. Kruse M, Rosorius O, Kratzer F, Stelz G, Kuhnt C, Schuler G, Hauber J, Steinkasserer A: Mature dendritic cells infected with herpes simplex virus type 1 exhibited inhibited T-cell stimulatory capacity. J Virol 2000, 74, 7127-7136

58. Bukreyev A, Volchkov VE, Blinov VM, Netesov SV: The GP-protein of Marburg virus contains the region similar to the 'immunosuppressive domain' of oncogenic retrovirus P15E proteins. FEBS Lett 1993, 323:183-187

59. Sanchez A, Kiley MP, Holloway BP, Auperin DD: Sequence analysis of the Ebola virus genome: organization, genetic elements, and comparison with the genome of Marburg virus. Virus Res 1993, 29:215-240

60. Sanchez A, Trappier SG, Mahy BW, Peters CJ, Nichol ST: The virion glycoproteins of Ebola viruses are encoded in two reading frames and are exposed through transcriptional editing. Proc Natl Acad Sci 1996, 93:3602-3607

61. Baize S, Leroy EM, Georges-Courbot M-C, Capron M, Lansoud-Soukate J, Debre P, Fisher-Hoch SP, McCormick JB, Georges AJ: Defective humoral responses and extensive intravascular apoptosis are associated with fatal outcome in Ebola virus-infected patients. Nature Med 1999, 5:423-426

62. Baize S, Leroy EM, Mavoungou E, Fisher-Hoch SP: Apoptosis in fatal Ebola infection. Does the virus toll the bell for immune system? Apoptosis 2000, 5:5-7

63. Andrade F, Bull HG, Thornberry NA, Ketner GW, Casciola-Rosen LA, Rosen A: Adenovirus L4-100K assembly protein is a granzyme B substrate that potently inhibits granzyme B-mediated cell death. Immunity 2001, 14:751-761

64. Kayagaki N, Yamaguchi N, Nakayama M, Eto H, Okumura K, Yagita H: Type I interferons (IFNs) regulate tumor necrosis factor-related apoptosis-inducing ligand (TRAIL) expression on human T cells: a novel mechanism for the antitumor effects of type I INFs. J Exp Med 1999, 189:1451-1460

65. Dhib-Jalbut SS, Cowan EP: Direct evidence that interferon-beta mediates enhanced HLA-class I expression in measles virus-infected cells. J Immunol 1993, 151:6248-6258

66. Griffith TS, Wiley SR, Kubin MZ, Sedger LM, Maliszewski CR, Fanger NA: Monocyte-mediated tumoricidal activity via the tumor necrosis factor-related cytokine, TRAIL. J Exp Med 1999, 189:1343-1353

67. Vidalain P-O, Azocar O, Lamouille B, Astier A, Rabourdin-Combe C, Servet-Delpart C: Measles virus induces functional TRAIL production by human dendritic cells. J Virol 2000, 74:556-559

68. Beaulieu S, Lafontaine M, Richer M, Courchesne I, Cohen EA, Bergeron D: Characterization of the cytotoxic factor(s) released from thymic dendritic cells upon human immunodeficiency virus type 1 infection. Virology 1998, 241:285-297

69. Katsikis PD, Garcia-Ojeda ME, Torres-Roca JF, Tijoe IM, Smith CA, Herzenberg LA, Herzenberg LA: Interleukin-1 beta converting enzyme-like protease involvement in Fas-induced and activation-induced peripheral blood T cell apoptosis in HIV infection. TNF-related apoptosis-inducing ligand can mediate activation-induced T cell death in HIV infection. J Exp Med 1997, 186:1365-1372

70. Jeremias I, Herr I, Boehler T, Debatin KM: TRAIL/Apo-2-ligand-induced apoptosis in human T cells. Eur J Immunol 1998, 28:143-152

71. Pavlovic J, Arzet HA, Hefti HP, Frese M, Rost D, Ernst B, Kolb E, Staeheli P, Haller O: Enhanced virus resistance of transgenic mice expressing the human MxA protein. J Virol 1995, 69:4506-4510

72. Cella M, Salio M, Sakakibara Y, Langen H, Julkunen I, Lanzavecchia A: Maturation, activation, and protection of dendritic cells induced by double-stranded RNA. J Exp Med 1999, 189:821-829

73. Wong BR, Josien R, Lee SY, Sauter B, Li HL, Steinman RM, Choi Y: TRANCE (tumor necrosis factor [TNF]-related activation-induced cytokine), a new TNF family member predominantly expressed in T cells, is a dendritic cell-specific survival factor. J Exp Med 1997, 186:2075-2080

74. Yeh WC, Shahinian A, Speiser D, Kraunus J, Billia F, Wakeham A, de la Pompa JL, Ferrick D, Hum B, Iscove N, Ohashi P, Rothe M, Goeddel DV, Mak TW: Early lethality, functional NF-κB activation, and increased sensitivity to TNF-induced cell death in TRAF2-deficient mice. Immunity 1997, 7:715-725

75. Takabayashi A, Kawai Y, Iwata S, Kanai M, Denno R, Kawada K, Obama K, Taki Y: Nitric oxide induces a decrease in the mitochondrial membrane potential of peripheral blood lymphocytes, especially in natural killer cells. Antioxid Redox Signal 2000, 2:673-680

76. Villinger F, Rollin PE, Brar SS, Chikkala NF, Winter J, Sundstrom JB, Zaki SR, Swanepoel R, Ansari AA, Peters CJ: Markedly elevated levels of interferon (IFN)-α, IFN-γ, interleukin (IL)-2, IL-10, and tumor necrosis factor-α associated with fatal Ebola virus infection. J Infect Dis 1999, 179(Suppl 1):S188-S191

77. Bailly S, Fay M, Gougerot-Pocidalo MA: Effects of antibiotics on production of cytokines by human monocytes. Pathol Biol (Paris) 1993, 41:838-844

78. Morikawa K, Watabe H, Araake M, Morikawa S: Modulatory effect of antibiotics on cytokine production by human monocytes in vitro. Antimicrob Agents Chemother 1996, 40:1366-1370

79. van Vlem B, Vanholder R, de Paepe P, Vogelaers D, Ringoir S: Immunomodulating effects of antibiotics: a literature review. Infection 1996, 24:275-291

80. Khan AA, Slifer TR, Araujo FG, Remington JS: Effect of clarithromycin and azithromycin on production of cytokines by human monocytes. Int J Antimicrob Agents 1999, 11:121-132

81. Guo W, Ding J, Huang Q, Jerrels T, Deitch EA: Alterations in intestinal bacterial flora modulate the systemic cytokine response to hemorrhagic shock. Am J Physiol 1995, 269:G827-G832

82. Guo W, Magnotti LJ, Ding J, Huang Q, Xu D, Deitch EA: Influence of gut microflora on mesenteric lymph cytokine production in rats with hemorrhagic shock. J Trauma 2002, 52:1178-1185

Figure 1. Representative gross necropsy lesions from cynomolgus monkeys experimentally infected with EBOV-Zaire. **A**, Characteristic petechial rash of the right arm at day 4. **B**, Petechial rash of the inguinal region at day 5. **C**, Mild enlargement and marked congestion/hemorrhage of inguinal lymph nodes at day 4. **D**, Multifocal to coalescing hemorrhages of mucosa of urinary bladder at day 5. **E** and **F**, Progression of marked congestion of the duodenum occurring between day 3 (**E**) and day 5 (**F**). Arrows indicate the gastroduodenal junction demarcating the stomach to the left and the duodenum to the right. The duodenum is markedly congested at day 5 (**F**). **G** and **H**, Progression of congestion of cecum occurring between day 3 (**G**) and day 5 (**H**). The cecum is opened up and the ileum extends outward from the cecum. Arrowheads indicate the ileocecal junction. Note the congested and thickened appearance of the cecum at day 5 (**H**).

Figure 1

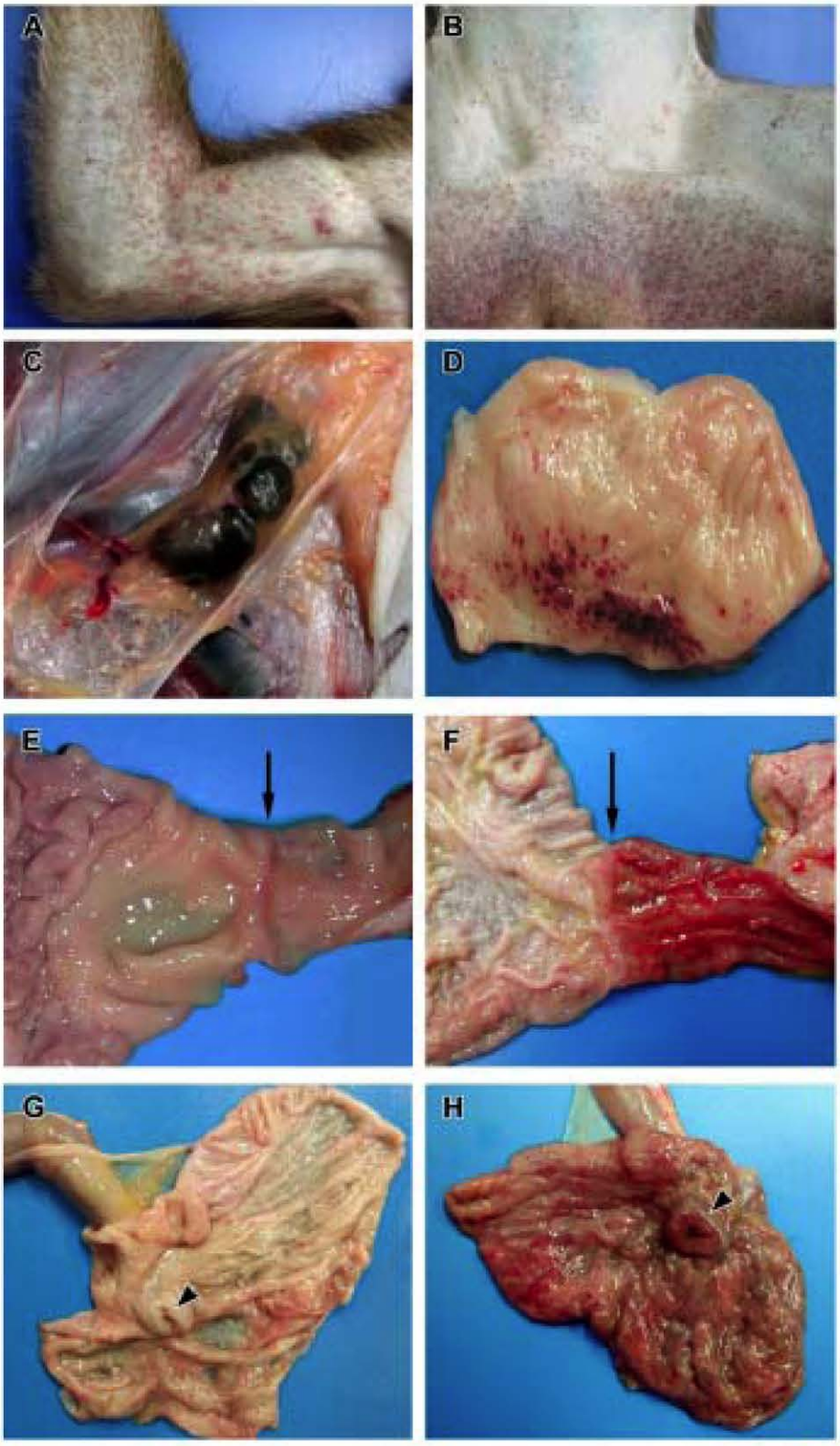

Figure 2. Hematology values after infection of cynomolgus monkeys with EBOV-Zaire. Total white blood cell counts (left panel) and differential white blood cell counts (center panel) show a developing leukocytosis due to an increased neutrophilia. Also, note concomitant lymphopenia. PMN = polymorphonuclear neutrophils; Lymphs = lymphocytes. Right panel, development of thrombocytopenia and D-dimers.

Figure 2

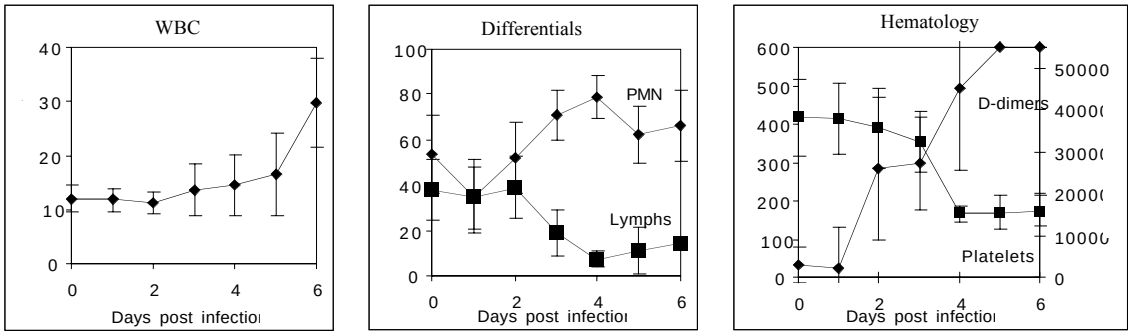
WBC
40
30
20
10
0
0
2
4
6
Days post infectio
Differentials
100
80
60
40
20
0
PMN
Lymphs
0
2
4
6
Days post infectio
Hematology
600
500
400
300
200
100
0
50000
4000(
3000(
2000(
10000
0
D-dimers
Platelets
0
2
4
6
Days post infectio

Figure 3. Flow cytometric analysis of cynomolgus monkey peripheral blood mononuclear cells after EBOV-Zaire infection. Note rapid decline in population of NK cells (blue fraction) by days 3 and 4.

Figure 3

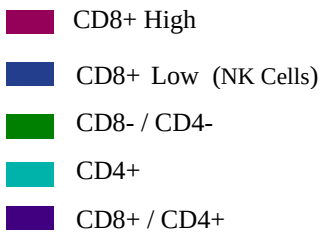

Figure 4. Clinical chemistry values after infection of cynomolgus monkeys with EBOV-Zaire showing elevated levels of serum enzymes primarily at the late stages of disease (days 5 and 6). Left panel, blood urea nitrogen (BUN) and creatinine. Center panel, gamma-glutamyl transferase (GGT) and ALP (alkaline phosphatase). Right panel, alanine aminotransferase (ALT) and aspartate aminotransferase (AST).

Figure 4

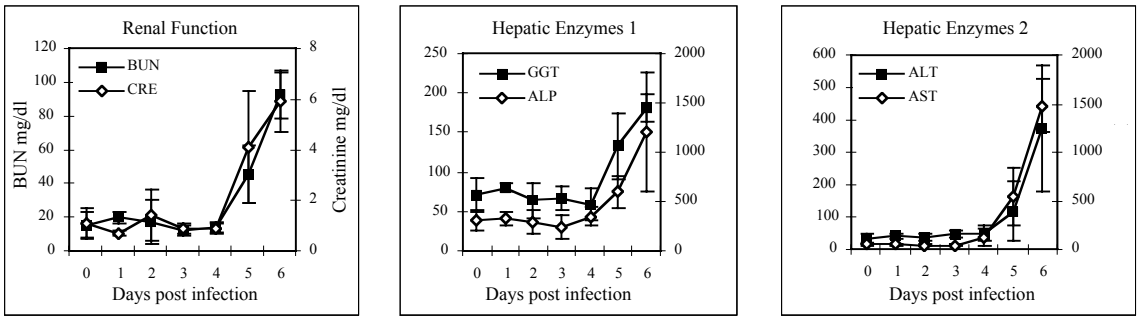
Renal Function
BUN
CRE
BUN mg/dl
Creatinine mg/dl
Days post infection
Hepatic Enzymes 1
GGT
ALP
Days post infection
Hepatic Enzymes 2
ALT
AST
Days post infection

Figure 5. Mean infectivity of cynomolgus monkey plasma and tissue homogenates (10% wt/vol) inoculated with EBOV-Zaire. LN = lymph node.

Figure 5

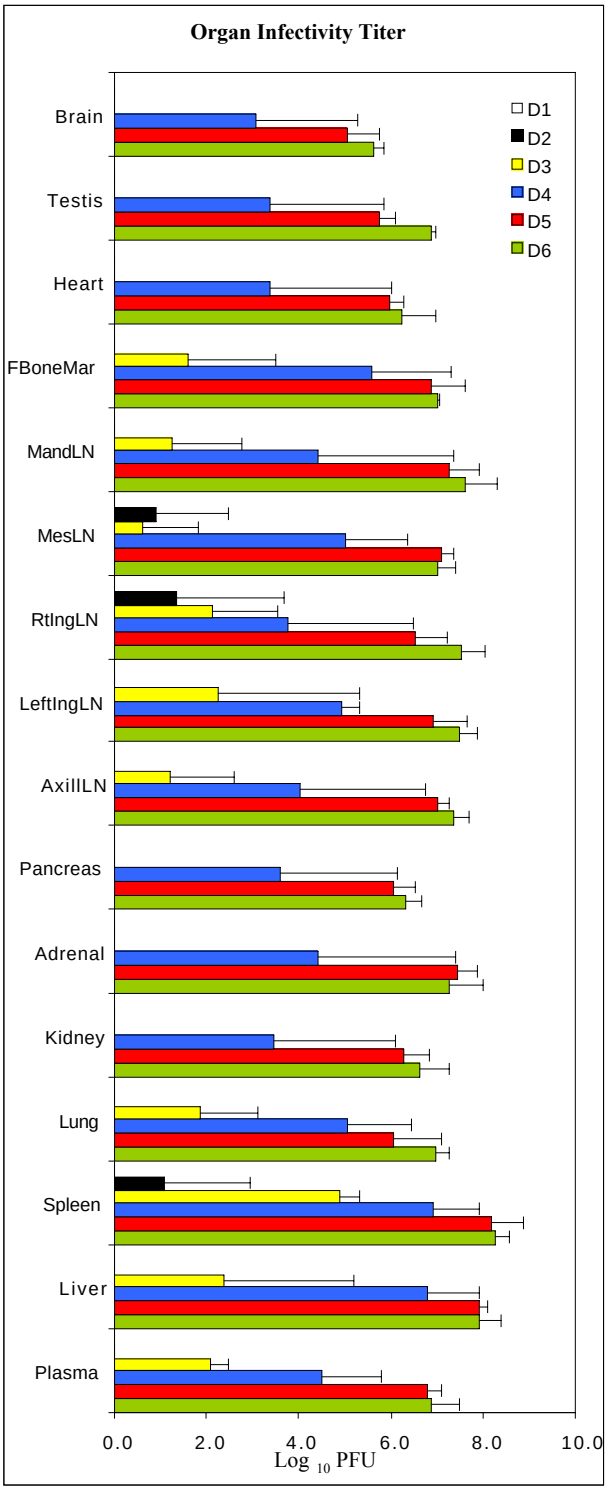
Organ Infectivity Titer
Brain
Testis
Heart
FBoneMar
MandLN
MesLN
RtIngLN
LeftIngLN
AxillLN
Pancreas
Adrenal
Kidney
Lung
Spleen
Liver
Plasma
D1
D2
D3
D4
D5
D6
0.0
2.0
4.0
6.0
8.0
10.0
Log 10 PFU

Figure 6. Analysis of mRNA of cynomolgus monkey peripheral blood mononuclear cells (PBMC) before and after infection with EBOV-Zaire. Representative RNase protection assays are shown. **A**, Chemokines. Comparison of preinfection PBMC (lanes A, D, F, J, M, P, T) with PBMC at postinfection day 1 (lanes B, E, G); day 2 (lanes H, N, R); day 3 (lanes C, I, K, O); day 4 (lanes L, Q); day 5 (lane U); and day 6 (lane S). **B**, IL-6. Comparison of preinfection PBMC (lanes A, D, F, I, L, P, R, T, V, X) with PBMC at postinfection day 1 (lanes B, G); day 2 (lanes C, E, J, M); day 3 (lanes H, K); day 4 (lanes N, Q, S); day 5 (lanes U, W); and day 6 (lanes O, Y). **C**, TNF-α. Comparison of preinfection PBMC (lanes A, C, F, H, K, N, R, T, V, X, Z) with PBMC at postinfection day 1 (lanes B, D, I); day 2 (lanes E, G, L, O); day 3 (lanes J, M); day 4 (lanes P,S,V); day 5 (lanes W,Y); and day 6 (lanes Q, a). **D**, IP-10. Comparison of PBMC at postinfection day 1 (lane A), day 3 (lane B), day 4 (lane C), day 5 (lane D) and day 6 (lane E).

Figure 6

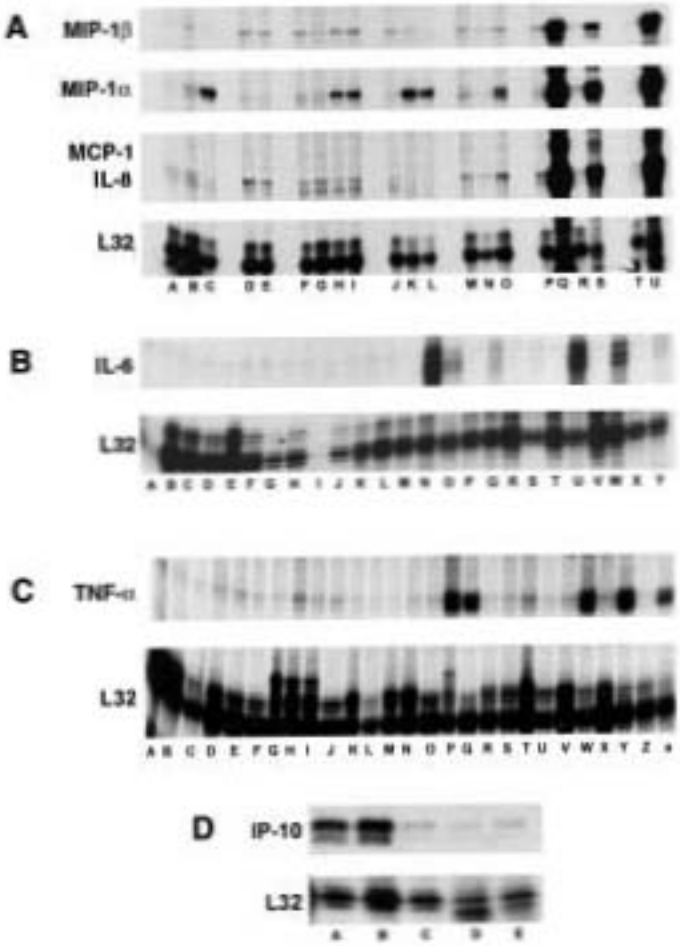

Figure 7. Analysis of cytokine/chemokine and nitrate accumulation in serum/plasma of EBOV-Zaire-infected cynomolgus monkeys.

Figure 7

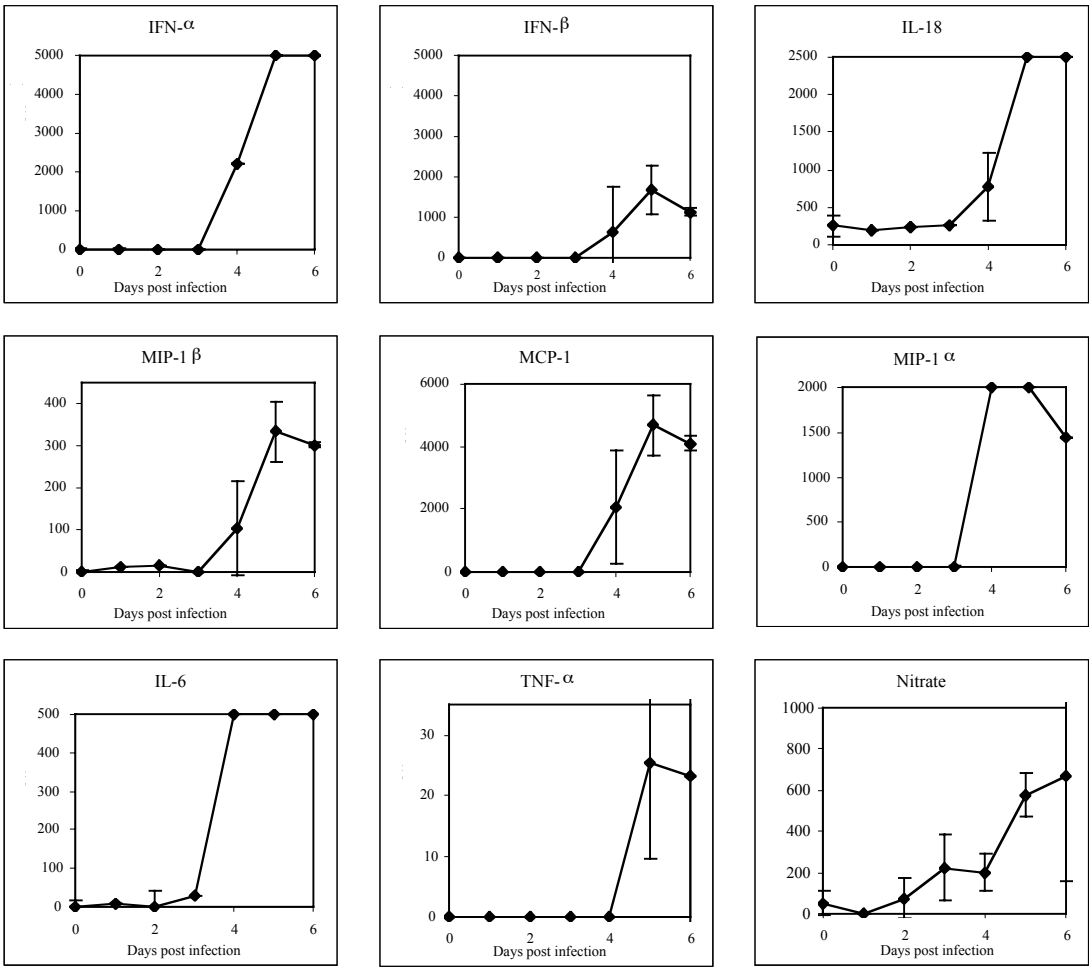
IFN-α
5000
4000
3000
2000
1000
0
0 2 4 6
Days post infection
IFN-β
5000
4000
3000
2000
1000
0
0 2 4 6
Days post infection
IL-18
2500
2000
1500
1000
500
0
0 2 4 6
Days post infection
MIP-1 β
400
300
200
100
0
0 2 4 6
Days post infection
MCP-1
6000
4000
2000
0
0 2 4 6
Days post infection
MIP-1 α
2000
1500
1000
500
0
0 2 4 6
Days post infection
IL-6
500
400
300
200
100
0
0 2 4 6
Days post infection
TNF-α
30
20
10
0
0 2 4 6
Days post infection
Nitrate
1000
800
600
400
200
0
0 2 4 6
Days post infection

Figure 8. Immunofluorescence staining of inguinal lymph nodes of EBOV-Zaire-infected cynomolgus monkeys for cell markers and EBOV. **A**, Double labeling for a macrophage marker (green) and EBOV antigens (red). Areas positive for both macrophage markers and EBOV antigens are stained gold as shown in the single EBOV-positive macrophage at day 3. **B** and **D**, Double labeling for a dendritic cell marker (DC-SIGN) (red) and EBOV antigens (green) showing a circulating EBOV-positive dendritic cell at day 3 (**B**) and large numbers of EBOV-positive dendritic cells (orange/gold) at day 5 (**D**). **C**, Double labeling for a macrophage marker (red) and EBOV antigens (green) demonstrating EBOV-positive macrophages (orange/gold) at day 5. **E**, Double labeling for a dendritic cell marker (DC-SIGN) (green) and EBOV antigens (red) demonstrating EBOV-positive dendritic cell (orange/gold) at day 4. Also, note EBOV-positive cell (red) with macrophage-like morphology and EBOV-negative dendritic cells (green) in this field. **Inset**: high-power view of the EBOV-positive dendritic cell in **E** by confocal microscopy. The nuclei were stained with DAPI (blue) in all panels. Original magnifications: X40 (**A**, **D**); X60 (**B**, **C**, **E**); X300 (**Inset**).

Figure 8

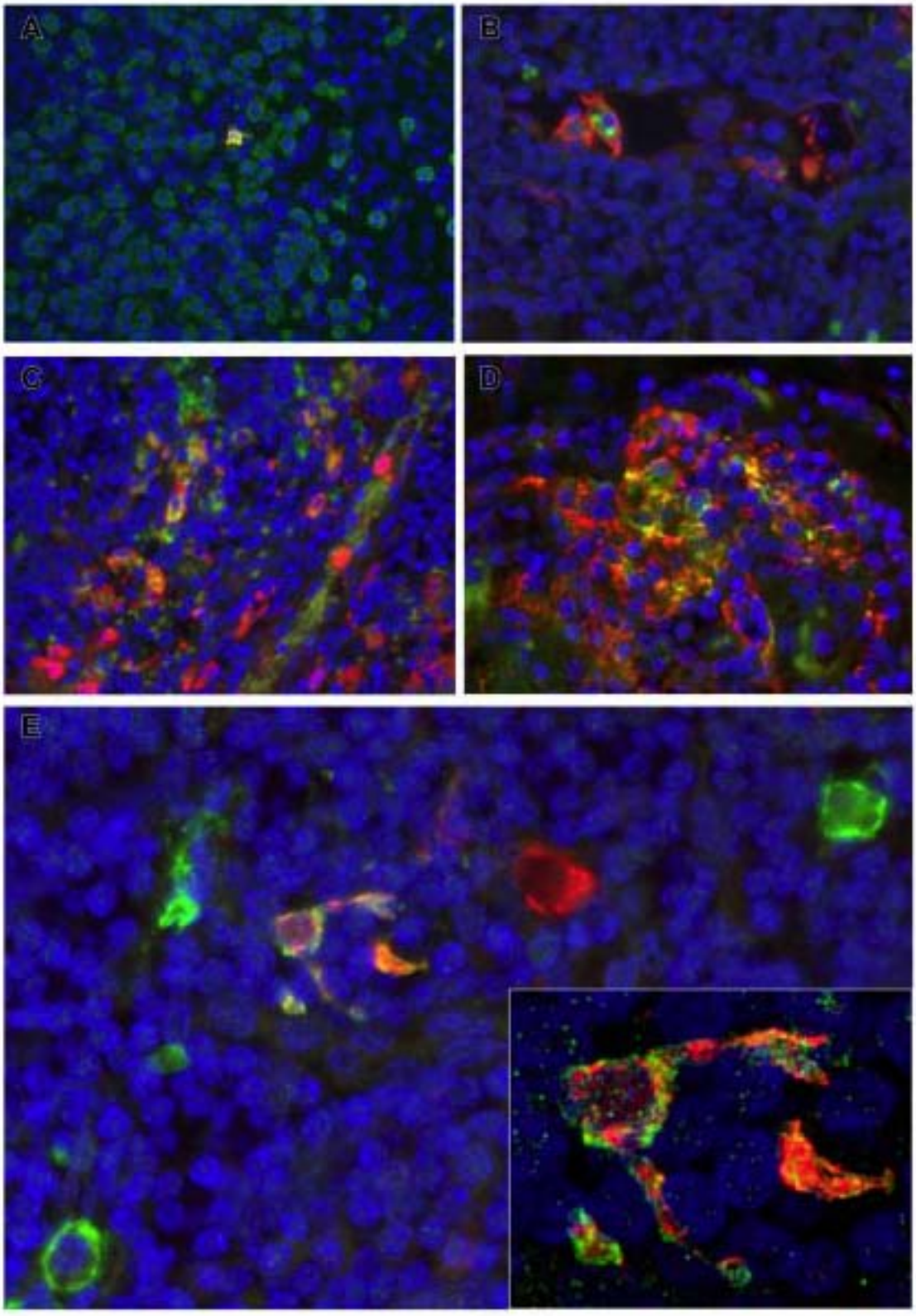

Figure 9. Localization of EBOV in cynomolgus monkey tissues. **A**, Immunopositive mononuclear cells (red) in the medullary sinus of a lymph node at day 3. The brown-pigmented cells are hemosiderin-ladened macrophages. **B**, Immunopositive (red) dendritic cells surrounding a high endothelial venule in a lymph node at day 4. **C**, EBOV RNA-positive circulating monocyte (arrow) in hepatic sinusoid at day 2. **D**, Immunopositive (red) Kupffer cell at day 3. **E**, Histology of liver showing small foci of hepatocellular degeneration and necrosis and foci of pleomorphic eosinophilic intracytoplasmic inclusions (arrows) in hepatocytes at day 5. **F**, Immunopositive Kupffer cells (red) and hepatocytes (red) at day 5. Alkaline phosphatase method: **A**, **B**, **D**, **F**; H&E stain, **E**. Original magnifications: X20 (**A**); X40 (**B**); X60 (**C**, **D**, **E**, **F**).

Figure 9

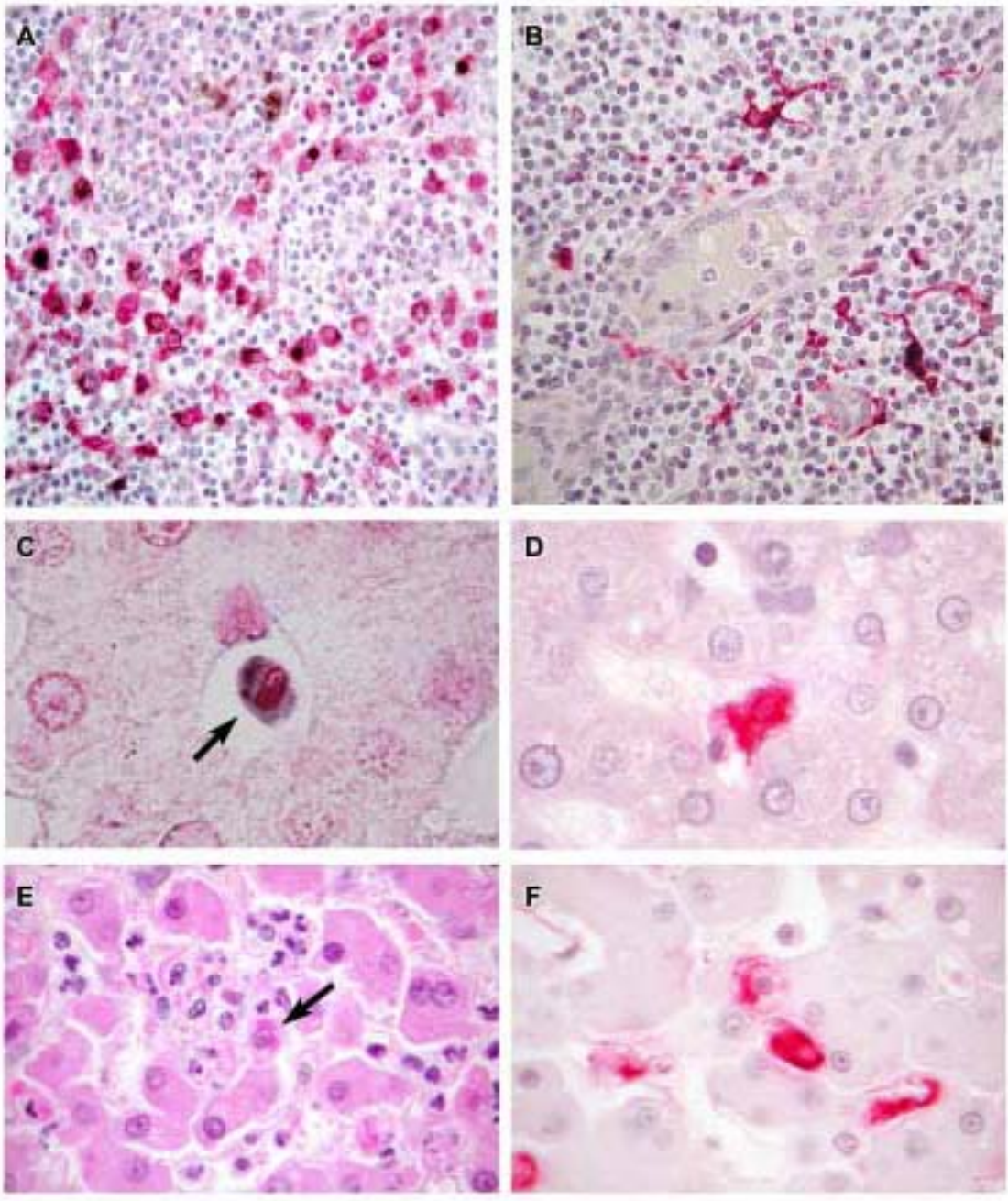

Figure 10. Ultrastuctural appearance of dendritic cells in marginal zone of spleen of EBOV-Zaire-infected cynomolgus monkeys. **A**, EBOV-infected dendritic cell at day 4 with typical branching processes (arrowheads). **Inset**: Enlargement of area marked by arrow in **A** shows virions budding from plasma membrane. **B**, Immunoelectron microscopy showing positive gold sphere (10 nm) labeling of plasma membrane and cytoplasm of EBOV-infected dendritic cell for DC-SIGN at day 3. Note virions budding from plasma membrane (arrowhead) and near absence of gold spheres on adjacent red blood cell (*). **Inset**: Low-power view of EBOV-infected, DC-SIGN-positive pale-staining cell interpreted as an immature dendritic cell. **C**, EBOV-infected pale-staining cell interpreted as an immature dendritic cell at day 3. Morphology is comparable to DC-SIGN positive cell in **Inset**, **B**. Note virions budding from plasma membrane (arrows), pale-staining cytoplasm and sparsity of organelles. Original magnifications: X6,500 (**A**, and **Inset B**); 12,500 (**C**); 16,000 (**Inset A**); X53,000 (**B**).

Figure 10

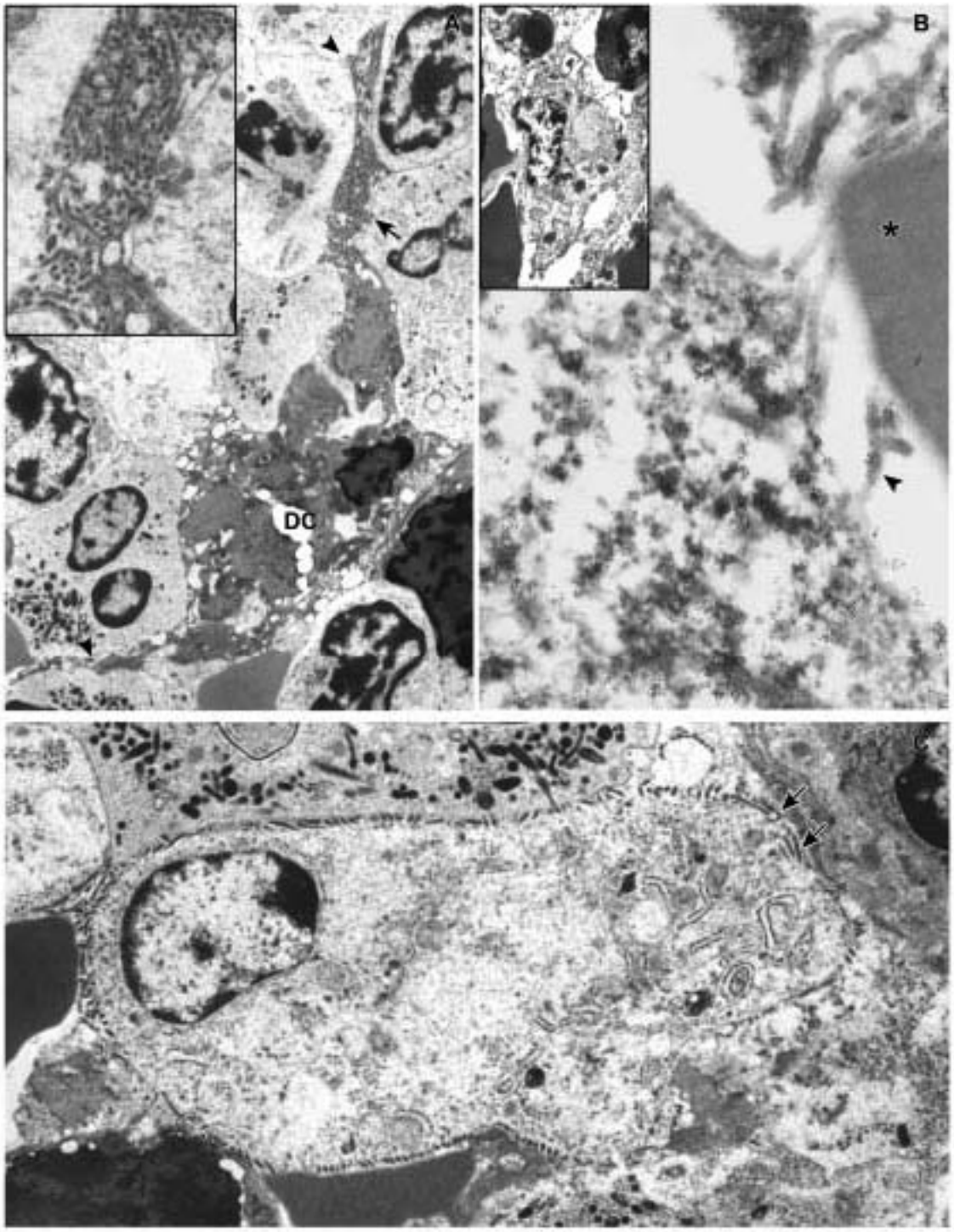

Figure 11. Analysis of peripheral blood mononuclear cells (PBMC) from EBOV-Zaire-infected cynomolgus monkeys for evidence of apoptosis. **A** and **B**, Transmission electron micrographs of peripheral blood mononuclear cells. **A**, Apoptosis of a large lymphocyte (~ 6 x 8 μM in cross-section) morphologically consistent with a NK cell at day 3. Arrowheads indicate cytoplasmic granules. Also, note abundance of mitochondria. **B**, Apoptotic small lymphocyte (arrow) and increased numbers of neutrophils at day 4. **C** and **D**, Analysis of PBMC mRNA; representative RNase protection assays are shown. **C**, Fas and TRAIL, Comparison of preinfection PBMC (lanes A, D, H, K, O, Q, S) with PBMC at postinfection day 1 (lanes B, E); day 2 (lanes F, I, L); day 3 (lanes C, G, J); day 4 (lane M); day 5 (lanes P, R); and day 6 (lanes N,T). **D**, NIAP and cIAP2. Comparison of preinfection PBMC (lanes A-C) with PBMC at postinfection day 1 (lanes D-F); day 2 (lanes G-I); day 3 (lanes J-L); day 4 (lanes M-O); day 5 (lanes P-R); and day 6 (lanes S,T). **E** and **F**, Analyses by TUNEL assay showing apoptotic mononuclear cells (black reaction product) within the lumen of a central hepatic vein and to the periphery of the vein at day 3 (**E**). Arrow in the inset points to an unaffected neutrophil and the arrowhead demonstrates the apoptotic lymphocyte. At day 4, follicles in a lymph node contain macrophages and dendritiform cells that have engulfed apoptotic bodies (**F**); single-strand breaks appear blue/black. Original magnifications: X20 (**E**, **F**); X6,500 (**B**); X16,000 (**A**).

Figure 11

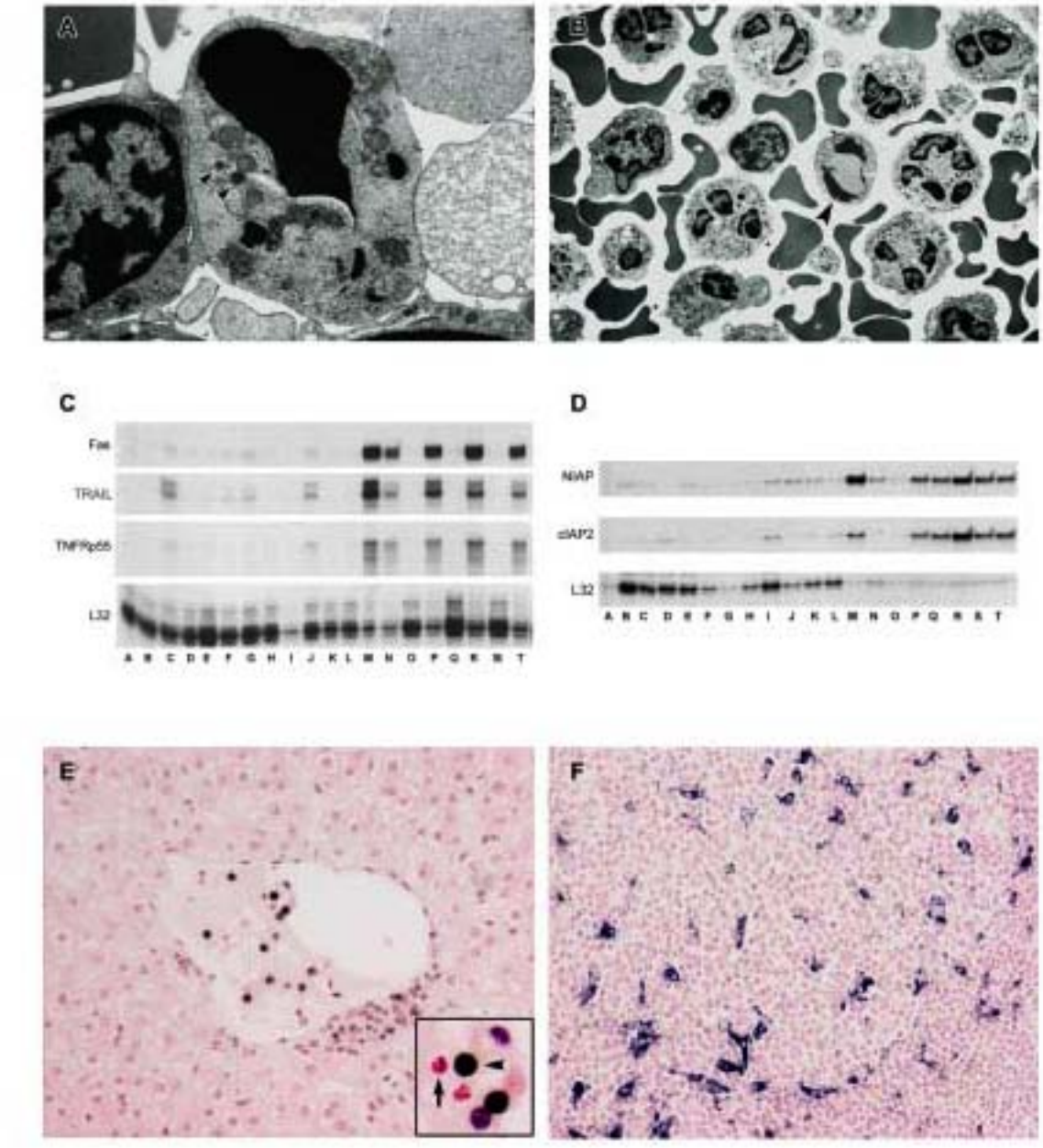

Pathogenesis of Ebola Hemorrhagic Fever in Primate Models: Evidence that Hemorrhage Is Not a Direct Effect of Virus-Induced Cytolysis of Endothelial Cells

Thomas W. Geisbert,[*, ‡] Howard A. Young,[†] Peter B. Jahrling,[*] Kelly J. Davis,[*] Tom Larsen,[*] Elliott Kagan,[‡] and Lisa E. Hensley[*]

From the United States Army Medical Institute of Infectious Diseases,[*] Fort Detrick, Maryland; Laboratory of Experimental Immunology, Center for Cancer Research, NCI-Frederick,[†] Frederick, MD; and the Uniformed Services University of the Health Sciences,[‡] Bethesda, MD

Corresponding author:

Thomas W. Geisbert
USAMRIID
Attn: MCMR-UIV
1425 Porter Street
Fort Detrick, MD 21702-5011

E-mail: tom.geisbert@amedd.army.mil
Phone: 301-619-4803
Fax: 301-619-4627

Abstract

Ebola virus (EBOV) infection causes a severe and often fatal hemorrhagic disease in humans and nonhuman primates. Whether infection of endothelial cells is central to the pathogenesis of EBOV hemorrhagic fever (HF) remains unknown. To clarify the role of endothelial cells in EBOV HF, we examined tissues of 21 EBOV-infected cynomolgus monkeys over time, and also evaluated EBOV infection of primary human umbilical vein endothelial cells (HUVEC) and primary human lung-derived microvascular endothelial cells (HMVEC-L) *in vitro*. Results showed that endothelial cells were not early cellular targets of EBOV *in vivo*, as viral replication was not consistently observed until day 5 postinfection, a full day after the onset of disseminated intravascular coagulation. Moreover, the endothelium remained relatively intact even at terminal stages of disease. While HUVEC and HMVEC-L were highly permissive to EBOV replication, significant cytopathic effects were not observed. Analysis of host cell gene response at 24-144 hours postinfection showed some evidence of endothelial cell activation, but changes were unremarkable considering the extent of viral replication. Together, these data suggest that coagulation abnormalities associated with EBOV HF are not the direct result of EBOV-induced cytolysis of endothelial cells, and are likely triggered by immune-mediated mechanisms.

Introduction

Ebola hemorrhagic fever is characterized by hypotension, generalized fluid distribution problems, lymphopenia, coagulative disorders, and hemorrhages. Disseminated intravascular coagulation (DIC) is a prominent manifestation of Ebola virus (EBOV) infection. DIC is a syndrome characterized by coagulation abnormalities including systemic intravascular activation of coagulation leading to widespread deposition of fibrin in the circulation, which contributes to the multiple organ failure and high mortality rates characteristic of EBOV infections. The mechanisms by which EBOV causes multisystemic disease are only partially understood. While viral replication in target tissues is clearly a factor, various strategies that restrict replication of EBOV have, at best, only delayed onset of lethal disease.[1-3] Recent studies suggested that the EBOV glycoprotein (GP) is the main determinant of vascular cell injury and consequently direct EBOV replication-induced structural damage of endothelial cells triggers the hemorrhagic diathesis.[4,5] This hypothesis has not been rigorously tested *in vitro* or *in vivo*.

Viral infections can exert changes in the vascular endothelium in a variety of ways, such as inducing endothelial cell activation indirectly by infecting and activating leukocytes and triggering the synthesis and local production of proinflammatory soluble factors or by directly inducing changes in endothelial cell expression of cytokines, chemokines, and cellular adhesion molecules in the absence of immune mediators (as a direct result of viral infection). Mediators released from activated endothelial cells that can modulate vascular tone, thrombosis, and/or inflammation include nitric oxide, prostacyclin,

interferons, IL-1, IL-6, and chemokines such as IL-8.[6,7] Few studies have evaluated the host gene response of endothelial cells infected with EBOV; Harcourt et al. reported that EBOV inhibits the induction of genes by double-stranded RNA in endothelial cells.[8]

Despite over 1,000 known fatal cases of EBOV infection, little has been learned from necropsies regarding the role of the endothelium in disease pathogenesis, as only a very limited number of tissues from a handful of cases in 1976 and 1996 have been examined.[9-11] EBOV infection of endothelial cells in post mortem tissues was demonstrated in one of these studies.[11] By comparison, EBOV infection of endothelial cells has been well documented in nonhuman primates.[12-16] However, with few exceptions, these investigations examined monkeys killed when moribund and shed little light on the pathogenesis of EBOV infection during times before death.

The specific goals of this study were: (1) to determine whether or not EBOV infection directly induces the activation and/or cytolysis of human endothelial cells *in vitro* and; (2) to determine the course of EBOV infection and detectable cytopathic disruption of endothelium in nonhuman primates, specifically, to determine whether or not EBOV infection of endothelial cells is an early event or a terminal event in the disease course relative to the first signs of any disruption/degeneration of the endothelium and/or evidence of DIC. The importance of this study is that it cannot be concluded that EBOV-induced damage to the endothelium is due exclusively to immune-mediated mechanisms without first examining the direct effects of EBOV infection on endothelial cell integrity

and vascular permeability. It is possible that EBOV mediates disruption of endothelia via an indirect route rather than only by direct infection of endothelial cells.

Materials and Methods

Cells and Viruses

Normal primary human umbilical vein endothelial cells (HUVEC) and primary human lung-derived microvascular endothelial cells (HMVEC-L) were obtained from Clonetics, Inc. (San Diego, CA), and maintained in endothelial cell growth medium (EGM; Clonetics), which was supplemented with human recombinant epidermal growth factor, hydrocortisone, fetal bovine serum, gentamicin, and bovine brain extract (Clonetics). HUVEC and HMVEC-L were maintained according to the supplier's recommendations. Viability was estimated by the trypan-blue exclusion procedure and was greater than 99% in all preparations. Experimental infection conditions consisted of 2.5 $x10^5$ HUVEC or HMVEC-L in segregated cultures. Cells were infected at a multiplicity of infection of 1.0 with EBOV that was originally obtained from a fatally infected human from the former Zaire in 1995.[2] After adsorption of virus for 1 hour at 37°C, cultures were washed twice with PBS, re-fed with fresh EGM, and incubated for various times at 37°C. Additional cultures of HUVEC and HMVEC-L were challenged with an equivalent dose of inactivated EBOV (i.e., virus inactivated by exposure to 6 million rads from a ^{60}Co source). Culture medium from Vero cells represented a "virus-free stock" in all mock infection experiments. Virus titration by plaque assay on Vero cells was performed as previously described.[17]

Animals and Inoculations

Healthy, filovirus-seronegative, adult male cynomolgus (*Macaca fascicularis*) macaques (n = 21, 4 to 6.5 kg) were used for these studies. The complete clinical and histopathological details of these animals are described in a companion paper.[18] Briefly, animals were inoculated i.m. with 1 ml of viral stock that contained 1,000 plaque-forming units (PFU) of EBOV-Zaire (1995 isolate). Scheduled necropsies were performed at 1 (n = 3), 2 (n = 3), 3 (n = 4), 4 (n = 4), 5 (n = 4), and 6 (n = 3) days postinfection.

Serum Albumin and Total Protein

Concentrations of serum albumin and total protein were measured using a Piccolo Point-Of-Care Blood Analyzer (Abaxis, Sunnyvale, CA).

Histology

Formalin-fixed tissues for histology and *in situ* hybridization were processed and embedded in paraffin according to conventional methods.[19] Histology sections were cut at 5 to 6 µm on a rotary microtome, mounted on glass slides, and stained with hemotoxylin and eosin. Replicate sections of all tissues were mounted on positively charged glass slides (Superfrost Plus, Fisher Scientific, Pittsburgh, PA) and immunohistochemically stained for detection of viral antigen by an immunoperoxidase (IPO) method according to kit procedures (Envision System, DAKO Corporation, Carpinteria, CA), or by a fluorescence-based method.

Immunohistochemistry

Immunoenzymatic methodology. Sections were deparaffinized and rehydrated through a series of graded ethanols, pretreated with DAKO Ready to Use Proteinase K (DAKO) for 6 minutes at room temperature, and blocked with DAKO's Serum Free Protein Block for 20 minutes before exposure to antibody. Tissue sections were incubated with primary antibody overnight a 4°C using an anti-EBOV rabbit polyclonal (kindly provided by Cindy Rossi) (1:500) or an equal mixture of mouse monoclonal antibodies to EBOV GP and VP40 (1:5000).[14] An alkaline phosphatase-labeled polymer (DAKO Envision® System, Alkaline phosphatase) was added for 30 minutes and color development was achieved by exposing tissue to the substrate 6-bromo-2-hydroxyl-3-naphtholic acid (Histomark Red®, Kirkegaard and Perry, Gaithersburg, MD) for 50 minutes in the dark. Sections were counterstained with hematoxylin. Negative controls included replicate sections exposed to anti-Marburg virus antibodies and unexposed cynomolgus monkey tissue; archived EBOV-infected cynomolgus tissue served as positive controls.

Immunofluorescence methodology. Tissue sections were deparaffinized, rehydrated, and incubated in 20 μg/ml of proteinase K for 30 minutes at room temperature. Sections were subsequently rinsed, placed in normal goat serum for 20 minutes and transferred to a mixture of the anti-EBOV antibodies as described above for 30 minutes at room temperature. After incubation, sections were rinsed and stained with goat anti-mouse alexa 594 (Molecular Probes, Eugene OR), incubated with a pan T cell marker, CD3 (DAKO), for 30 minutes at room temperature, rinsed, and incubated in goat anti-mouse alexa 488 (Molecular Probes).

For localization of EBOV antigens in endothelial cells, double stains using a marker for endothelial cells and a pool of anti-EBOV antibodies was employed. Briefly, tissue sections were pretreated with proteinase K (20 μg/ml) for 30 minutes at room temperature and incubated in normal goat serum for 20 minutes. Sections were then incubated in a rabbit polyclonal antibody for von Willebrand's factor (DAKO) for 30 minutes at room temperature. After incubation, sections were placed in goat anti-rabbit alexa 488 (Molecular Probes) for 30 minutes at room temperature, rinsed, and incubated in a mixture of the anti-EBOV antibodies described above. Sections were rinsed and incubated in goat anti-mouse alexa 594 (Molecular Probes) for 30 minutes at room temperature. After rinsing in PBS, sections were mounted in an aqueous mounting medium containing 4',6'-diamidino-2-phenylindole (DAPI) (Vector Laboratories, Burlingame, CA) and examined with a Nikon E600 fluorescence microscope (Nikon Instech Co., Ltd., Kanagawa, Japan).

In vitro staining for cell adhesion molecules was performed on acetone-fixed, gamma-irradiated (6 million rads from a ^{60}Co source) endothelial cells grown on coverslips. Briefly, coverlips were rehydrated, incubated in normal goat serum for 20 minutes, transferred to either a murine monoclonal antibody for intercellular adhesion molecule-1 (ICAM-1) or vascular cell adhesion molecule-1 (VCAM-1) (Pharmingen, San Diego, CA), rinsed, and incubated in alexa 594 (Molecular Probes) as described above.

In Situ Hybridization

EBOV GP and VP40 RNA were localized in tissues using digoxigenin-labeled DNA probes. Probe constructs were plasmids (pCR2.1, Invitrogen, San Diego, CA) containing complementary DNA sequences for EBOV GP or VP40. Probes were labeled by nick translation with digoxigenin-11-UTP (Boehringer Mannheim, Indianapolis, IN) according to the manufacturer's recommendations. Before hybridization, tissue sections were incubated with 40 μg/ml of nuclease-free proteinase K (Boehringer Mannheim) in Tris-buffered saline, pH 7.6, for 30 minutes at 37ºC. For hybridization, probes were denatured at 95ºC for 5 minutes, placed on ice, and then applied to tissue sections and incubated overnight at 42ºC. After hybridization, sections were washed in buffer, and incubated in alkaline phophatase-conjugated, antidigoxigenin antibody (Boehringer Mannheim), diluted 1:600, for 1 hour at 37ºC. Sections were washed and the color was developed with 5-bromo-4-chloro-3-indolyl phosphate (NBT/BCIP, Life Technologies, Gaithersburg, MD) as the substrate and nitro blue tetrazolium salt (NBT) as the chromagen for 1 hour at 37ºC. Sections were counterstained with nuclear fast red (Vector Laboratories). Tissue sections incubated in the pCR2.1 plasmid lacking the EBOV gene inserts served as negative controls.

Electron Microscopy

HUVEC and HMVEC-L were processed by conventional methods for transmission electron microscopy (TEM) as previously described for cultured cells.[20] Also, portions of liver, spleen, lung, kidney, adrenal gland, skin, and mesenteric, axillary, and inguinal lymph nodes from EBOV-infected monkeys were immersion-fixed in 4%

paraformaldehyde + 1% glutaraldehyde in 0.1 M Millonig's phosphate buffer (pH 7.4) and processed for TEM as previously described.[14,15] Briefly, tissues and cultured cells were postfixed in 1% osmium tetroxide in 0.1 mol/L Millonig's phosphate buffer, rinsed, stained with 0.5% uranyl acetate in ethanol, dehydrated in graded ethanol and propylene oxide, and embedded in Poly/Bed 812 resin (Polysciences, Warrington, PA). Areas to be examined by TEM were selected from 1-μm sections stained with toluidine blue. Ultrathin sections were cut, placed on 200-mesh copper electron microscopy grids, stained with uranyl acetate and lead citrate, and examined using a JEOL 1200 EX transmission electron microscope (JEOL Ltd., Peabody, MA) at 80 kV.

HUVEC and HMVEC-L were also processed by conventional methods for scanning electron microscopy (SEM). Briefly, cells grown on coverslips were treated with 4% paraformaldehyde + 1% glutaraldehyde in 0.1 M Millonig's phosphate buffer (pH 7.4) for 2 hours. The specimens were postfixed in 1% osmium tetroxide, rinsed, dehydrated in ethanol, dried by the critical point method in liquid carbon dioxide, and mounted on aluminum SEM stubs with silver paint. Samples were viewed in a Hitachi S-4500 scanning electron microscope (Nissei Sangyo America Ltd., Gaithersburg, MD).

Cytokine/chemokine and Prostacyclin Production

Cytokine/chemokine levels in HUVEC or HMVEC-L cultures were assayed using commercially available ELISA kits according to the manufacturer's directions. Cytokines/chemokines assayed included IFN-α, IL-6, and RANTES (BioSource International, Inc., Camarillo, CA); and IL-8 and IFN-β (R & D Systems, Minneapolis,

MN). Prostacyclin levels were determined by measuring its stable metabolite 6-keto-prostaglandin $F_{1\alpha}$ by ELISA (R & D Systems).

RNAse Protection Assays

Total RNA was extracted from infected/treated HUVEC and HMVEC-L by using Trizol (Life Technologies, Gaithersburg MD) and was stored at -70°C until RNA isolations could be performed. Probe sets were obtained from Pharmingen. The Multiprobe RNAse Protection assay was performed according to the manufacturer's directions (Pharmingen) with minor modifications.[18]

Results

Susceptibility of Primary Human Endothelial Cells to Ebola Virus

Vascular endothelia are remarkably heterogeneous in terms of morphology, marker expression, and function. In order to determine the susceptibility of macrovascular and microvascular endothelial cells to EBOV, cultures of HUVEC and HMVEC-L were inoculated with EBOV and analyzed for production of infectious virus and also evaluated for virus-induced cytopathic effects. Viral infectivity titration showed production of approximately 6 log10 PFU/ml of infectious EBOV in both HUVEC and HMVEC-L by day 6 postinfection (Figure 1). At day 4, few ultrastructural differences were noted between EBOV-infected cells and mock-infected control cultures with the exception of the characteristic EBOV inclusion material and budding virions, which were striking features (Figure 2). Surprisingly, we detected little cytopathic effect by inverted phase microscopy at day 4. By day 6, mild cytopathic effects were observed including swelling

of some EBOV-infected cells with detachment infrequently detected in some areas (Figure 3). Ultrastructural evaluation at day 6 showed that nearly all cells in the EBOV-infected cultures contained characteristic EBOV inclusion material and/or budding virions (Figure 4B); occasional EBOV-infected cells showed morphological evidence of necrosis (Figure 4C). Ultrastructural evidence of apoptosis was not detected in any of the cultures examined.

Transcriptional Responses of Endothelial Cells to Ebola Virus Infection

As a first step to determine whether EBOV infection induces activation of endothelial cells, we examined mRNA levels of selected genes and compared transcriptional responses of EBOV-infected cells to mock-infected endothelial cell controls and to cultures inoculated with EBOV inactivated by exposure to gamma rays. Analysis of total RNA from EBOV-infected HUVEC revealed increased mRNA transcripts for cyclooxygenase (COX)-2 (Figure 5A), inducible nitric oxide synthase (iNOS) (Figure 5A), IL-6 (Figure 6A), IL-8 (Figure 6A), ICAM-1 (Figure 7A), and monocyte chemotactic protein-1 (MCP-1) (Figure 6A) by 1 hour. At 24 hours, increased levels of mRNA transcripts for IFN-β and regulated on activation normal T cell expressed and secreted (RANTES) (Figure 6A) were detected in EBOV-infected HUVEC, while increased transcripts for cellular inhibitor of apoptosis protein (cIAP)-2 (Figure 7B), growth-related oncongene (Gro)-α, IL-1α (Figure 6A), I-309, and macrophage inflammatory protein (MIP)-3β were observed by 96 hours. While mRNA levels for these transcripts were sustained through the course of the infection, transient increases were noted for other mRNA transcripts. Specifically, transcripts for VCAM-1 were

increased from 1 hour through 24 hours and then returned to baseline levels; transcripts for tissue factor and lipoxygenase were elevated at 1 hour only; transcripts for IFN-γ-inducible protein 10 (IP-10) and TNF-related apoptosis-inducing ligand (TRAIL) were increased only at 24 hours. A transient increase in transcripts for COX-1 was detected at 1 hour; transcripts returned to baseline levels by 24 hours, and were substantially decreased by day 6 (Figure 5A).

For EBOV-infected HMVEC-L, increased mRNA transcripts for RANTES (Figure 6B) and TRAIL were detected by 24 hours, while increased levels of transcripts for COX-2 and IL-8 were noted at 48 hours (Figure 5B) and transcripts for IL-1α were elevated by 96 hours (Figure 6B); VCAM-1 transcripts were downregulated by 2 hours (Figure 7A). Changes in mRNA transcripts for cIAP2, COX-1, Gro-α, ICAM-1, IL-6, IFN-β, iNOS, IP-10, I-309, lipoxygenase, MCP-1, and MIP-3β, which were detected in EBOV-infected HUVEC, were not observed in EBOV-infected HMVEC-L. In most cases, it appeared that EBOV replication was required to induce changes in levels of mRNA transcripts for the endothelial cell cultures; the only changes noted when cultures were treated with inactivated EBOV was an increase in COX-2 and MCP-1 transcripts detected in HUVEC. Changes in levels of transcripts for IL-1β, IL-4, IL-12, IFNγ, leukotriene A4, leukotriene B4, MIP-1α, MIP-1β, P-Selectin, TGFβ1, TGFβ2, TGFβ3, TNFα, TNFβ, bcl-2, caspase 3, caspase 8, endothelial nitric oxide synthase (eNOS), decoy receptor (DCR)-1, DCR2, death receptor (DR)-3, DR4, DR5, Fas, FasL, TNFRp55, TNF receptor type 1-associated death domain (TRADD), receptor interacting protein (RIP), TNF receptor-associated factor (TRAF)-1, TRAF2, TRAF3, TRAF4, testosterone-repressed prostate message-2

(TRPM2), cIAP1, neuronal apoptosis inhibitory protein (NAIP), and X-linked inhibitor of apoptosis protein (XIAP) were not detected in any of the endothelial cell cultures.

Cytokine/Chemokine and Prostacyclin Expression in EBOV-Infected Endothelial Cells

Levels of cytokines/chemokines and prostacyclin were determined at regular intervals after inoculation of endothelial cell cultures to confirm transcriptional responses and to further investigate the temporal response of endothelial cells to EBOV infection. Analysis of fluids from EBOV-infected HUVEC showed increased levels of IFN-β, IL-6, IL-8, RANTES, and 6-keto-prostaglandin $F_{1\alpha}$ (as a measure of prostacyclin) (Figure 8), while elevated levels of IL-8, RANTES, and 6-keto-prostaglandin $F_{1\alpha}$ were detected in EBOV-infected HMVEC-L (Figure 8). Results were recorded as positive if OD values were greater than twice the OD of the mock-infected controls. Increased levels of IL-6 were initially detected at 24 hours in EBOV-infected HUVEC. The accumulated levels rose sharply at day 4 (>12,000 pg/ml) and were maintained through 6 days. Elevated levels of IL-6 were not detected in EBOV-infected HMVEC-L. By 48 hours, increased levels of IFN-α, RANTES, and prostacyclin were observed in EBOV-infected HUVEC. Accumulated levels of RANTES markedly increased at day 4 (> 16,000 pg/ml) and were sustained through day 6, while levels of IFN-α and prostacyclin continued to increase from 48 hours through day 6. Increased levels of IFN-α were not detected in HMVEC-L. Detectable levels of RANTES were first seen at day 4 in EBOV-infected HMVEC-L and increased through day 6, while accumulated levels of prostacylin were only noted at day 6. Constitutive expression of IL-8 was high (> 1000 pg/ml) for HUVEC and HMVEC-L. EBOV infection induced two- to threefold increases in the levels of IL-8 at days 4 and 6

in these cultures. Increases in accumulated levels of IFN-α were not detected in any of the endothelial cell cultures. Likewise, EBOV rendered noninfectious by treatment with gamma rays failed to induce increased production of cytokines/chemokines or prostacyclin in any of these cultures.

Effects of EBOV Infection on CAM Protein Expression

Although some changes in the levels of mRNA transcripts were observed for cell adhesion molecules in EBOV-infected HUVEC and HMVEC-L, we were unable to demonstrate substantial changes in protein expression of ICAM-1 or VCAM-1 by immunofluorescence staining of formalin-fixed cells.

Effects of EBOV Infection on Levels of Total Serum Proteins and Albumin

We evaluated levels of total serum proteins and albumin in EBOV-infected monkeys as an indicator of the impairment of endothelial barrier integrity and increased endothelial permeability to macromolecules. Total serum proteins did not fluctuate during the course of EBOV infection; however, decreases in serum albumin levels were seen by day 4 indicating a loss of only small molecular weight proteins (Figure 9).

Evaluation of Endothelial Cell Infection and Cytopathology In Vivo

We evaluated tissues longitudinally collected from 21 EBOV-infected cynomolgus monkeys by immunohistochemistry, *in situ* hybridization, and electron microscopy in order to determine whether EBOV infection of endothelial cells is an early event or a terminal event in the disease course relative the first signs of any morphological

disruption of the endothelium or evidence of DIC. Endothelial cell immunoreactivity was not detected in any tissue of any animal until day 4, and even by this time was only an infrequent observation. At day 4, EBOV antigen was very rarely seen in endothelial-like cells lining hepatic and adrenal cortical sinusoids (3/4 animals). Also, single endothelial cells lining high endothelial venules in the tonsil contained EBOV antigen in one monkey.

By day 5, EBOV RNA and antigen-positive endothelial cells had increased in number and distribution but were still eclipsed in magnitude by the overwhelming numbers of immunoreactive monocytes, macrophages and dendritic cells (Figure 10A). Immunostaining for von Willebrand's factor, as a marker for endothelial cells, and EBOV antigens, confirmed that endothelial cells were an infrequent target of EBOV infection (Figure 10B-D), and also demonstrated the structural intactness of the endothelium. When observed, immunoreactive endothelial cells were most apparent lining high endothelial venules in lymph nodes (4/4), tonsils (4/4), and gut-associated lymphoid tissue (4/4). Multiple foci of RNA- and antigen-positive endothelial cells were seen in thymus (2/4) and heart (1/4), while immunoreactive endothelial cells were infrequently observed in spleen (4/4); superficial lamina propria of tongue, nares, lip, and larynx (4/4); lamina propria of intestines (4/4); large blood vessels of mediastinum (4/4); renal capillaries (4/4); testes, epididymus and prostate (4/4); skeletal muscle (3/4); brachial plexus (3/4) (Figure 10E); aleveolar capillaries (2/4); capillaries and venules in the brain (1/4); and capillaries and venules of the conjunctiva (1/4). At day 6, an increase in the

number of EBOV-positive endothelial cells was noted with a distribution paralleling that shown above at day 5 (3/3).

Ultrastructural changes in endothelia were not detected until day 4 when nonviral tubuloreticular inclusions (TRI), identical to TRI previously described in moribund EBOV-infected monkeys,[13] were observed in occasional endothelial cells in lymphoid tissues (3/4). Infrequent fields in lymphoid tissues also contained endothelial cells that showed morphological evidence of activation (Figure 11A and B), e.g., abnormal adhesion to platelets, vacuolization of cytoplasm, increased numbers of intracytoplasmic granules, increased presence of cytoplasmic projections and membrane blebbing, and increased cell thickness.

Evidence of EBOV replication in endothelial cells was not detected by electron microscopy until day 5 when rare endothelial cells lining hepatic sinusoids in two of four monkeys contained characteristic EBOV intracytoplasmic inclusions.[20] Nonetheless evidence suggestive of DIC, as demonstrated by intravascular fibrin deposits and adherence of platelets to vascular endothelium was detected as early as day 4 (3/4) (Figure 11A) in lymphoid tissues and in hepatic sinusoids; perivascular edema was also evident in occasional foci of lymphoid tissues at day 4. At day 5, extensive intravascular and extravascular deposits of fibrin and fibrinocellular debris were detected in all lymphoid tissues (Figure 11C) and in hepatic sinusoids (4/4). Foci of endothelial cells in lymphoid tissues showing morphological evidence of activation were more numerous than at day 4. Extravasation of red blood cells was sporadically detected in areas where

vessels were obstructed by fibrin thrombi; perivascular edema was evident in these foci and small numbers of macrophages showing evidence of erythrophagocytosis were noted. Also at day 5, higher numbers of endothelial cells containing nonviral TRI were detected in lymphoid tissues. It is worthy to note that these nonviral TRI were not seen in the EBOV-infected endothelial cells *in vitro* nor was there any association between EBOV inclusions and nonviral TRI *in vivo*; nonviral TRI were detected in cells with EBOV inclusions and in cells with no morphological evidence of EBOV infection. By day 6, EBOV inclusions were occasionally seen in hepatic sinusoidal endothelial lining cells (3/3) and in high endothelial venules of lymph nodes (3/3). In addition to ultrastructural findings described for day 5, partial detachment of endothelial cells from basement membrane and disruption of basement membrane were infrequent findings in lymphoid tissues at day 6 (3/3). Frank disruption of endothelial integrity was occasionally noted in hepatic sinusoids of all three animals. No morphological evidence of apoptosis was detected in endothelial cells of any tissues of any animal examined at any time point.

Discussion

Dysregulation of endothelial cell functions can cause a wide range of vascular effects that lead to changes in vascular permeability or hemorrhage.[21,22] Vascular damage can be induced by immunologic mechanisms and/or by direct infection of the vascular tissue. Several microbial diseases are characterized by severe vascular lesions attributed to direct microbial replication-induced damage to endothelial cells. For example, intracellular replication of *Rickettsia rickettsii*, the etiologic agent of Rocky Mountain spotted fever, directly induces lethal injury to host endothelial cells causing pathophysiological changes

including thrombosis, hemorrhage, and vasculitis.[23,24] Another example is Nipah virus infection, where a systemic vasculitis with extensive thrombosis was attributed to infection, damage and necrosis of endothelial cells.[25] The etiology of the hemorrhagic diatheses in fatal cases caused by the filoviruses, Marburg virus and EBOV, was searched for in tissues from initial outbreaks in 1967 and 1976, but no vascular lesions were identified.[10] Nonetheless, there has been much speculation that EBOV replication-induced structural damage of endothelial cells triggers the hemorrhagic diathesis.

In our study, and consistent with the original histologic observations of Murphy in fatal human cases,[10] we found that EBOV infection of endothelial cells did not extensively disrupt the architecture of the vascular endothelium in EBOV-infected cynomolgus monkeys. While EBOV replicated in endothelial cells of these animals, endothelial cell infection was only seen focally at late stages of disease, after the onset of the hemorrhagic abnormalities that characterize EBOV HF.[18] Although we observed ultrastructural evidence of endothelial cell activation and disruption, it is likely that the vasoactive effects on endothelial cells are mediated indirectly as we were unable to associate these changes with the presence of intracytoplasmic EBOV antigens. Additionally, our data showed that while EBOV was capable of replicating in microvascular and macrovascular human endothelial cells *in vitro*, replication did not directly induce cytopathology.

A notable finding in our EBOV-infected cynomolgus monkey model, was the observation that total serum protein levels did not fluctuate during the course of infection; however,

decreases in serum albumin levels were seen by day 4. A decrease in the level of total proteins would be predicted in cases of severe necrosis and damage to the endothelium versus selective loss of a small molecular weight protein, such as albumin. Because albumin is the serum protein most responsible for maintaining colloid osmotic pressure, excessive loss would result in a reduced plasma osmotic pressure, producing edema. A decrease in osmotic pressure may also be attributed to a reduced synthesis of albumin, and it cannot be discounted that EBOV-induced impairment of hepatocyte function contributes to the decreased levels of serum albumin. Previous studies demonstrated that TNF-α can increase albumin permeation in the systemic vasculature,[26] but surprisingly only small increases in circulating levels of TNF-α were detected during the late stages of EBOV-infection in our cynomolgus monkeys.[18] However, previous studies showed a priming effect for TNF-α in the presence of agents such as H_2O_2.[27] Because substantially increased systemic serum nitrate levels, indicating increased *in vivo* nitric oxide production, were observed in these EBOV-infected monkeys,[18] the impact of low concentrations of TNF-α on vascular permeability cannot be discounted.

To confirm *in vivo* findings, primary cultures of endothelial cells were employed. *In vitro* infection of these cells resulted in a noncytolytic infection, with the production of progeny virus and induced cells to secrete chemoattractants, such as the CXC chemokine IL-8, the proinflammatory cytokine IL-6, and transcripts for the proinflammatory protein COX-2. Although very high levels of IFN-α were detected in our EBOV-infected monkeys by day 4,[18] and nonviral TRI that are known to be associated with the production of IFN-α,[28] were observed in endothelial cells *in vivo*, we failed to detect

production of IFN-α in EBOV-infected HUVEC or HMVEC. These observations strongly suggest that other factors triggered by EBOV infection induce endothelial cells to produce IFN-α *in vivo* and support the hypothesis that endothelial cell disturbances *in vivo* are largely unrelated to overt cytopathology induced by EBOV replication. Interestingly, the predominate Type I IFN species observed in our *in vitro* infections was IFN-β. This observation is distinct from previous *in vitro* work using primate monocytes/macrophages, an early cellular target of EBOV, where IFN-α was the predominant Type I IFN species produced.[29] The observation of increased circulating levels of IFN-β at late stages of disease, after the onset of DIC, and the lack of IFN-β produced from EBOV-infected monocytes/macrophages *in vitro* is consistent with the observation that endothelial cells were late targets of EBOV infection *in vivo*.

It is worthy to note that EBOV infection did not induce apoptosis either directly or indirectly in endothelial cells *in vitro* or *in vivo*. Relatively strong increases in transcripts for the anti-apoptotic gene cIAP2, and COX-2, which is known to have anti-apoptotic properties,[30,31] were detected in EBOV-infected HUVEC. Pro-apoptotic transcripts were not seen in any of the EBOV-infected endothelial cell cultures, consistent with the hypothesis that EBOV induces protective modalities in cells that it infects. Furthermore, these observations support the view that development of vascular hemorrhage/leakage is not a direct result of destruction of the endothelium by EBOV replication. These findings are in contrast with results reported for other viral hemorrhagic fevers including dengue[32] and African swine fever,[33] which induce apoptosis in endothelial cells *in vitro*, but are consistent with Lassa virus.[34]

Although endothelial cells were readily infected *in vitro*, the predilection of EBOV for endothelial cells *in vivo* was not consistent and developed according to anatomic location. While this phenomenon may be a function of the remarkably heterogeneous nature of vascular endothelia in terms of morphology, receptor/marker expression, and function, it is also possible that the host factor required for EBOV replication in endothelial cells is located on the basolateral surface and *in vivo* is somewhat protected from viremia. For example, over 4 $\log_{10}$ PFU/ml of EBOV was detected in circulation of these monkeys at day 4[18] yet the only endothelial cells containing EBOV RNA and antigens were endothelial cells lining hepatic sinusoids. As illustrated by Schnittler and Feldmann in postulating a model for routes of filoviral dissemination,[35] the portal liver sinuses are lined by a discontinuous endothelium that does not rest on a regular basement membrane. This endothelium contains transcellular gaps, allowing virions to enter the space of Disse. In addition to providing more immediate access to hepatocytes as proposed,[35] these gaps may also enhance access to the basolateral aspects of the sinusoidal endothelial cells. It is also worthy of note that sinusoidal endothelial lining cells express the receptor DC-SIGNR, which was recently postulated to be a receptor for EBOV.[36] HEV were also earlier targets of EBOV than other endothelial cells, and it is possible that increased trafficking of EBOV-infected monocytes and dendritic cells through these vessels disseminated virus more readily to HEV.

Although we have defined endothelial cell transcriptional and protein responses, our findings are limited by their intended focus on the endothelium. These findings exclude

responses from immune cells and complex immune cell-endothelial cell interactions that are also likely to contribute to multifactoral causes of EBOV HF. However, in focusing on an important cellular target of EBOV disease, we have addressed key vascular responses and identified many factors that regulate immune cell responses and endothelial cell barrier functions central to EBOV HF. The potential role of endothelial cell responses in EBOV pathogenesis remains speculative, but these results are vital for defining factors that contribute to EBOV HF. Our data imply that EBOV infection largely affects the function rather than the structure of endothelial cells. We conclude that EBOV-induced coagulopathy results primarily from vascular disruption induced by factors secreted from infected monocytes/macrophages and dendritic cells, while direct virus-induced cytolysis of endothelial cells plays a minimal, secondary role in the hemorrhagic diathesis.

Acknowledgements

Opinions, interpretations, conclusions, and recommendations are those of the authors and are not necessarily endorsed by the U.S. Army. Research was conducted in compliance with the Animal Welfare Act and other Federal statutes and regulations relating to animals and experiments involving animals and adheres to principles stated in the Guide for the Care and Use of Laboratory Animals, National Research Council, 1996. The facility where this research was conducted is fully accredited by the Association for Assessment and Accreditation of Laboratory Animal Care International. The research described herein was sponsored by the Medical Chemical/Biological Defense Research

Program, U.S. Army Medical Research and Material Command (Project No. 02-4-4J-081).

The authors thank Denise Braun, Joan Geisbert, Lynda Miller, Roswita Moxley, Jeff Brubaker, Steve Moon, Neil Davis, and Larry Ostby for their expert technical assistance. The authors also express thanks to Gabriela Dveksler, Aileen Marty, Rahda Maheshwari, and Chou-Zen Giam for helpful discussions and comments and to Dana Scott for skillful assistance with necropsies.

References

1. Huggins JW: Prospects for treatment of viral hemorrhagic fevers with ribavirin, a broad-spectrum antiviral drug. Rev Infect Dis Suppl 1989, 4:S750-61
2. Jahrling PB, Geisbert J, Swearengen JR, Jaax GP, Lewis T, Huggins JW, Schmidt JJ, LeDuc JW, Peters CJ: Passive immunization of Ebola virus-infected cynomolgus monkeys with immunoglobulin from hyperimmune horses. Arch Virol Suppl 1996, 11:135-140
3. Jahrling PB, Geisbert TW, Geisbert JB, Swearengen JR, Bray M, Jaax NK, Huggins JW, LeDuc JW, Peters CJ: Evaluation of immune globulin and recombinant Interferon-α2b for treatment of experimental Ebola virus infections. J Infect Dis Suppl 1999, 179: S224-S234
4. Yang Z, Delgado R, Xu L, Todd RF, Nabel EG, Sanchez A, Nabel GJ: Distinct cellular interactions of secreted and transmembrane Ebola virus glycoproteins. Science 1998, 279:1034-1037
5. Yang Z, Duckers HJ, Sullivan NJ, Sanchez A, Nabel EG, Nabel GJ: Identification of the Ebola virus glycoprotein as the main viral determinant of vascular cell cytotoxicity and injury. Nature Med 2000, 6:886-889
6. Moncada S, Palmer RMJ, Higgs EA: Relationship between prostacyclin and nitric oxide in the thrombotic process. Thromb Res Suppl 1990, XI:3-13
7. Mantovani A, Bussolino F, Dejana E: Cytokine regulation of endothelial cell function. FASEB J 1992, 6:2591-2599
8. Harcourt BH, Sanchez A, Offermann MK: Ebola virus inhibits induction of genes by double-stranded RNA in endothelial cells. Virology 1998, 252:179-188

9. Dietrich M, Schumacher HH, Peters D, Knobloch J: Human pathology of Ebola (Maridi) virus infection in the Sudan. Ebola Virus Haemorrhagic Fever. Edited by SR Pattyn. New York, Elsevier/North-Holland Biomedical Press, 1978, pp 37-42
10. Murphy FA: Pathology of Ebola virus infection. Ebola Virus Haemorrhagic Fever. Edited by SR Pattyn. New York, Elsevier/North-Holland Biomedical Press, 1978, pp 43-60
11. Zaki SR, Goldsmith CS: Pathologic features of filovirus infections in humans. Curr Top Microbiol Immunol 1999, 235:97-116
12. Baskerville A, Fisher-Hoch SP, Neild GH, Dowsett AB: Ultrastructural pathology of experimental Ebola haemorrhagic fever virus infection. J Pathol 1985, 147: 199-209
13. Geisbert TW, Jahrling PB, Hanes MA, Zack PM: Association of Ebola related Reston virus particles and antigen with tissue lesions of monkeys imported to the United States. J Comp Pathol 1992, 106:137-152
14. Jaax NK, Davis KJ, Geisbert TW, Vogel P, Jaax GP, Topper M, Jahrling PB: Lethal experimental infection of rhesus monkeys with Ebola-Zaire (Mayinga) virus by the oral and conjunctival route of exposure. Arch Pathol Lab Med 1996, 120:140-155
15. Davis KJ, Anderson AO, Geisbert TW, Steele KE, Geisbert JB, Vogel P, Connolly BM, Huggins JW, Jahrling PB, Jaax NK: Pathology of experimental Ebola virus infection in African green monkeys. Arch Pathol Lab Med 1997, 121:805-819

16. Ryabchikova EI, Kolesnikova LV, Netesov SV: Animal pathology of filoviral infections. Curr Top Microbiol Immunol 1999, 235:145-173

17. Jahrling PB: Filoviruses and Arenaviruses. Manual of Clinical Microbiology. Edited by PR Murray, EJ Baron, M Pfaller, FC Tenover, RH Yolken. Washington, DC, ASM Press, 1999, pp 1125-1136

18. Geisbert TW, Hensley LE, Larsen T, Young HA, Reed D, Geisbert JB, Scott DP, Kagan E, Jahrling PB, Davis KJ: Pathogenesis of Ebola Hemorrhagic Fever in Cynomolgus Macaques: Evidence that Dendritic Cells Are Early and Sustained Targets of Infection, submitted

19. Prophet EB, Mills B, Arrington JB, Sobin LH, editors: Laboratory Methods in Histotechnology. Washington, DC, Armed Forces Institute of Pathology, 1992, pp 25-59

20. Geisbert TW, Jahrling PB: Differentiation of filoviruses by electron microscopy. Virus Res 1995, 39:129-150

21. Dvorak HF, Brown LF, Detmar M, Dvorak AM: Vascular permeability factor/vascular endothelial growth factor, microvascular hyperpermeability, and angiogenesis. Am J Pathol 1995, 146:1029-39

22. Kevil CG, Payne DK, Mire E, Alexander JS: Vascular permeability factor/vascular endothelial cell growth factor-mediated permeability occurs through disorganization of endothelial junctional proteins. J Biol Chem 1998, 273:15099-103

23. Walker DH: Pathology and pathogenesis of the vasculotropic rickettsioses. Biology of Rickettsial Diseases. Edited by DH Walker. Boca Raton, CRC Press, 1988, pp 115-138

24. Eremeeva ME, Silverman DJ: Rickettsia rickettsii infection of the EA.hy 926 endothelial cell line: morphological response to infection and evidence for oxidative injury. Microbiology 1998, 144:2037-2048

25. Wong KT, Shieh WJ, Kumar S, Norain K, Abdullah W, Guarner J, Goldsmith CS, Chua KB, Lam SK, Tan CT, Goh KJ, Chong HT, Jusoh R, Rollin PE, Ksiazek TG, Zaki SR: Nipah virus infection: pathology and pathogenesis of an emerging paramyxoviral zoonosis. Am J Pathol 2002, 161:2153-67

26. Worrall NK, Chang K, LeJeune WS, Misko TP, Sullivan PM, Ferguson TB Jr, Williamson JR: TNF-alpha causes reversible in vivo systemic vascular barrier dysfunction via NO-dependent and -independent mechanisms. Am J Physiol 1997, 273:H2565-2574

27. Feldmann H, Bugany H, Mahner F, Klenk H-D, Drenckhahn D, Schnittler H-J: Filovirus-induced endothelial leakage triggered by infected monocytes/macrophages. J Virol 1996, 70:2208-2214

28. Grimley PM, Kang YH, Silverman RH, Davis G, Hoofnagle JH: Blood lymphocyte inclusions associated with alpha interferon. Lab Invest 1983, 48:30A-31A

29. Hensley LE, Young HA, Jahrling PB, Geisbert TW: Proinflammatory response during Ebola virus infection of primate models: possible involvement of the tumor necrosis factor receptor superfamily. Immunol Lett 2002, 80:169-179

30. Teruyama K, Abe M, Nakano T, Iwasaka-Yagi C, Takahashi S, Yamada S, Sato Y: Role of transcription factor Ets-1 in the apoptosis of human vascular endothelial cells. J Cell Physiol 2001, 188:243-252

31. Cao Y, Prescott SM: Many actions of cyclooxygenase-2 in cellular dynamics and in cancer. J Cell Physiol 2002, 190:279-286

32. Avirutnan P, Malasit P, Seliger B, Bhakdi S, Husmann M: Dengue virus infection of human endothelial cells leads to chemokine production, complement activation, and apoptosis. J Immunol 1998, 161:6338-6346

33. Vallee I, Tait SW, Powell PP: African swine fever virus infection of porcine aortic endothelial cells leads to inhibition of inflammatory responses, activation of the thrombotic state, and apoptosis. J Virol 2001, 75:10372-82

34. Lukashevich IS, Maryankova R, Vladyko AS, Nashkevich N, Koleda S, Djavani M, Horejsh D, Voitenok NN, Salvato MS: Lassa and Mopeia virus replication in human monocytes/macrophages and in endothelial cells: different effects on IL-8 and TNF-alpha gene expression. J Med Virol 1999, 59:552-60

35. Schnittler H-J, Feldmann H: Marburg and Ebola hemorrhagic fevers: does the primary course of infection depend on the accessibility of organ-specific macrophages? Clin Infect Dis 1998, 27:404-406

36. Simmons G, Reeves JD, Grogan CC, Vandenberghe LH, Baribaud F, Whitbeck JC, Burke E, Buchmeier MJ, Soilleux EJ, Riley JL, Doms RW, Bates P, Pohlmann S: DC-SIGN and DC-SIGNR Bind Ebola Glycoproteins and Enhance Infection of Macrophages and Endothelial Cells. Virology 2003, 305:115-23

Figure 1. EBOV replication in HUVEC and HMVEC-L by infectivity titration.

Figure 1

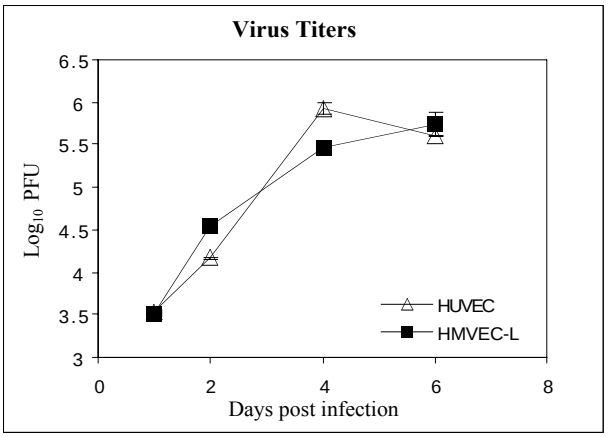
Virus Titers
6.5
6
5.5
5
4.5
4
3.5
3
Log10 PFU
0
2
4
6
8
Days post infection
HUVEC
HMVEC-L

Figure 2. Scanning electron micrograph of EBOV-infected HUVEC at day 4 illustrating large numbers of virions budding from the cell surface. Original magnification: X20,000.

Figure 2

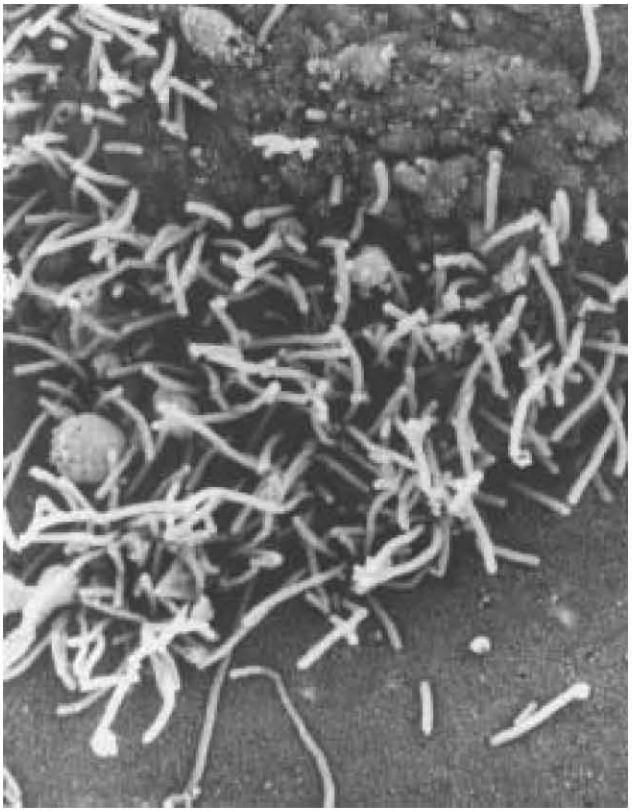

Figure 3. Comparison of mock-infected (A) and EBOV-infected (B) HUVEC at day 6. Note that there are relatively minor differences in cytopathology; cultures were indistinguishable at day 4.

Figure 3

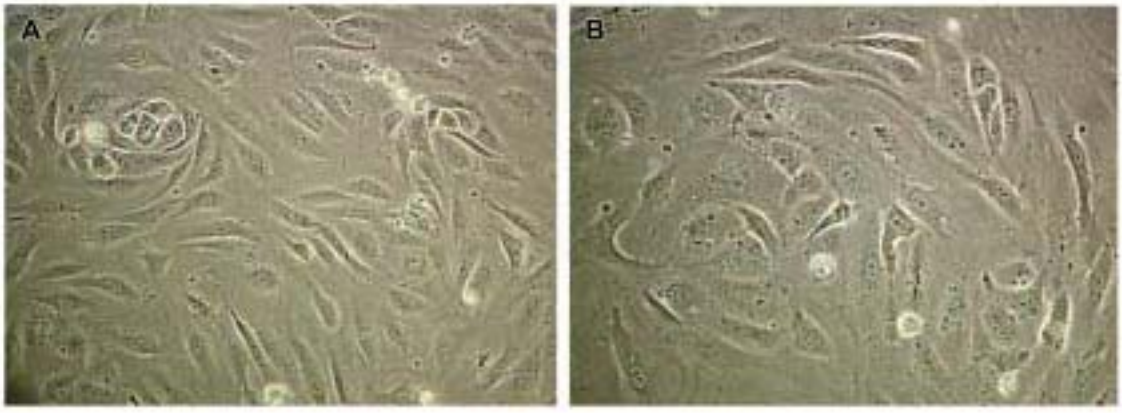

Figure 4. Ultrastructural appearance of EBOV-infected HMVEC-L at day 6. **A**, Mock-infected cells. **B**, EBOV-infected cell with typical EBOV intracytoplasmic inclusion (arrowhead). **C**, EBOV-infected cells with typical EBOV intracytoplasmic inclusions (arrowheads) and morphological evidence of necrosis. Note comparable nuclear morphology in **A** and **B**, while nuclei in **C** show degenerative necrotic change as evidenced by pale-staining and random clumping of chromatin. Original magnifications: X3,000 (**A-C**).

Figure 4

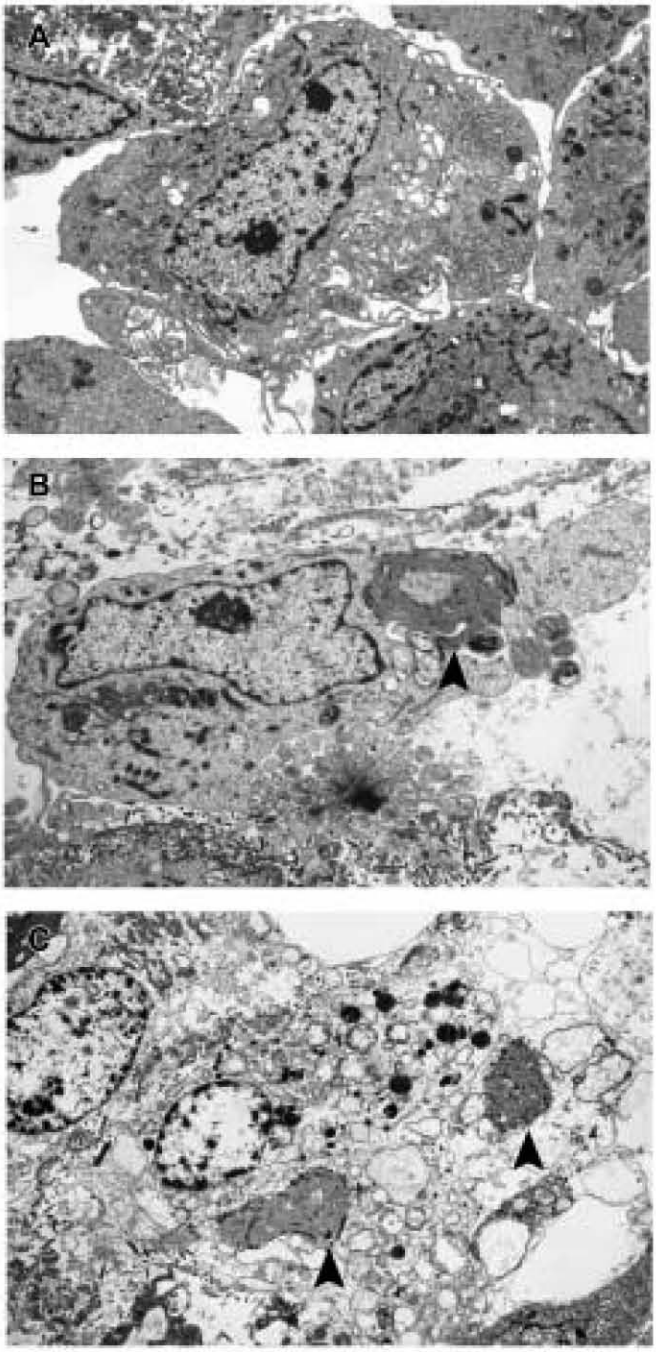

Figure 5. Analysis of mRNA production in EBOV-infected endothelial cell cultures. Representative RNase protection assays are shown. **A**, COX-1, COX-2, iNOS, Fas; Comparison of mock-infected HUVEC at 1 hour (lane 1), 24 hours (lane 2), 96 hours, (lane 3), and 144 hours (lane 4) with EBOV-infected HUVEC at 1 hour (lane 5), 24 hours (lane 6), 96 hours (lane 7), and 144 hours (lane 8), and HUVEC treated with inactivated EBOV at 144 hours (lane 9). **B**, COX-1, COX-2, iNOS, Fas; Comparison of mock-infected HMVEC-L at 1 hour (lane 1), 24 hours (lane 2), 96 hours, (lane 3), and 144 hours (lane 4) with EBOV-infected HMVEC-L at 1 hour (lane 5), 24 hours (lane 6), 96 hours (lane 7), and 144 hours (lane 8).

Figure 5

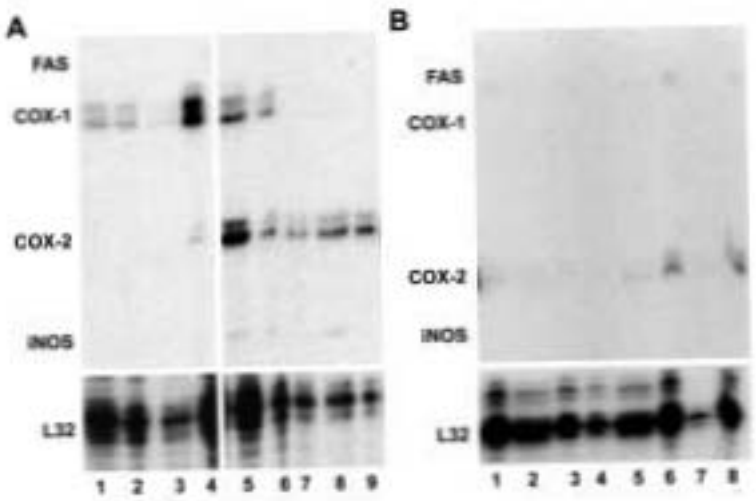
A
FAS
COX-1
COX-2
iNOS
L32
1 2 3 4 5 6 7 8 9
B
FAS
COX-1
COX-2
iNOS
L32
1 2 3 4 5 6 7 8

Figure 6. Analysis of mRNA production in EBOV-infected endothelial cell cultures. Representative RNase protection assays are shown. **A**, Cytokines/chemokines; Comparison of mock-infected HUVEC at 1 hour (lane 1), 24 hours (lane 2), 96 hours, (lane 3), and 144 hours (lane 4) with EBOV-infected HUVEC at 1 hour (lane 5), 24 hours (lane 6), 96 hours (lane 7), and 144 hours (lane 8). **B**, Cytokines/Chemokines; Comparison of mock-infected HMVEC-L at 1 hour (lane 1), 24 hours (lane 2), 96 hours, (lane 3), and 144 hours (lane 4) with EBOV-infected HMVEC-L at 1 hour (lane 5), 24 hours (lane 6), 96 hours (lane 7), and 144 hours (lane 8).

Figure 6

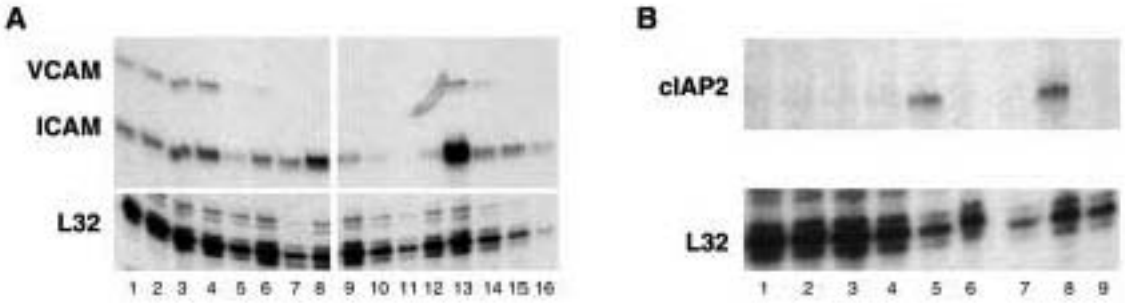
A
VCAM
ICAM
L32
1 2 3 4 5 6 7 8 9 10 11 12 13 14 15 16
B
cIAP2
L32
1 2 3 4 5 6 7 8 9

Figure 7. Analysis of mRNA production in EBOV-infected endothelial cell cultures. Representative RNase protection assays are shown. **A**, VCAM-1, ICAM-1; Comparison of mock-infected HMVEC-L at 1 hour (lane 1), 24 hours (lane 2), 96 hours, (lane 3), and 144 hours (lane 4) with EBOV-infected HMVEC-L at 1 hour (lane 5), 24 hours (lane 6), 96 hours (lane 7), and 144 hours (lane 8), and mock-infected HUVEC at 1 hour (lane 9), 24 hours (lane 10), 96 hours, (lane 11), and 144 hours (lane 12) with EBOV-infected HUVEC at 1 hour (lane 13), 24 hours (lane 14), 96 hours (lane 15), and 144 hours (lane 16), and HUVEC treated with inactivated EBOV at 144 hours (lane 17). **B**, cIAP2; Comparison of mock-infected HUVEC at 24 hours (lane 1), 96 hours (lane 4), and 144 hours (lane 7) with EBOV-infected HUVEC at 24 hours (lane 2), 96 hours (lane 5), and 144 hours (lane 8), and HUVEC treated with inactivated EBOV at 24 hours (lane 3), 96 hours (lane 6), and 144 hours (lane 9).

Figure 7

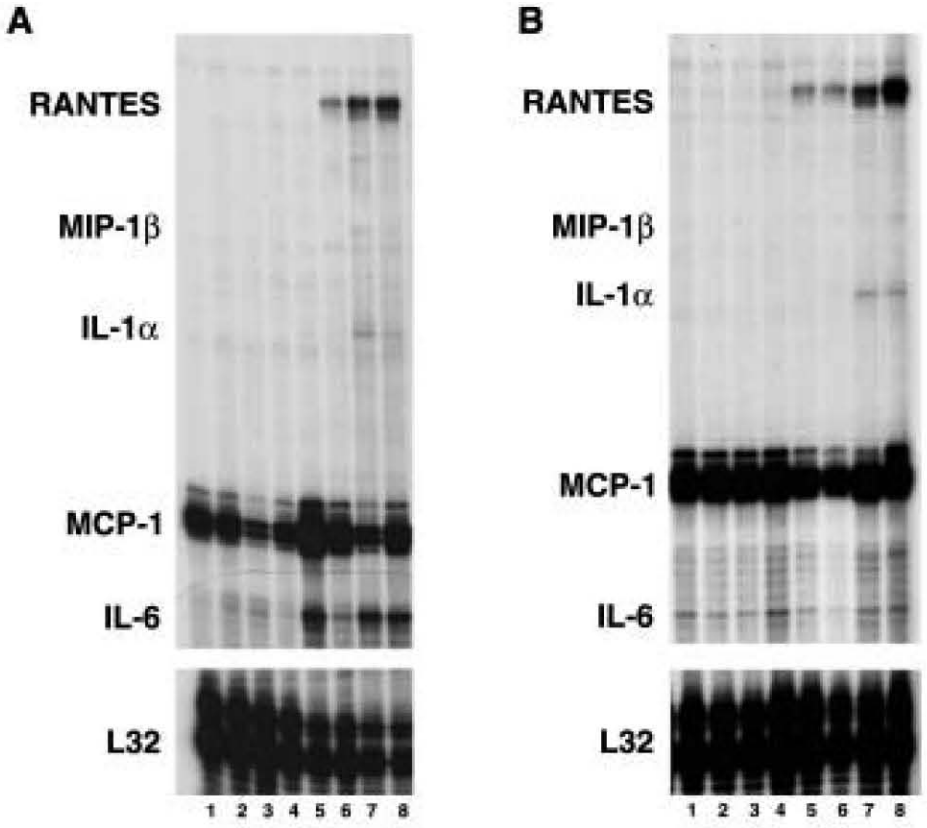
A
RANTES
MIP-1β
IL-1α
MCP-1
IL-6
L32
1 2 3 4 5 6 7 8
B
RANTES
MIP-1β
IL-1α
MCP-1
IL-6
L32
1 2 3 4 5 6 7 8

Figure 8. Analysis of cytokine/chemokine and prostacyclin (measuring its stable metabolite, 6-keto-prostaglandin $F_{1\alpha}$) accumulation in culture fluids of EBOV-infected HUVEC and HMVEC-L.

Figure 8

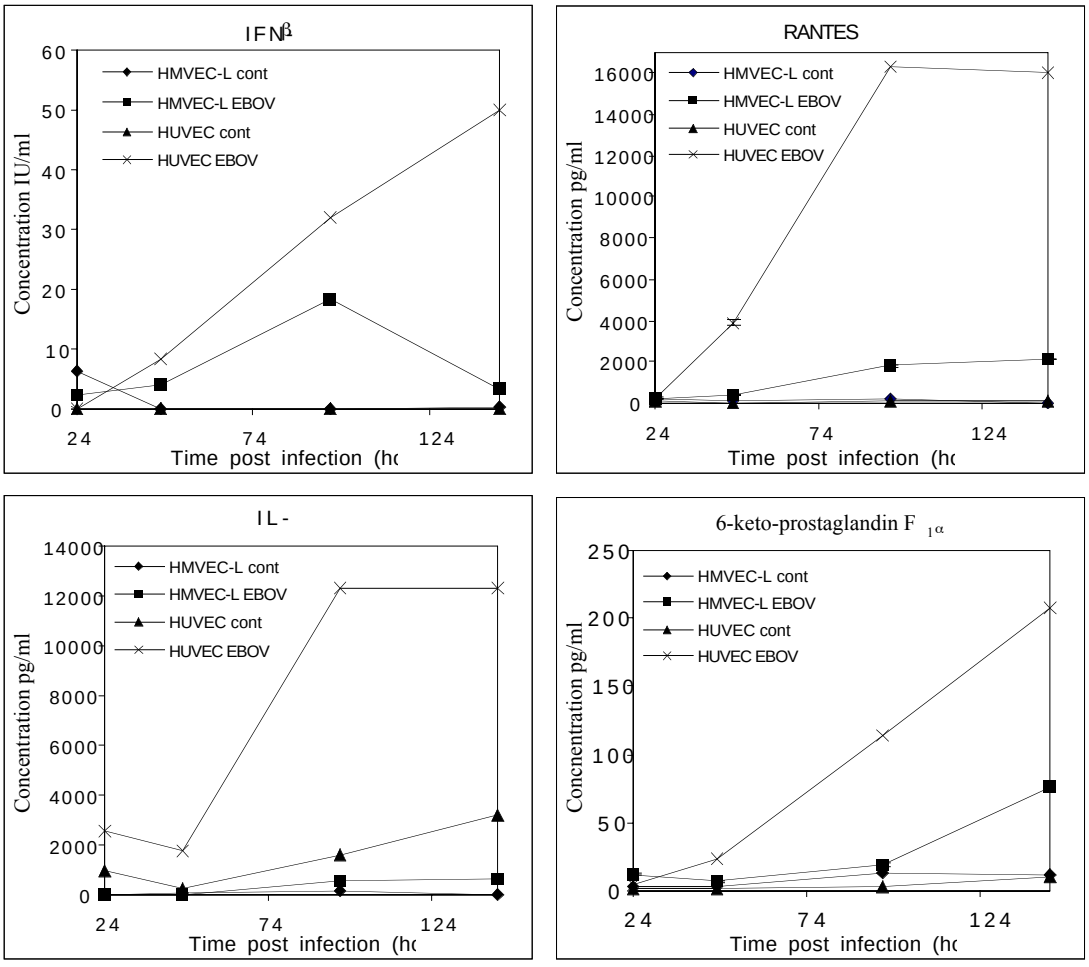
IFNβ
Concentration IU/ml
HMVEC-L cont
HMVEC-L EBOV
HUVEC cont
HUVEC EBOV
Time post infection (hc
RANTES
Concentration pg/ml
IL-
6-keto-prostaglandin F 1α
Concnentration pg/ml

Figure 9. Total serum protein and albumin values after infection of cynomolgus monkeys with EBOV-Zaire.

Figure 9

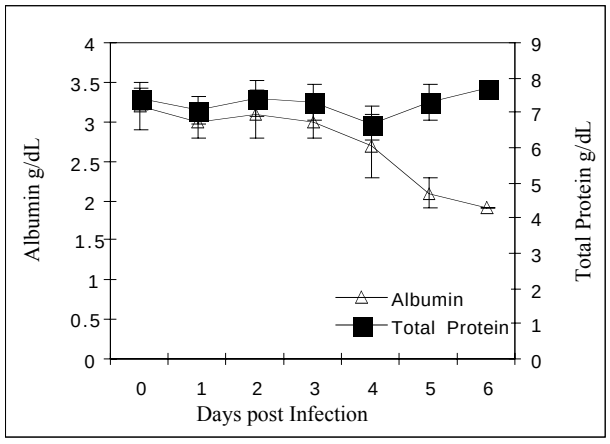
Albumin g/dL
Total Protein g/dL
Days post Infection
Albumin
Total Protein
0
0.5
1
1.5
2
2.5
3
3.5
4
0
1
2
3
4
5
6
7
8
9

Figure 10. Immunohistochemistry of inguinal lymph nodes of EBOV-Zaire-infected cynomolgus monkeys for cell markers and EBOV at day 5. **A**, Abundance of EBOV-positive mononuclear cells (red) and extracellular EBOV antigen in extravascular area. Note absence of EBOV-positive endothelial cells. **B-D**, Double labeling for an endothelial cell marker (von Willebrand's factor) (green) and EBOV antigens (red). Note that endothelium appears intact and there is no evidence of EBOV-positive endothelial cells; EBOV antigens are localized to extravascular foci or fibrinocellular thrombi in vessels. **E**, Venule, brachial plexus. Rare EBOV-positive endothelial cell (arrow) and typical EBOV-positive monocyte (within lumen). **A-D**, Immuofluorescence method with DAPI counterstain; **E**, Alkaline phosphatase method. Original magnifications: X20 (**C**); X40 (**A**, **B**, **D**, **E**).

Figure 10

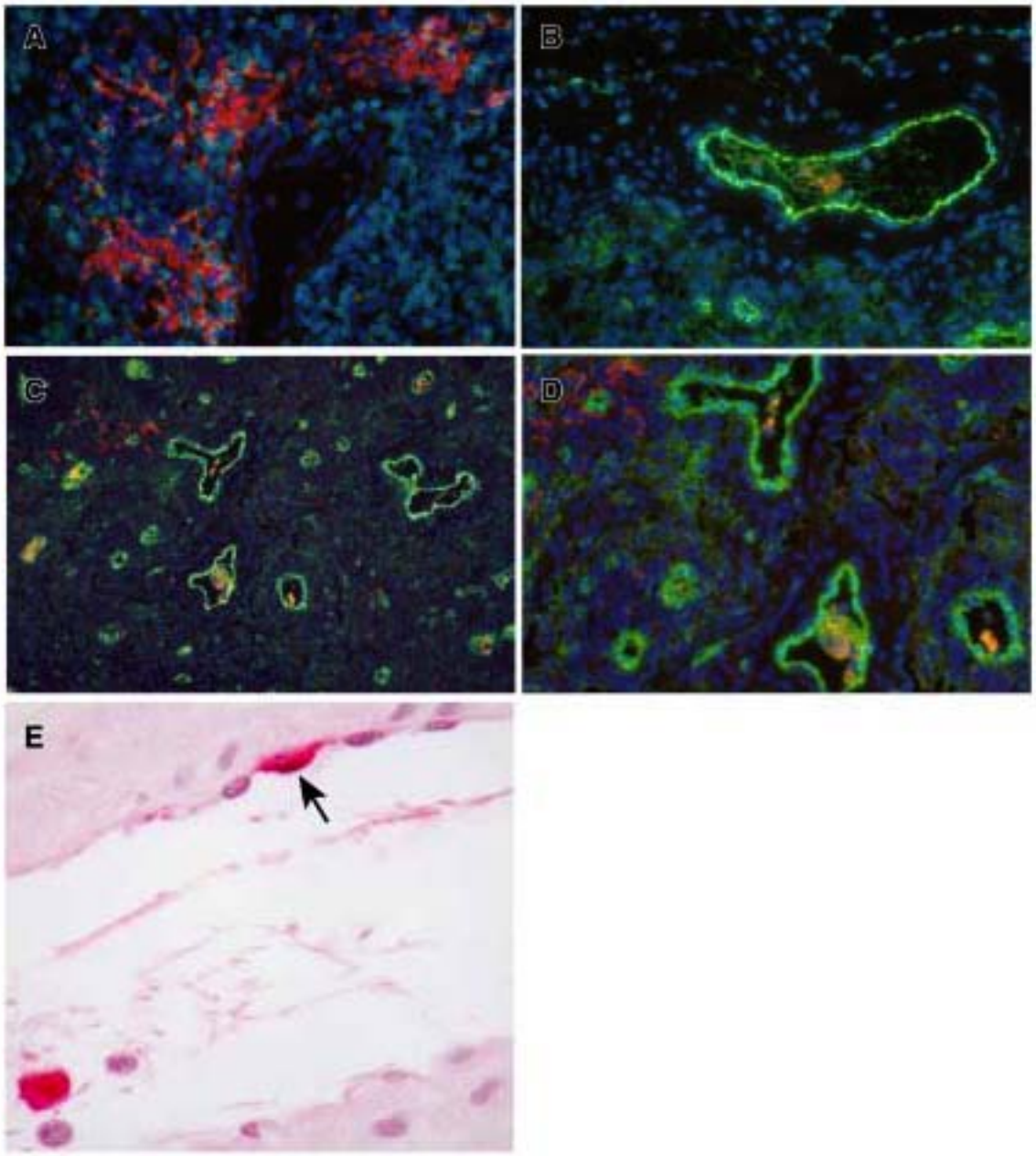

Figure 11. Ultrastuctural appearance of vessels in lymph nodes of EBOV-Zaire-infected cynomolgus monkeys. **A**, Intravascular fibrin deposits (arrowhead) and adherence of platelets (arrow) to vascular endothelium at day 4. **B**, Intravascular fibrin deposits (arrowheads), vacuolization of endothelial cell cytoplasm (arrow), and evidence of mild edema (*) at day 4. **C**, Obstruction of vessel lumen with fibrin and fibrinocellar debris (F). Despite observed coagulopathy, endothelial cells (E) show no evidence of EBOV infection. Original magnification: X6,500 (**A-C**).

Figure 11

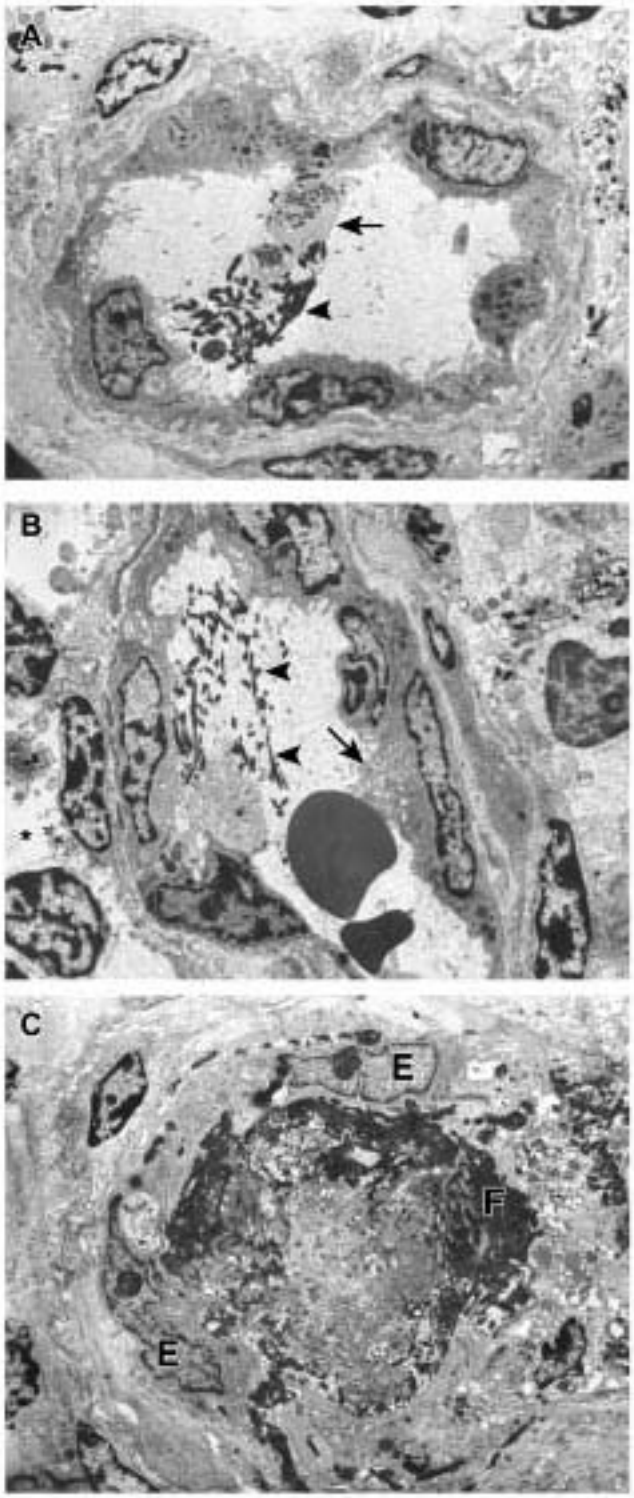

Mechanisms Underlying Coagulation Abnormalities in Ebola Hemorrhagic Fever: Overexpression of Tissue Factor in Primate Monocytes/Macrophages is a Key Event

Thomas W. Geisbert,[1,4] Howard A. Young,[3] Peter B. Jahrling,[2] Kelly J. Davis,[2] Elliott Kagan,[4] and Lisa E. Hensley[1]

[1]*Virology Division and* [2]*Headquarters, United States Army Medical Research Institute of Infectious Diseases, Fort Detrick, Maryland;* [3]*Cellular and Molecular Immunology Section, Laboratory of Experimental Immunology, NCI-FCRDC, Frederick, Maryland;* [4]*Department of Pathology, Uniformed Services University of the Health Sciences, Bethesda, Maryland*

Running head: Coagulation Abnormalities in Ebola Fever

Word count of Abstract: 150

Word count of Text: 4,825

Corresponding author:

Thomas W. Geisbert
USAMRIID
Attn: MCMR-UIV
1425 Porter Street
Fort Detrick, MD 21702-5011
Phone: 301-619-4803 Fax: 301-619-4627
Email: tom.geisbert@amedd.army.mil

Footnotes

Presented in part: XIIth International Congress of Virology, Paris, France, 27 July-1 August 2002 (Symposium V-293).

The views, opinions, and findings contained herein are those of the authors and should not be construed as an official Department of the Army position, policy, or decision unless so designated by other documentation. In conducting this research, the investigators adhered to the *Guide for the Care and Use of Laboratory Animals*, prepared by the Institute of Laboratory Animal Resources, National Research Council (National Academy Press, Washington, D.C., 1996). The facilities are fully accredited by the Association for Assessment and Accreditation of Laboratory Animal Care International. Human leukocytes employed in this study were obtained from healthy donors after informed consent. These cells were obtained in accordance with a protocol (FY99-21) approved by the USAMRIID Office of Human Use and Ethics.

Corresponding author:

Thomas W. Geisbert
USAMRIID
Attn: MCMR-UIV
1425 Porter Street
Fort Detrick, MD 21702-5011
Phone: 301-619-4803 Fax: 301-619-4627
Email: tom.geisbert@amedd.army.mil

Abstract

Disseminated intravascular coagulation is a prominent manifestation of Ebola virus (EBOV) infection. Here we report that tissue factor (TF) plays an important role in triggering the hemorrhagic complications that characterize EBOV infections. Analysis of samples collected from 25 nonhuman primates showed increased levels of TF associated with lymphoid macrophages, while analysis of peripheral blood cell RNA showed increased TF transcripts by day 3. Plasma from monkeys contained increased numbers of TF-expressing membrane microparticles. Dysregulation of the fibrinolytic system developed during the course of infection including a rapid drop in levels of plasma protein C. Infection of primary human monocytes/macrophages (PHM) was employed to further evaluate the role of TF in EBOV infections. Analysis of PHM RNA at 1-48 hours showed increased TF transcripts while levels of TF protein were dramatically increased by day 2. Thus, chemotherapeutic strategies aimed at controlling TF overexpression may ameliorate the effects of EBOV hemorrhagic fever.

Introduction

Among viruses causing hemorrhagic fever (HF), and among emerging infectious diseases with global impact in general, Ebola virus (EBOV) stands out for its impressive lethality. Along with Marburg virus (MBGV), the four species of EBOV (Zaire, Sudan, Reston, Ivory Coast) make up the negative-stranded, enveloped RNA virus family *Filoviridae*. Acute mortality caused by the Zaire species of EBOV has been approximately 80% in human outbreaks [1] and greater than 90% in monkey models of the genus *Macaca* [2-4]. As with septic shock caused by bacterial pathogens, the fulminant end of the spectrum of disease triggered by EBOV infection is thought to involve inappropriate or maladaptive host responses. The parallels of EBOV hemorrhagic fever (HF) with septic shock are instructive. Among processes or mediators or pathways thought to be dysregulated in both EBOV HF and septic shock are: 1) lymphocyte apoptosis (massive apoptosis of lymphocytes both intravascularly and in lymphoid organs); 2) proinflammatory cytokines; and 3) the coagulation cascade (disseminated intravascular coagulation [DIC]).

DIC is neither a disease nor symptom, rather it is a syndrome characterized by activation of the coagulation system, either in a localized region or throughout the entire vascular system, leading to histologically visible microthrombi generated in the microvasculature [5-7]. These microthrombi may hamper adequate blood supply and thereby contribute to the multiple organ dysfunction and high mortality rates characteristic of EBOV infections. In fact, there is ample experimental and pathological evidence that fibrin deposition contributes to multiple organ failure [8, 9]. Before acute DIC can become apparent, there must be sufficient stimulus to deplete or overwhelm the natural

anticoagulant systems, such as the protein C system. During activation of the clotting system the host will make an effort to block the process through inhibitors of the clotting system. In this process, however, the inhibitors are consumed, and if the rate of consumption exceeds the rate synthesized by liver parenchymal cells, plasma levels of inhibitors will decline. A number of studies have found positive correlations between plasma levels of inhibitors and the degree of DIC [6,10].

During DIC, the extrinsic tissue factor (TF)-dependent pathway is the dominant route to thrombin generation that leads to fibrin deposition [6, 11]. Overexpresssion of TF, a 47-kDa transmembrane glycoprotein that functions as the primary cellular initiator of the coagulation protease cascades represents one leading cause of DIC and thrombosis-related organ failure [12]. In many cases, TF exposed to the circulation is the sole culprit underlying the initiation of DIC. Although endothelial cells can express large amounts of TF *in vitro*, most studies suggest that this is an artificial observation that is not relevant to *in vivo* settings. In contrast, synthesis and exposure of endothelial TF is very limited and not likely significant in emerging and ongoing DIC [13, 14]. Monocytic TF expression can promote widespread clot formation in other diseases [14, 15]. Furthermore, increased levels of TF mRNA have been shown in mononuclear, but not endothelial, cells in lipopolysaccharide-treated rats [12, 16].

While DIC is often viewed as a prominent manifestation of EBOV infection in primates, the presence of DIC in human filoviral infections has been a controversial topic; cultural mores and logistical problems have hampered systematic studies. No single laboratory

test is sufficient to permit a definitive diagnosis of DIC; however, a positive D-dimer test is particularly useful in supporting a diagnosis of DIC as it indicates activation of both the clotting and fibrinolytic systems, and elevated levels are found in about 95% of all DIC cases [6]. In most instances, a diagnosis of DIC can be made by taking into consideration the underlying disease in conjunction with a combination of laboratory findings [5-7]. With regard to human filoviral cases, fibrin deposition has been documented at autopsy [17-19]; furthermore, clinical laboratory data suggest that DIC is likely to be a prominent feature of human disease [20-23]. The coagulation picture is clearer for nonhuman primates. Numerous studies have shown histologic and biochemical evidence of DIC syndrome during EBOV infection in a variety of nonhuman primate species [2-4, 24-27]. However, with few exceptions, these investigations examined monkeys killed when moribund and shed little light on the pathogenesis of EBOV infection during the period before death. Despite progress made during the last decade to identify key modulators of EBOV pathogenesis, there is no universal concept on the triggering mechanism of the hemorrhagic diathesis of EBOV infection.

The aim of this study was to investigate the process(es) triggering the coagulation abnormalities characteristic of both human and nonhuman primate EBOV infections and to identify key targets for potential chemotherapeutic interventions. The *in vivo* portion of this study focused on longitudinal evaluation of various coagulation parameters in nonhuman primates that were experimentally infected with EBOV. In addition, we inoculated primary human monocytes/macrophages (PHM) to further evaluate the potential triggers for DIC including TF expression.

Materials and Methods

Animals and Inoculations. Twenty-one healthy, filovirus-seronegative, adult male cynomolgus macaques (*Macaca fascicularis*) and four rhesus macaques (*Macaca mulatta*) were used for this study. Animals were inoculated i.m. with 1 ml of viral stock that contained 1000 pfu of EBOV (Zaire '95 isolate). Scheduled necropsies were performed at 1 (n = 3 cynomolgus), 2 (n = 3 cynomolgus), 3 (n = 4 cynomolgus, 1 rhesus), 4 (n = 4 cynomolgus, 1 rhesus), 5 (n = 4 cynomolgus, 1 rhesus), 6 (n = 3 cynomolgus) and 9 (n = 1 rhesus) days postinfection. Longitudinal blood samples were analyzed by coagulation assays described below.

Cell Cultures and Viruses. Elutriated monocytes were obtained from healthy human donors, isolated according to conventional procedures, and cultured/differentiated in 6-well plates [28]. Normal primary human umbilical vein endothelial cells (HUVEC) and primary human lung-derived microvascular endothelial cells (HMVEC-L) were obtained from Clonetics, Inc. (San Diego, CA), and maintained according to the supplier's recommendations. Cultures were challenged with EBOV (Zaire '95 isolate) at a multiplicity of infection of 1.0. Culture medium from Vero cells represented a "virus-free stock" in all mock infection experiments. Total RNA was extracted from infected/treated cells using Trizol (Life Technologies, Gaithersburg MD). Titration for infectious EBOV was determined as previously described [3].

Coagulation Tests. Plasma levels of D-dimers were measured by an enzyme-linked immunosorbent assay (ELISA) according to the manufacturer's directions

(Diagnostica Stago, Parsippany, NJ). Plasma levels of protein C were determined by a chromatic hydrolysis assay (DiaPharma, West Chester, OH) according to the manufacturer's recommendations. To control background for nonspecific hydrolysis, sterile water was substituted for the protein C activator. Plasma levels of tissue-type plasminogen activator antigen (tPA), urokinase-type plasminogen activator (uPA), and Factor VIIa (FVIIa) were determined by ELISA (American Diagnostica, Greenwich, CT) according to the manufacturer's instructions.

Histopathology. Tissues were collected and immersion-fixed in 10% neutral-buffered formalin and processed for histopathology, immunohistochemistry, and TEM as previously described [3, 4]. Replicate sections of spleen, liver, and axillary lymph nodes were stained with PTAH to demonstrate polymerized fibrin [4].

Electron Microscopy of Tissues. Paraformaldehyde/glutaraldehyde-fixed tissues and PBMC for TEM were postfixed in 1% osmium tetroxide in 0.1 mol/L phosphate buffer, rinsed, stained with 0.5% uranyl acetate in ethanol, dehydrated in graded ethanol and propylene oxide, and embedded in Poly/Bed 812 resin (Polysciences, Warrington, PA). Ultrathin sections were cut, placed on 300-mesh nickel TEM grids, and stained with uranyl acetate and lead citrate.

Immunoelectron Microscopy of Cell Cultures. For TF staining of cells, PHM cultured in 6-well plates were incubated with dilutions (1:100) of an anti-TF murine monoclonal antibody against human TF (American Diagnostica) or an isotype identical

irrelevant murine antibody. PHM were incubated with primary antibodies for 2 h, washed with Tris-buffered saline (TBS), and then incubated with dilutions (1:25) of a goat anti-mouse IgG conjugated to 10 nm colloidal gold (Ted Pella, Redding, CA) for 1 h. Cultures were washed in TBS, fixed in 2% glutaraldehyde in 0.1 M phosphate buffer for 1 h, washed, postfixed in 1% osmium tetroxide, and processed for embedment in Poly/Bed 812 resin as described above.

Immunoelectron Microscopy of Plasma and Culture Fluids. For TF staining of MP in culture medium or plasma, 1.5 ml aliquots of culture fluid or 0.5 ml aliquots of plasma were centrifuged at 16,000 x g for 20 min. Pellets from culture fluid were resuspended in 50 µl of PBS while pellets from plasma were recentrifuged in PBS (0.5 ml) and resuspended in 200 µl of PBS. Drops (5-10 µl) of the suspensions were applied to 300-mesh, nickel TEM grids pre-coated with Formvar and carbon. Grids were immersed for 1 h in dilutions (1:100) of a murine monoclonal antibody against human TF (American Diagnostica) or an identical isotype of an irrelevant murine antibody in TBS containing 0.1% bovine serum albumin and 0.05% Tween-20. Grids were washed and transferred for 1 h to goat anti-mouse IgG labeled with 10 nm gold spheres (Ted Pella) diluted 1:25 in TBS. Grids were then washed by successive immersion in drops of TBS, PBS, and fixed in drops of 2% glutaraldehyde for 1 h. After rinsing in drops of PBS, grids were postfixed in drops of 1% osmium tetroxide, washed in distilled water, and negatively stained with 1% uranyl acetate.

Flow Cytometric Analysis. MP were collected from plasma samples as described above, resuspended in PBS containing a murine anti-TF antibody (American Diagnostica) or an isotype control and incubated for 30 min. Samples were concentrated, washed in PBS, resusupended in PBS containing goat anti-mouse FITC for 30 min, reconcentrated, rinsed in PBS, and resuspended in 500 µl of PBS. Samples were analyzed in a FACScan flow cytometer with CellQuest software (Becton Dickinson, San Jose, CA).

Immunofluorescence. Formalin-fixed tissue sections were deparafinized and rehydrated as previously described [28]. Slides were placed in normal goat serum for 30 min, transferred to an anti-TF murine antibody (American Diagnostica), incubated overnight at 4 °C, rinsed, incubated in goat anti-mouse alexa 594 (Molecular Probes, Eugene, OR) for 30 min, rinsed and mounted in aqueous mounting medium containing 4',6'-diamidino-2-phenylindole (DAPI; Vector Laboratories). Cytospins or coverslips were rehydrated, rinsed in PBS, placed in normal goat serum for 30 min, transferred to the anti-TF antibody (American Diagnostica) or an EBOV antibody pool [26] for 1.5 h, incubated in goat anti-mouse alexa 594 (Molecular Probes) for 30 min, rinsed, and mounted in aqueous mounting medium containing DAPI.

RNAse Protection Assays. PBMC were separated from EDTA-treated peripheral blood collected from monkeys before and after exposure to EBOV [28]. Custom Probe sets were obtained from Pharmingen (San Diego, CA). The Multiprobe RNAse

Protection Assay was performed according to manufacturer's directions (Pharmingen,) with minor modifications [28].

Results

Development of Coagulation Abnormalities. In order to evaluate the role of the natural anticoagulant systems in the development of DIC during EBOV HF, we assessed several fibrinolytic pathways using plasma and/or sera temporally collected from EBOV-infected macaques. Because of a limited amount of available test material, we focused our efforts on the most definitive assays, which had been validated in nonhuman primates, and could readily be performed under BSL-4 containment. As an example of assay utility, preliminary studies showed that available assays for plasminogen activator inhibitor 1 (PAI-1) were not compatible with cynomolgus or rhesus macaques.

Our most striking finding was the rapid drop in plasma protein C levels (figure 1A), which developed early during the course of disease and was evident in all monkeys at day 2, and beyond. At days 2 and 3, levels dropped > 40% (2/4 monkeys each day) versus prechallenge levels. By days 4 and 5, levels dropped > 50% (3/4 each day) from prechallenge values. Protein C levels rebounded at day 6, but only to 60% versus baseline levels (2/2). Tissue-type plasminogen activator antigen (tPA) levels rose sharply between days 3 and 4, from no detectable difference versus preinfection levels at day 3, to an approximate 5.5-fold increase over baseline levels at day 4; this elevation continued to rise through days 5 and 6 (14- and 18-fold over baseline, respectively) (figure 1B). Urokinase-type plasminogen activator (uPA) levels increased in a similar manner with

elevations being approximately 2-fold over preinfection levels on day 4, 4.5 fold-over baseline on day 5, and rising to nearly 8-fold over prechallenge values on day 6. Factor VIIa levels showed a general decline in most animals during the course of disease beginning with a greater than 2-fold decline at days 1 and 2 (2/3 and 3/4, respectively) and increasing to more than a 3-fold decline by days 5 and 6 (2/4 and 2/2, respectively). Development of fibrin degradation products (D-dimers) showed rapid increases of 45-fold by day 4 and 55-fold by day 5 (figure 1C). Also of relevance in this study, thrombocytopenia developed as platelets declined from a preinfection mean of 412 x $10^3/mm^3$ to 154 x $10^3/mm^3$ on day 6.

Evidence of Fibrin in Tissues: Association With Viral Antigen. To further characterize the development of coagulation abnormalities during EBOV infections, the formation of fibrin deposition was longitudinally analyzed in EBOV-infected monkey tissues by transmission electron microscopy (TEM) and histologic demonstration of polymerized fibrin. TEM at day 2 postinfection showed rare deposits of fibrin in association with activated (increase in size of nucleus, numbers of lysosomes, cytoplasmic flaps) tissue macrophages in the splenic marginal zone (1/3 animals). By day 3, small focal deposits of fibrin were associated with activated tissue macrophages in red pulp and marginal zone (2/4). Phosphotungstic acid hematoxylin (PTAH)-positive fibrin was evident by day 4; multifocal deposits were present in the sinusoids and marginal zones of spleen (figure 2A) and were less frequently observed in the cords of Bilroth (3/4). Fibrin was occasionally observed in hepatic sinusoids usually closely associated with Kupffer cells (3/4), and multiple foci of PTAH-positive fibrin were

detected in blood vessels of the renal medulla (2/4) (figure 2B). By day 5, the presence of fibrin deposits dramatically increased. Fibrin thrombi and fibrinocellular thrombi, composed of monocytes enmeshed in fibrin, were focally identified in vessels of most tissues evaluated. PTAH-positive fibrin was occasionally seen in hepatic sinusoids usually closely associated with Kupffer cells (4/4), frequently present in red pulp sinusoids, marginal zones, and cords of Bilroth (4/4), and was especially prominent in blood vessels of the renal medulla (4/4). TEM findings at day 5 were similar. A high proportion of hepatic sinusoids were filled with fibrin deposits, fibrinocellular debris, and free virions. Deposits of fibrin and fibrinocellular debris in spleen were so heavy and widespread that normal architecture was almost completely lost (4/4); there was a strong demarcation of venous sinuses by fibrin deposits between the basement membrane and cords of Bilroth. Day 6 animals showed similar patterns of splenic fibrin deposition, but with more abundant fibrin, and PTAH-positive fibrin thrombi were also present in pulmonary vessels (2/3) and renal glomeruli (1/3).

It is noteworthy that the presence of fibrin appeared to be closely associated with the presence of EBOV-infected cells. For example, PTAH staining did not show deposition of fibrin in the liver until day 4, the time when infected cells were readily detected by indirect fluorescent antibody analysis (IFA) (figure 2C-D). Likewise, the abundance of fibrin paralleled the level of EBOV antigen detected. Organ infectivity titers corroborated these findings. Specifically, by day 3 postinfection, 2/4 animals had infectious virus in the liver (mean organ titer 2.40 ± 2.77 per gram of tissue); by day 4, infectious virus was detected in liver of all four animals (mean 6.89 ± 1.01). In spleen,

infectious virus was detected in 1/3 animals by day 2 (mean 1.08 ± 1.87); interestingly, the single animal with infectious virus in spleen was also the only day 2 animal with detectable fibrin by TEM. By day 3, all animals had detectable infectious virus in spleen (mean 4.88 ± 0.43), and by day 4 the mean viral titer was 6.91 ± 1.03 per gram of tissue.

TEM also demonstrated a close association between fibrin deposits and EBOV-infected cells. The most remarkable TEM observation at day 4 was the appearance of fibrin mesh networks that completely encased many EBOV-infected lymphoid tissue macrophages (figure 3A), particularly in the subcapsular sinuses of inguinal lymph nodes (2/4). These fibrin mesh networks were also observed by TEM around EBOV-infected Kupffer cells and cells with morphology consistent with dendritic cells or fibroblastic reticular cells. This fibrin encapsulation was only observed in cells with characteristic EBOV intracellular inclusion material and/or budding virions and proliferated membranes (29); neighboring cells (neutrophils, lymphocytes, red blood cells, macrophages) that did not exhibit morphological evidence of EBOV infection were not associated with these fibrin mesh networks (figure 3B).

Expression of TF mRNA and Protein in Peripheral Blood Mononuclear Cells In Vivo. To explore the potential role of TF in inducing the coagulation cascade during EBOV-infection, peripheral blood mononuclear cells (PBMC) were collected from EBOV-infected macaques and mRNA transcripts were analyzed. Increased TF transcripts were observed in 3/4 monkeys by day 3 postinfecton and in all macaques from day 4, and beyond (figure 4A). IFA for TF was also performed on cytospins prepared from

available blood samples. IFA confirmed TF expression and showed increased numbers of TF-positive cells during the course of the infection (figure 4B-C).

Expression of TF Protein in Tissues. Immunohistochemistry was performed on liver and spleen from EBOV-infected monkeys. Early-stage tissues, collected at days 1 and 2, were compared with those collected at mid- to late-stages of infection (days 4 and 5). Although antigen retrieval for TF proved problematic in tissues that had been stored in formalin for 4 weeks, clear increases in the number of cells expressing TF, particularly splenic macrophages, were seen at days 4 and 5. In addition to macrophages, other cells positive for TF antigen included polymorphonuclear neutrophils (PMN) and endothelial cells. Interestingly, TF expression in endothelial cells appeared to be focal, and TF expression was not uniform (e.g., occasional vessels displayed intense staining while many others showed mild to no staining). Circulating TF-positive cells were also observed in larger vessels (figure 4D). To confirm these findings, and to circumvent problems associated with storing tissues in formalin for extended periods of time, cytospins were prepared from dissociated spleen of available EBOV-infected monkeys. IFA for TF on these samples confirmed increasing numbers of TF-positive cells during the disease course (figure 4E-F).

Production of Membrane Microparticles In Vivo. Membrane microparticles (MP) are shed from the plasma membrane of most eukaryotic cells undergoing activation or apoptosis [30-32]. To test the hypothesis that TF-expressing MP are formed during EBOV infection, flow cytometry and immunoelectron microscopy (IEM) were performed

on a cohort of plasma samples from EBOV-infected monkeys. Flow cytometry demonstrated the development of a TF-positive MP population (figure 5A). IEM analysis of these samples confirmed that the MP were fragments of cell membranes, of a variety of sizes (range of 0.1 μM to 1.0 μM) and conformations, and that the labeling of TF on these MP was very specific (Figure 5B-C). TF-positive MP were infrequently seen at day 1 (less than one TF-positive MP per field of 300 field EM grid) but by days 4 and 5 gold sphere-labeled MP were readily detected in plasma of all animals analysed (> 40 TF-positive MP per field). In addition, the intensity of gold sphere labeling of MP increased during the infection, e.g., at day 1, MP were often decorated with only three to four gold spheres while more than 10 spheres were usually seen on MP by day 4.

Expression of TF mRNA and Protein In Vitro. To confirm TF expression in mononuclear phagocytes, cultures of PHM were established from three separate donors and infected with EBOV. Primary human endothelial cells, macrovascular HUVEC and microvascular HMVEC-L, were employed for comparative purposes. Analysis of PHM and endothelial cell gene response showed increased TF transcripts in PHM as early as 1 hour postinfection (figure 6A); increased TF transcripts were also seen in PHM at 24 and 48 hours. Increased TF transcripts were not detected in HUVEC or HMVEC-L even though EBOV replicated in these cells as evidenced by viral infectivity titration, which showed nearly 6 log10 pfu/ml of infectious EBOV in culture fluid. IFA confirmed TF protein expression in PHM at 48 hours (figure 6B-D). IEM also corroborated TF expression and revealed that TF was primarily localized to PHM showing morphological evidence of EBOV infection [29]. TF-positive gold sphere labeling was only rarely seen

in PHM that showed no morphologic evidence of infection. In many cases, TF was co-localized with areas of EBOV-induced proliferated membranes [29] (figure 6E-F). Occasional foci of TF were localized to nondescript areas along and just beneath the plasma membrane. Analysis of fluids from PHM cultures by IEM showed TF-positive MP ranging in size from 0.1 μM to nearly 1.0 μM (figure 6G). Some of these MP had attached viral particles and were interpreted to be portions of the EBOV-induced proliferated membranes seen in thin sections of EBOV-infected PHM. It is noteworthy that the EBOV virions did not express TF yet the attached membranes were TF-positive.

Discussion

Development of DIC is a characteristic clinical manifestation of EBOV infection in primates; however, the mechanism(s) for triggering the coagulation abnormalities remain unknown. This study provides the first insight into the pathogenesis of coagulation system dysregulation and suggests that development of coagulation abnormalities may occur much earlier than previously thought. Although it is likely that the coagulopathy seen in EBOV HF is caused by multiple factors, particularly during the later stages of disease, the data presented here strongly implicate TF expression/release from EBOV-infected monocytes/macrophages as key a factor that induces the development of coagulation irregularities seen in EBOV infections. Dysregulation of the protein C system also appears to play an important role in the observed coagulopathy.

The appearance of fibrin deposits in tissues coinciding with detectable viremia and infectious virus in these tissues strongly supports a direct link with viral infection. The

appearance of fibrin mesh networks that selectively encased EBOV-infected lymphoid tissue macrophages and Kupffer cells by day 4, and dendritic cells by day 5, not only corroborate this observation but suggest that viral infection resulted in upregulation of a protein capable of triggering the coagulation cascade. RNA analysis, IFA, and TEM all show that TF expression is upregulated during EBOV infection and that expression of TF likely triggers activation of the coagulation system producing the marked fibrin encasement of EBOV-infected cells.

Analysis of macaque PBMC mRNA demonstrated increased TF transcripts by day 3; IFA confirmed these findings. Because monocytes/macrophages are the only cells in the blood circulation compartment that express TF on their surface [15, 33], and differential counts show that monocytes represented only 1 to 6 % of the total white blood cells of any of the 25 monkeys in this study, it is likely that the transcript level in monocytes is more marked than that from total PBMC. Cells morphologically consistent with monocytes/macrophages or PMN were positive for TF. TEM analysis of macaque tissues demonstrated fibrin formation only around EBOV-infected cells including lymphoid monocytes/macrophages, Kupffer cells, and dendritic cells. Fibrin formation was not observed around PMN, which are nonpermissive to EBOV. It is not surprising that PMN may phagocytose and store TF protein released by monocytes/macrophages but unless they are induced to upregulate mRNA transcripts and express TF protein on the cell surface, PMN are not likely to trigger the coagulation system. The observation of TF by IFA, but lack of fibrin associated with these cell types by TEM is consistent with this view and also implicates monocytes/macrophages as key sources for TF protein during

EBOV infection. Moreover, upregulation of TF mRNA and protein in EBOV-infected monocytes/macrophages *in vitro* further corroborates this hypothesis.

Levels of TF expression may also be affected by the production of various cytokines and chemokines. Proinflammatory cytokines such as interleukin (IL)-6 have been shown to effectively upregulate TF expression on monocytes [34, 35]. Elevations of IL-6 have been reported by day 4 postinfection in EBOV-infected monkeys [28]. Splenocyte stimulation with TF also induces the selective release of the monocyte chemoattractant molecule MIP-1α in vitro [36]. Increased levels of MIP-1α have been demonstrated in EBOV-infected monkeys and cultures of infected monocytes/macrophages [28]. Taken together, these findings suggest that TF expression can be amplified during the later stages of disease when EBOV-infected cells, which selectively express TF, release cytokines/chemokines that may either directly upregulate levels of TF or attract additional preferred target cells to foci of infection, thereby exacerbating activation of the extrinsic coagulation pathway. TF expression may also be amplified in the latter stages of disease as a result of tissue damage caused by the formation of microthrombi. Specifically, development of these microclots during disease, as a result of TF overexpression, can produce tissue infarcts, as evidenced by the strong increase in plasma levels of tPA noted at days 5 and 6; these areas of tissue damage may then augment the effect by inducing local upregulation of TF.

This study also implicates TF expressed on MP that may be generated by EBOV infection of monocytes/macrophages as playing an important role in disease

pathogenesis. Mechanistically, we have demonstrated that MP expressing TF are shed from EBOV-infected monocytes/macrophages in vitro, and furthermore, we have shown increased numbers of TF-positive MP in plasma of EBOV-infected monkeys. The procoagulant potential of MP is supported by clinical studies showing elevated levels of circulating MP in patients with an increased risk for thromboembolic events (e.g., DIC) [31, 32]. Our observation of MP during EBOV infection is not unprecedented. Recently, it was reported that patients with fulminant meningococcal sepsis contained MP expressing CD14 and TF and these MP also induced extreme thrombin generation in vitro [31]. As about 85% of the TF-positive MP were also CD14 positive, it was concluded that the overall procoagulant activity was due to an increased number of monocyte-derived MP.

Leukocyte-derived MP circulate in the bloodstream under normal conditions and are rapidly upregulated by inflammatory stimulation [37]. Furthermore, blood-derived MP induce the release of proinflammatory and chemotactic cytokines in endothelial cells [30, 37]. This may be potentially relevant to endothelial cell dysfunction during vascular diseases further exacerbating vessel wall dysfunction and procoagulant activity. In this study, it is likely that the contribution of TF to the overall procoagulant activity was boosted by the increased number of monocyte/macrophage-derived MP as monocytes/macrophages are well established as the preferred target of EBOV [25, 38] and undergo necrotic changes during the course of infection [38]. The abundance of TF-expressing MP inducing vascular procoagulant activity is also relevant to DIC states, in

which secondary injuries to the vessel wall are frequently prevalent, providing for sustained exposure of TF activity to the blood.

This study suggests that protein C may be a critical component to the observed coagulation dysfunction in EBOV HF. The protein C system is one of the main anticoagulant mechanisms in blood [39]. The key factor is a vitamin K-dependent proenzyme, protein C, which, upon activation on the endothelial surface by thrombin-thrombomodulin complex, imparts a potent anticoagulant activity via degradation of activated factors V and VIII. Growing evidence also suggests that protein C has direct anti-inflammatory properties and modulating activity on cellular functions, likely by blocking NF-κB nuclear translocation [40-42]. The rapid decline in plasma protein C levels concomitant with disease progression was a prominent finding in the current study. Reduced levels of protein C are found in the majority of patients with sepsis and are associated with an increased risk of death [43, 44]. Moreover, protein C deficiency appears to develop well before the onset of defined clinical variables of severe sepsis or septic shock (44, 45) and may be considered a prognostic indicator [46]. Clearly, identifying protein C abnormalities in this EBOV primate model (that so closely parallel protein C anomalies in human coagulopathies) offers an ideal target for chemotherapeutic interventions. Administration of activated protein C was protective in a baboon model of lethal *Escherichia coli* sepsis [47]. More recently, treatment with recombinant human activated protein C significantly reduced mortality in patients with severe sepsis [48]; furthermore, biological activity of the activated protein C was demonstrated by finding

greater decreases in D-dimer and IL-6 levels in patients who received activated protein C than in those who received placebo.

Identifying TF as an initiating aspect of DIC, and dysregulation of protein C as a potentially exacerbating factor, may be central to explaining the mechanisms triggering the hemorrhagic diathesis of EBOV infection. This report represents a first step in demonstrating that chemotherapeutic strategies aimed at controlling TF overexpression, and dysregulation of the protein C system, may ameliorate the effects of EBOV hemorrhagic fever. Strategies that have proven successful for treating patients with similar clinical pictures, such as administering activated protein C in severe sepsis, may also have utility in treating EBOV infections. It is also likely that combination therapy with multiple coagulation-modulating agents may ultimately prove to be the best approach for treating the inherent DIC. Rodent models of EBOV HF do not exhibit the hemorrhagic manifestations that characterize primate EBOV infections [4, 27], yet rodents are relatively easy to protect from lethal disease by a variety of antiviral approaches that are not protective in primates [4], thus, use of these strategies aimed at controlling EBOV replication should also provide a significant boost to therapies aimed at regulating coagulation in primates.

Acknowledgements

The authors thank Denise Braun, Joan Geisbert, Lynda Miller, Roswita Moxley, Jeff Brubaker, Steve Moon, Neil Davis, and Larry Ostby for their expert technical assistance. The authors also express thanks to Michael Hensley, Brad Stiles, and Doug Reed for helpful discussions and comments and to Tom Larsen for skillful assistance with necropsies.

References

1. Sanchez A, Khan AS, Zaki SR, Nabel GJ, Ksiazek TG, Peters CJ. Filoviridae. In: Fields Virology. Knipe DM and Howley PM, eds. Philadelphia: Lippincott Williams & Wilkins, **2001:**1279-1304.
2. Fisher-Hoch SP, Brammer LT, Trappier SG, et al. Pathogenic potential of filoviruses: role of geographic origin of primate host and virus strain. J Infect Dis **1992;**166:753-763.
3. Jaax NK, Davis KJ, Geisbert TW, et al. Lethal experimental infection of rhesus monkeys with Ebola-Zaire (Mayinga) virus by the oral and conjunctival route of exposure. Arch Pathol Lab Med **1996;**120:140-155.
4. Geisbert TW, Pushko P, Anderson K, Smith J, Davis KJ, Jahrling PB. Evaluation in nonhuman primates of vaccines against Ebola virus. Emerg Infect Dis **2002;**8:503-507.
5. Levi M, de Jonge E, van der Poll T, ten Cate H. Disseminated intravascular coagulation. Thromb Haemost **1999;**82:695-705.
6. Mammen EF. Disseminated intravascular coagulation (DIC). Clin Lab Sci **2000;**13:239-245.
7. Levi M. Pathogenesis and treatment of disseminated intravascular coagulation in the septic patient. J Crit Care **2001;**16:167-177.
8. Gando S, Nanzaki S, Kemmotsu O. Disseminated intravascular coagulation and sustained systemic inflammatory response syndrome predict organ dysfunctions after trauma: application of clinical decision analysis. Ann Surg **1999;**229:121-127.

9. Levi M, de Jonge E, van der Poll T, ten Cate H. Advances in the understanding of the pathogenetic pathways of disseminated intravascular coagualtion result in more insight in the clinical picture and better management strategies. Semin Thromb Hemost **2001;** 27:569-575.

10. Wilson RF, Mammen EF, Tyburski JG, Warsow KM, Kubinec SM. Antithrombin levels related to infections and outcome. J Trauma **1996;**40:384-387.

11. Taylor FB Jr, Chang A, Ruf W, et al. Lethal E. coli septic shock is prevented by blocking tissue factor with monoclonal antibody. Circ Shock **1991;**33:127-134.

12. Arai A, Hirano H, Ueta Y, Hamada T, Mita T, Shirahata A. Detection of mononuclear cells as the source of the increased tissue factor mRNA in the liver from lipopolysaccharide-treated rats. Thromb Res **2000;**97:153-162.

13. Drake TA, Cheng J, Chang A, Taylor FB Jr. Expression of tissue factor, thrombomodulin, and E-selectin in baboons with lethal *escherichia coli* sepsis. Am J Pathol **1993;**142:1458-1470.

14. Osterud B, Bjorklid E. The tissue factor pathway in disseminated intravascular coagulation. Semin Thromb Hemost **2001;**27:605-617.

15. Tremoli E, Camera M, Toschi V, Colli S. Tissue factor in atherosclerosis. Atherosclerosis **1999;**144:273-283.

16. Hara S, Asada Y, Hatakeyama K, et al. Expression of tissue factor and tissue factor pathway inhibitor in rat lungs with lipopolysaccharide-induced disseminated intravascular coagulation. Lab Invest **1997;**77:581-589.

17. Gedigk P, Bechtelsheimer H, Korb G. Die pathologische anatomie der Marburg-virus-Krankheit. Dtsch Med Wochenschr **1968;**93:590-601.

18. Murphy FA. Pathology of Ebola virus infection. In: Pattyn SR, ed. Ebola Virus Haemorrhagic Fever. New York: Elsevier/North-Holland Biomedical Press, **1978:**43-60.

19. Geisbert TW, Jaax NK. Marburg hemorrhagic fever: report of a case studied by immunohistochemistry and electron microscopy. Ultrastruct Pathol **1998;**22:3-17.

20. Egbring R, Slenczka W, Baltzer G. Clinical manifestations and mechanism of the hemorrhagic diathesis in Marburg virus disease. In: Martini GA, Siegert R, eds. Marburg Virus Disease. New York: Springer-Verlag, **1971:**41-49.

21. Gear JS, Cassel GA, Gear AJ, et al. Outbreak of Marburg virus disease in Johannesburg. Br J Med **1975;**4:489-493.

22. Isaacson M, Sureau P, Courteille G, Pattyn SR. Clinical aspects of Ebola virus disease at the Ngaliema Hospital, Kinshasa, Zaire, 1976. In: Pattyn SR, ed. Ebola Virus Haemorrhagic Fever. New York: Elsevier/North-Holland Biomedical Press, **1978:**15-20.

23. WHO. Ebola haemorrhagic fever in Zaire, 1976. Report of an international commission. Bull World Health Organ **1978;**56:271-293.

24. Fisher-Hoch SP, Platt GS, Neild GH, et al. Pathophysiology of shock and hemorrhage in a fulminating viral infection (Ebola). J Infect Dis **1985;**152:887-894.

25. Geisbert TW, Jahrling PB, Hanes MA, Zack PM. Association of Ebola related Reston virus particles and antigen with tissue lesions of monkeys imported to the United States. J Comp Pathol **1992;**106:137-152.

26. Davis KJ, Anderson AO, Geisbert TW, et al. Pathology of experimental Ebola virus infection in African green monkeys. Arch Pathol Lab Med **1997;**121:805-819.

27. Bray M, Hatfill S, Hensley L, Huggins JW. Haematological, biochemical and coagulation changes in mice, guinea-pigs and monkeys infected with a mouse-adapted variant of Ebola Zaire virus. J Comp Pathol **2001;**125:243-253.

28. Hensley LE, Young HA, Jahrling PB, Geisbert TW. Proinflammatory response during Ebola virus infection of primate models: possible involvement of the tumor necrosis factor receptor superfamily. Immunol Lett **2002;**80:169-179.

29. Geisbert TW, Jahrling PB. Differentiation of filoviruses by electron microscopy. Virus Res **1995;**39:129-150.

30. Mesri M, Altieri DC. Endothelial cell activation by leukocyte microparticles. J Immunol **1998;**161:4382-4387.

31. Nieuwland R, Berckmans RJ, McGregor S, et al. Cellular origin and procoagulant properties of microparticles in meningococcal sepsis. Blood **2000;**95:930-935.

32. Sabatier F, Roux V, Anfosso F, Camoin L, Sampol J, Dignat-George F. Interaction of endothelial microparticles with monocytic cells in vitro induces tissue factor-dependent procoagulant activity. Blood. **2002;**99:3962-3970.

33. Giesen PL, Rauch U, Bohrmann B, et al. Blood-borne tissue factor: another view of thrombosis. Proc Natl Acad Sci USA **1999;**96:2311-2315.

34. Neumann F-J, Ott I, Marx N, et al. Effect of human recombinant interleukin-6 and interleukin-8 on monocyte procoagulant activity. Arterioscler Thromb Vasc Biol **1997;**17:3399-3405.

35. Grignani G, Maiolo A. Cytokines and hemostasis. Haematologica **2000;**85:967-972.

36. Bokarewa MI, Morissey JH, Tarkowski A. Tissue factor as a proinflammatory agent. Arthritis Res **2002;**4:190-195.

37. Mesri M, Altieri DC. Leukocyte microparticles stimulate endothelial cell cytokine release and tissue factor induction in a JNK1 signaling pathway. J Biol Chem **1999;**274:23111-23118.

38. Geisbert TW, Hensley LE, Gibb TR, Steele KE, Jaax NK, Jahrling PB. Apoptosis induced in vitro and in vivo during infection by Ebola and Marburg viruses. Lab Invest **2000;**80:171-186.

39. Esmon CT. Regulation of blood coagulation. Biochim Biophys Acta **2000;**1477:349-360.

40. Yan SB, Grinnell BW. Antithrombotic and anti-inflammatory agents of the protein C anticoagulant pathway. Ann Rep Med Chem **1994;**11:103-112.

41. Murakami K, Okajima K, Uchiba M, et al. Activated protein C prevents LPS-induced pulmonary vascular injury by inhibiting cytokine production. Am J Physiol **1997;**272:L197-L202.

42. Esmon CT. Protein C anticoagulant pathway and its role in controlling microvascular thrombosis and inflammation. Crit Care Med **2001;**29:S48-S52.

43. Fourrier F, Chopin C, Goudemand J, et al. Septic shock, multiple organ failure, and disseminated intravascular coagulation: compared patterns of antithrombin III, protein C, and protein S deficiencies. Chest. **1992;**101:816-823.

44. Lorente JA, Garcia-Frade LJ, Landin L, et al. Time course of hemostatic abnormalities in sepsis and its relation to outcome. Chest. **1993;**103:1536-1542.

45. Kidokoro A, Iba T, Fukunaga M, Yagi Y. Alterations in coagulation and fibrinolysis during sepsis. Shock **1996;5:**223-228.

46. Fisher CJ, Yan B. Protein C levels as a prognostic indicator of outcome in sepsis and related diseases. Crit Care Med **2000;**28:S49-S56.

47. Taylor FB Jr, Chang A, Esmon CT, D'Angelo A, Vigano-D'Angelo S, Blick KE. Protein C prevents the coagulopathic and lethal effects of *Escherichia coli* infusion in the baboon. J Clin Invest **1987;**79:918-925.

48. Bernard GR, Vincent JL, Laterre PF, et al. Efficacy and safety of recombinant human activated protein C for severe sepsis. N Engl J Med **2001;**344:699-709.

Figure 1. Development of coagulation abnormalities during EBOV infection of cynomolgus monkeys. **A**, plasma levels of activated protein C measured by a chromatic hydrolysis assay at days 1 through 6 postinfection. **B**, plasma levels of tPA determined by ELISA at days 1 through 6. **c**, plasma levels of D-dimers measured by ELISA at days 1 through 6.

Figure 1

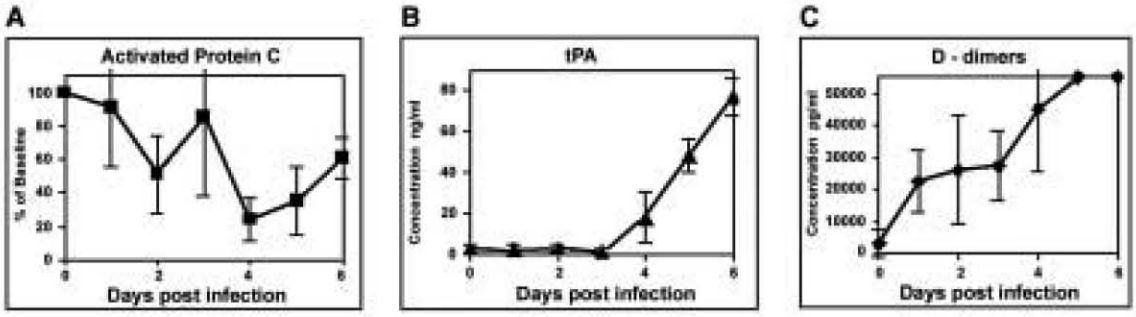
A
Activated Protein C
% of Baseline
Days post infection
B
tPA
Concentration ng/ml
Days post infection
C
D - dimers
Concentration pg/ml
Days post infection

Figure 2. Development of fibrin and association with EBOV antigen. **A,** PTAH-positive fibrin in marginal zone of spleen of cynomolgus monkey at day 4 postinfection. **B,** PTAH-positive fibrin in blood vessels of renal medulla of cynomolgus monkey at day 4. **C,** IFA showing abundance of EBOV-positive cells in spleen of cynomolgus monkey at day 4. **D,** IFA showing EBOV antigen in Kupffer cells and hepatic sinusoids of cynomolgus monkey at day 4.

Figure 2

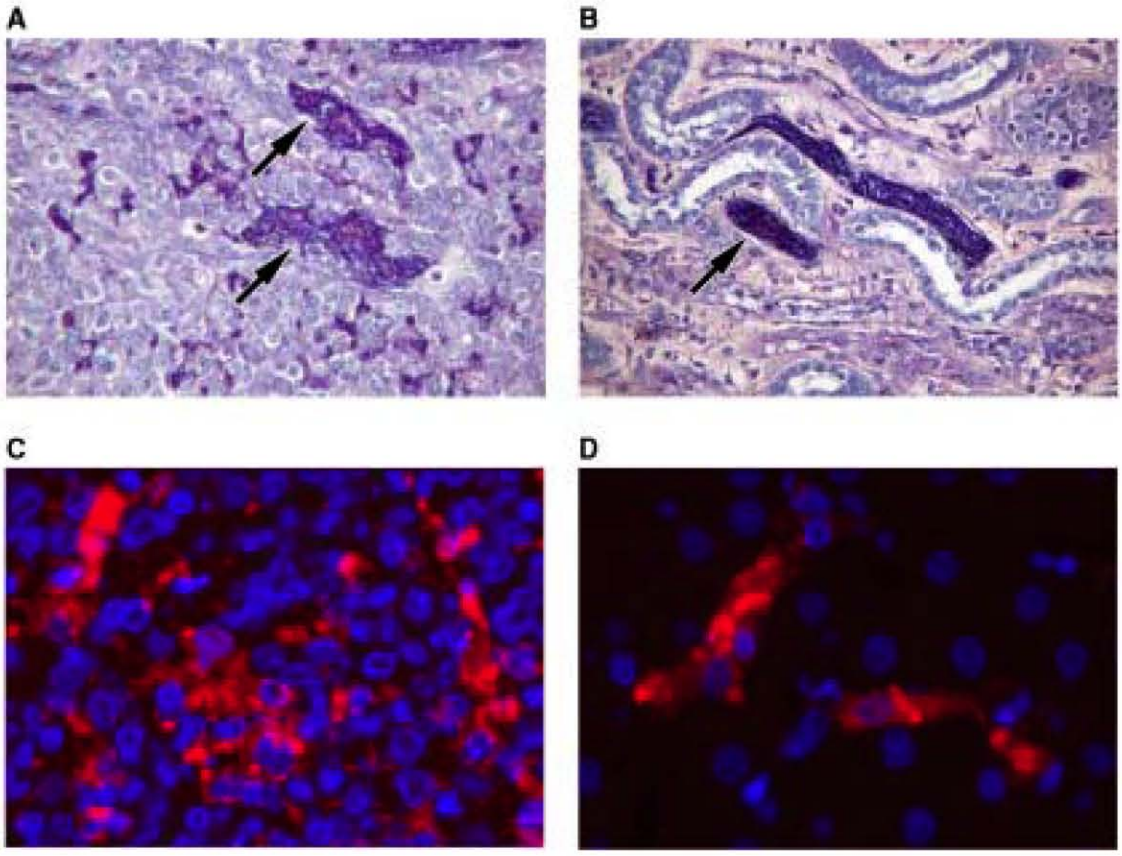

Figure 3. Association of fibrin with EBOV-infected cells by TEM. **A,** Encasement of EBOV-infected tissue macrophages with fibrin in subcapsular sinus of inguinal lymph node of cynomolgus monkey at day 4 postinfection. Bar = 1.5 μM. **B,** fibrin encapsulation of EBOV-infected tissue macrophage in same area of different macaque at day 5. Note that adjacent PMN (P) show no association with fibrin. Bar = 2.5 μM. Arrowheads in each panel identify EBOV inclusion material and arrows indicate fibrin.

Figure 3

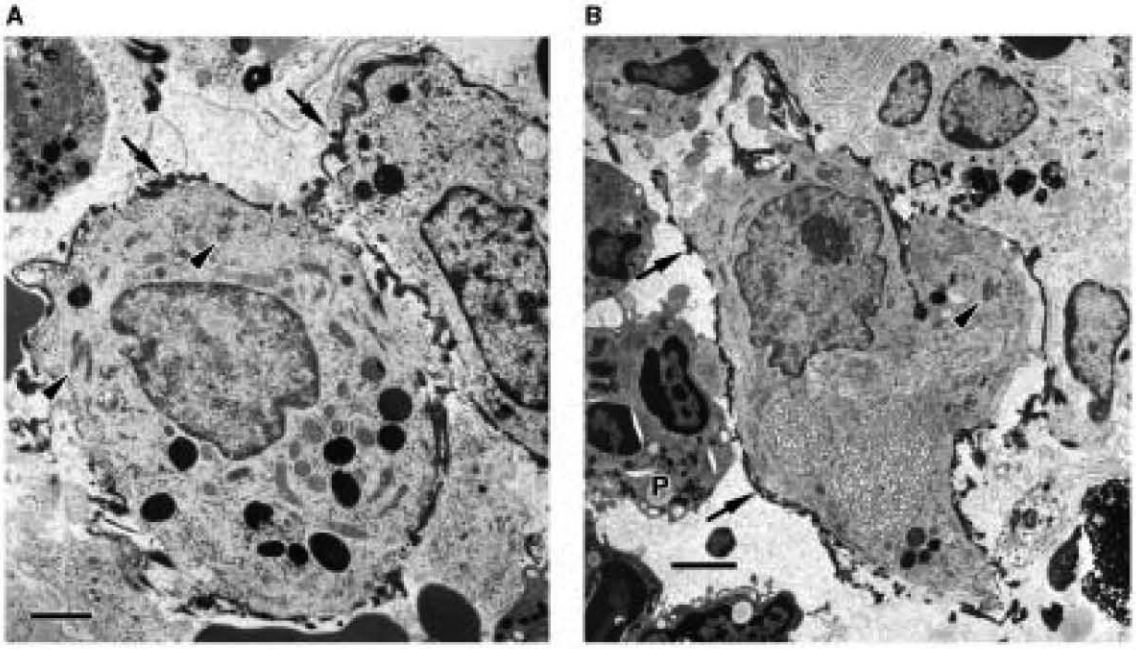

Figure 4. Expression of TF mRNA and protein in vivo. **A,** analysis of TF mRNA production in peripheral blood mononuclear cells of EBOV-infected monkeys. Representative RNase protection assay comparing three different animals preinfection (lanes 1-3), and two animals postinfection per day at days 1 (lanes 4-5), 2 (lanes 6-7), 3 (lanes 8-9), 4 (lanes 10-11), 5 (lanes 12-13), and 6 (lanes 14-15). **B,** IFA for TF of cytospins prepared from peripheral blood mononuclear cells of an EBOV-infected rhesus monkey at day 2 and **C,** at day 5 postinfection. **D,** IFA for TF showing TF-positive circulating cells in large hepatic vessel of a cynomolgus monkey at day 5. **E,** IFA for TF of cytospins prepared from spleen of EBOV-infected cynomolgus monkeys at day 3, and **F,** at day 5.

Figure 4

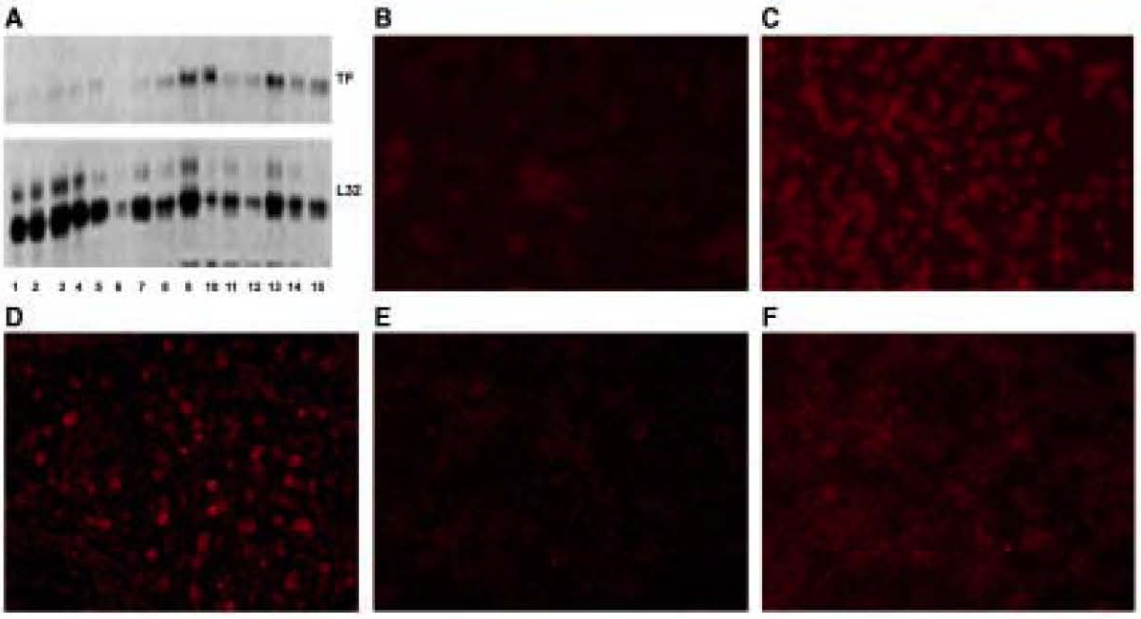

Figure 5. Detection of membrane microparticles (MP) in vivo. **A,** Flow cytometric analysis showing development of a distinct population of TF-positive MP during EBOV infection of cynomolgus monkeys. Dashed line represents MP collected from plasma of a monkey at day 1 postinfection; solid line represents MP from a monkey at day 5. **B,** IEM showing specific gold sphere labeling (arrows) for TF of MP isolated from plasma of an EBOV-infected rhesus monkey at day 9. Bar = 100 nm. **C,** IEM showing intense gold-sphere labeling (arrows) for TF of MP isolated from plasma of EBOV-infected cynomolgus monkey at day 4. Bar = 100 nm.

Figure 5

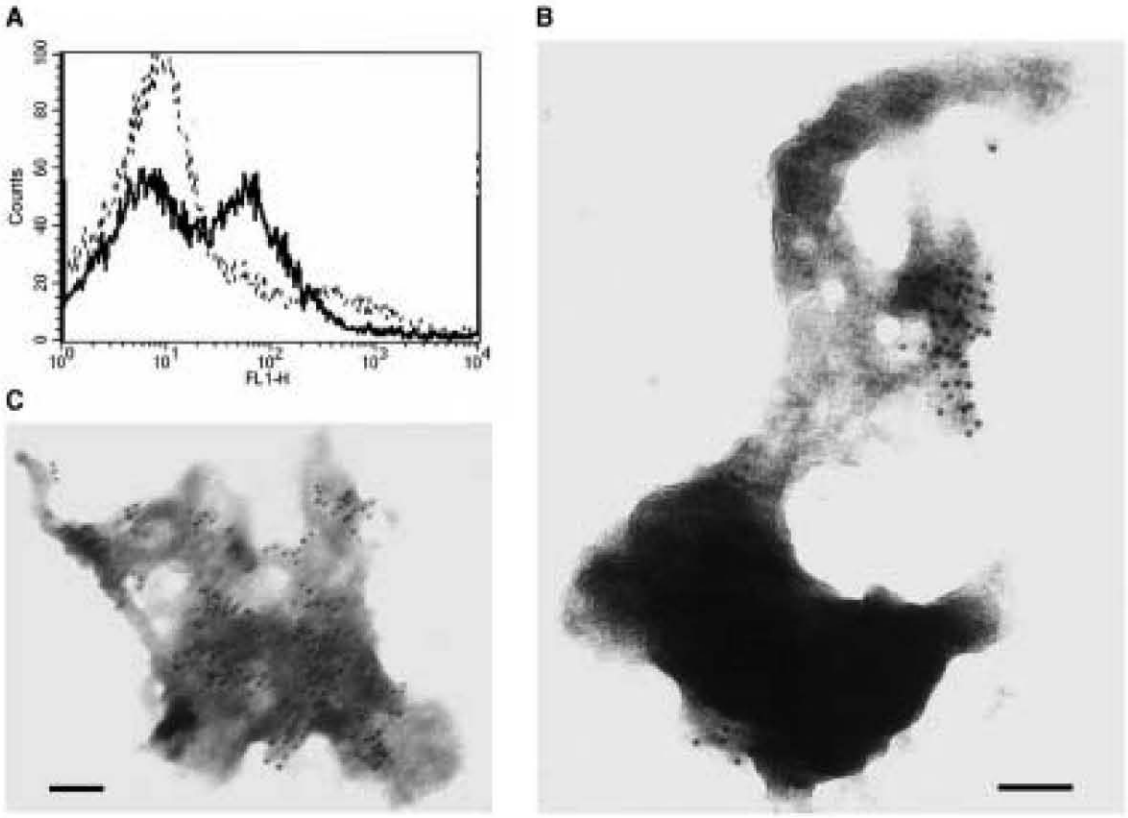

Figure 6. Expression of TF mRNA and protein in vitro. **A,** analysis of TF mRNA production in EBOV-infected cultures. Representative RNase protection assays are shown comparing mock-infected PHM at 1, 24, and 48 hours (lanes 1-3, respectively); and EBOV-infected PHM at 1, 24, and 48 hours (lanes 4-6, respectively). **B,** IFA for TF from mock-infected PHM at 48 hours postinfection, and **C,** EBOV-infected PHM at 48 hours. **D,** high power view of EBOV-infected PHM at 48 hours similar to field shown in panel c. **E,** pre-embedment IEM of EBOV-infected PHM at 48 hours postinfection incubated with irrelevant murine antibody, and **F,** incubated with anti-TF antibody showing 10 nm gold sphere labeling of proliferated membranes. **G,** IEM showing gold sphere labeling (arrows) for TF of MP isolated from culture fluid of EBOV-infected PHM at 48 hours. Bar = 150 nm.

Figure 6

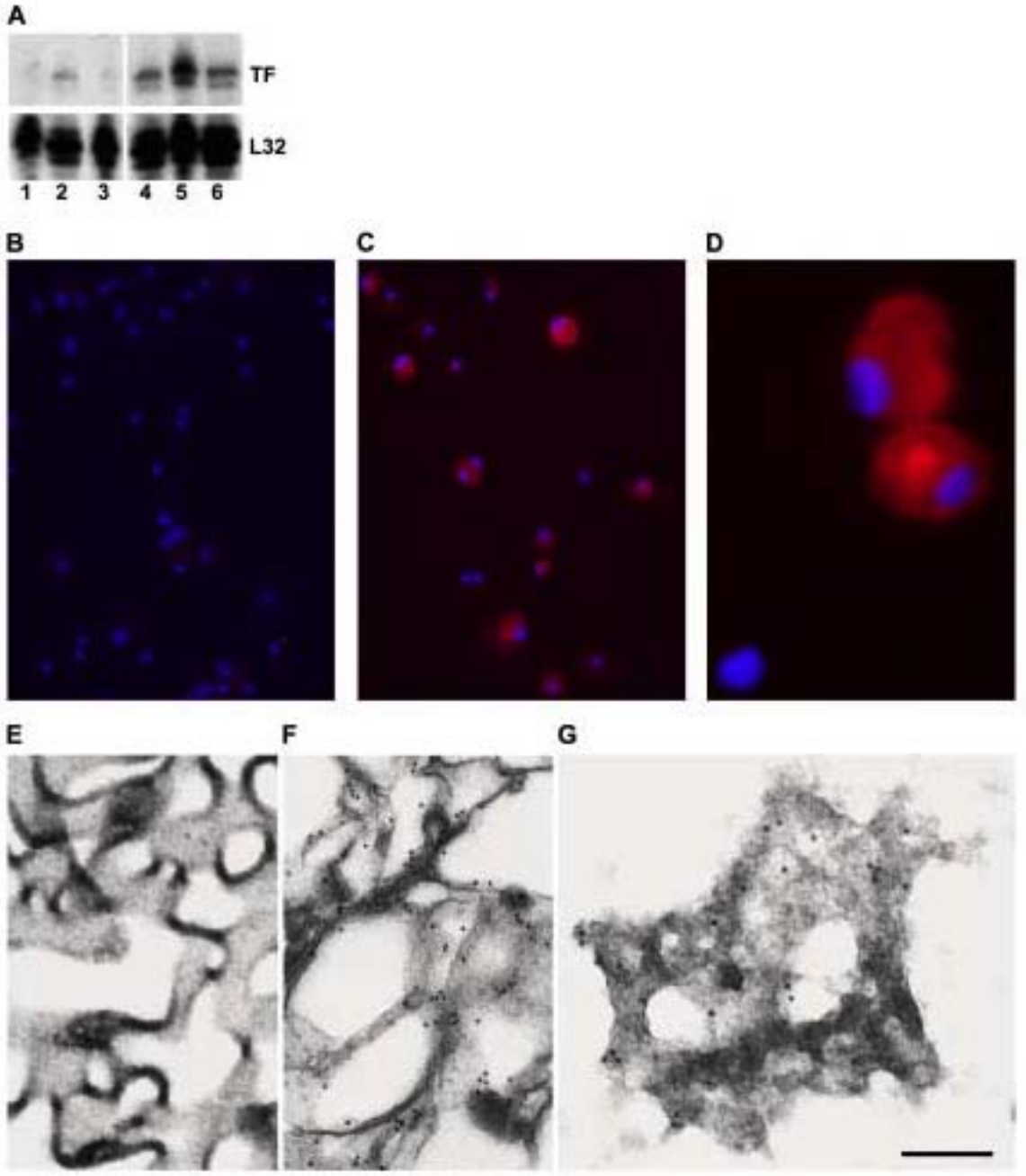

DISCUSSION

Identification of critical pathogenetic processes is important for the rational development of vaccines and chemotherapeutics against microbial pathogens. In the case of EBOV HF, few studies have addressed the underlying mechanisms of disease in primates, and very little is known about early host-pathogen interactions. This thesis presents the results of three specific aims: to determine whether dendritic cells are early cellular targets of EBOV *in vivo* and to determine whether bystander lymphocyte apoptosis is an early or late event in EBOV HF; to determine whether EBOV infection directly induces the activation/cytopathic disruption of the vascular endothelium; and to determine whether EBOV infection of primate monocytes/macrophages induces tissue factor gene transcription and tissue factor expression. This discussion attempts to integrate these results with previous findings on EBOV pathogenesis in primates and identify future avenues of research.

Results from Chapter 2 demonstrate, for the first time, that dendritic cells are early and sustained cellular targets of EBOV in macaques; that lymphocyte apoptosis is a relatively early event in disease progression; and furthermore, it is the NK cell fraction that is likely lost by increased apoptosis early in the course of infection. We also observed early and sustained infection of monocytes and macrophages, with EBOV RNA initially detected at day 2 postinfection. As monocytes and macrophages are usually the cells that elicit the response cascade in the acute phase of inflammation (Baumann and Gauldie, 1994), their early infection represents an effective strategy for evasion of the host defense system as well as facilitating dissemination of the virus.

Regarding the importance of EBOV predilection for dendritic cells in disease pathogenesis, EBOV may act in a manner similar to other viruses that are known to disable the host immune response by attacking and manipulating the very cells that play the most critical roles in initiating the antiviral immune response. Infection of dendritic cells by human cytomegalovirus was proposed to induce immunosuppression through a multilayered defense strategy that included partially downregulating MHC molecules, upregulating apoptosis-inducing ligands CD95L and tumor necrosis factor (TNF)-related apoptosis-inducing ligand (TRAIL) to delete activated T lymphocytes, complemented by a nondeletional mechanism involving undefined viral proteins that suppresses surviving T lymphocytes (Raftery *et al*., 2001). Of note, increased TRAIL expression and partial suppression of MHC II were associated with EBOV infection of immature dendritic cells *in vitro* (Hensley *et al*., 2002); apoptosis of bystander lymphocytes is a characteristic feature of EBOV infections (Geisbert *et al*., 2000); and furthermore, the well-chronicled discovery of an immunosuppressive motif in the C-terminal region of filoviral glycoproteins (Sanchez *et al*., 1993; Sanchez *et al*., 1996) lends some additional credence to this comparison. Thus, it is evident that interactions of viruses with dendritic cells are crucial for the outcomes of viral infections.

Pathological apoptosis of lymphocytes is likely to ablate protective immune responses. It is evident from results shown in Chapter 2 of this thesis that dysregulation of apoptosis is critical to the pathogenesis of EBOV HF. Analysis of peripheral blood mononuclear cell gene expression showed temporal increases in TRAIL and Fas transcripts revealing a possible mechanism for the observed bystander apoptosis, while upregulation of neuronal apoptosis inhibitory protein (NAIP) and cellular inhibitor of

apoptosis protein 2 (cIAP2) mRNA suggest that EBOV has evolved additional mechanisms to resist host defenses by inducing protective transcripts in cells that it infects. The early destruction of intravascular and extravascular lymphocytes likely prevents the immune system from clearing the virus. Classical apoptosis is dependent upon the activity of caspases, a family of cysteine proteases with key roles in the initiation and execution of cell death (reviewed in Zimmerman *et al*., 2001). There is also clear evidence that conserved caspase-independent pathways of apoptosis exist as well (reviewed in Bidere and Senik, 2001). Potent poly-caspase inhibitors, and small-molecule inhibitors of caspase-independent pathways, have been developed by various biotechnology companies (Podak 1999; Hotchkiss *et al*., 2000). Future studies to test the hypothesis that blockade of the pathological apoptosis of lymphocytes during EBOV HF will improve the survival of EBOV-infected nonhuman primates may now be warranted.

Whether infection of endothelial cells is central to the pathogenesis of EBOV HF has been debated for some time. Several recent studies suggested that the EBOV GP is the main determinant of vascular cell injury and therefore it is direct infection of endothelial cells that causes the hemorrhagic diathesis (Yang *et al*., 1998; Yang *et al*., 2000). This hypothesis has not been rigorously tested *in vitro* or *in vivo*. Viral infections can exert changes in the vascular endothelium in a variety of ways, such as inducing endothelial cell activation indirectly by infecting and activating leukocytes and triggering the synthesis and local production of proinflammatory soluble factors or by directly inducing changes in endothelial cell expression of cytokines, chemokines, and cellular adhesion molecules in the absence of immune mediators (as a direct result of viral infection). Mediators released from activated endothelial cells that can modulate vascular

tone, thrombosis, and/or inflammation include nitric oxide, prostacyclin, interferons, interleukin 1 (IL-1), IL-6, and chemokines such as IL-8 (Mantovani *et al*., 1992; Laroux *et al*., 2000). Few studies have evaluated the host gene response of endothelial cells infected with EBOV; work is restricted to a report of EBOV inhibiting induction of genes by double-stranded RNA (Harcourt *et al*., 1998).

Previous studies showed EBOV infection of endothelial cells in postmortem tissues from humans and nonhuman primates (Baskerville *et al*., 1985; Geisbert *et al*., 1992; Jaax *et al*., 1996; Davis *et al*., 1997; Zaki and Goldsmith, 1999a). In Chapter 3, we show that endothelial cells do not appear to be a primary early cellular target of EBOV. Replication of EBOV in endothelial cells was not consistently observed until day 5 postinfection in cynomolgus monkeys and, in fact, was an infrequent observation in most tissues at this late stage of disease. Of note, detection of EBOV in endothelial cells occurred a full day after the onset of indicators consistent with DIC, e.g., elevated levels of D-dimers. Electron microscopy confirmed that endothelium remained relatively intact even during terminal stages of disease.

Development of DIC is a characteristic clinical manifestation of EBOV infection in nonhuman primates, however the mechanism(s) for triggering the coagulation abnormalities remains unknown. Results from Chapter 4 provide the first insight into the pathogenesis of coagulation system dysregulation, and suggest that development of coagulation abnormalities may occur much earlier than previously thought. Although it is likely that the coagulopathy seen in EBOV HF is caused by multiple factors, particularly during the latter stages of disease, these new findings strongly implicate tissue factor expression/release from EBOV-infected monocytes/macrophages, and

dysregulation of the protein C system, as key factors that induce the development of coagulation irregularities seen in EBOV infections. Interestingly, increased transcripts for tissue factor were not detected in EBOV-infected endothelial cells *in vitro* consistent with studies showing that synthesis and exposure of endothelial tissue factor is very limited and not likely significant in emerging and ongoing DIC (Drake *et al*., 1993; Osterud and Bjorklid, 2001). Moreover, plasma from EBOV-infected monkeys at early- to mid-stages of disease contained increased numbers of tissue factor-expressing membrane microparticles. The procoagulant potential of membrane microparticles is supported by data from clinical studies showing elevated levels of circulating membrane microparticles in patients with an increased risk for thromboembolic events (e.g., DIC) (Nieuwland *et al*., 2000; Sabatier *et al*., 2002).

Levels of tissue factor expression may also be affected by the production of various cytokines and chemokines. Proinflammatory cytokines, such as IL-6, effectively upregulate tissue factor expression on monocytes (Neumann *et al*., 1997; Grignani and Maiolo, 2000). Elevated levels of IL-6 have been reported by day 4 postinfection in EBOV-infected monkeys (Hensley *et al*., 2002), and were seen by day 4 in the current study (Chapter 2). Splenocyte stimulation with tissue factor also induces the selective release of the monocyte chemoattractant molecule MIP-1α *in vitro* (Bokarewa *et al*., 2002). Increased levels of MIP-1α were previously reported in EBOV-infected monkeys and cultures of infected monocytes/macrophages (Hensley *et al*., 2002), and were highly elevated in monkeys by day 4 as shown in Chapter 2. Taken together, these findings suggest that tissue factor expression can be amplified during the later stages of diseases when EBOV-infected cells, which selectively express tissue factor, release chemokines.

Chemokine release may either directly upregulate levels of tissue factor or attract additional preferred target cells to foci of infection, thereby exacerbating activation of the extrinsic blood coagulation pathway. Tissue factor expression may also be amplified in the latter stages of disease as a result of tissue damage caused by the formation of microthrombi. Specifically, development of these microthrombi during disease, as a result of tissue factor overexpression, can produce tissue damage, as evidenced by the strong increase in plasma levels of tissue-type plasminogen activator noted in EBOV-infected monkeys (Chapter 4); these areas of tissue damage may then augment the effect by inducing local upregulation of tissue factor.

Identifying tissue factor as an initiating aspect of DIC, and dysregulation of protein C as an exacerbating factor, may be central to explaining the mechanisms triggering the hemorrhagic diathesis of EBOV infection. The results presented in Chapter 4 represent a first step in demonstrating that chemotherapeutic strategies aimed at controlling tissue factor overexpression, and dysregulation of the protein C system, may ameliorate the effects of EBOV HF. Others have shown that inhibition of the tissue factor pathway attenuates coagulopathy and reduces and/or prevents lethal effects in nonhuman primate models of septic shock (Taylor *et al*., 1991; Carr *et al*., 1994). Moreover, strategies that have proven successful for treating patients with similar clinical pictures, such as administering activated protein C in severe sepsis (Bernard *et al*., 2001), may also have utility in treating EBOV infections.

The results of the work presented in this thesis, and insight gained from historical studies, demonstrate that the nonhuman primate system is an extremely relevant model for studying EBOV pathogenesis. Despite the lack of inbred or pedigreed strains, and

practical and ethical considerations that limit sizes of experiments, nonhuman primates remain the most useful and valid model of EBOV HF. Rodent models have been developed, and clearly have utility, but require serial adaptation of the virus to produce lethal disease (Bray *et al*., 1998; Connolly *et al*., 1999). Furthermore, because of differences in the disease pathology (Geisbert *et al*., 2002) there are numerous scientific questions that cannot be satisfactorily addressed by an evaluation only in rodents. Nonhuman primates are phylogenetically closely related to humans and most genes, serum proteins, and other factors that require analysis, are biochemically and antigenically similar to those of humans. Several species of nonhuman primates have been used to model EBOV HF, and which species most accurately reproduces human disease is debatable. Nonetheless, the cynomolgus and rhesus macaques appear to be excellent animal models for human EBOV HF.

The pathogenesis studies described in this thesis employed a parenteral route of exposure for several reasons including applicability to laboratory-acquired exposures and comparison with previously published and ongoing studies. Importantly, all of the current EBOV candidate vaccines in development employ an intramuscular challenge. However, additional research needs to be done in the area of aerosol-acquired infections before these vaccines become a reality. When planning defenses against biological warfare agents such as filoviruses, it is important to consider that the inhalation route is the most likely portal of entry for agents disseminated as aerosols (Eitzen, 1997; Jahrling, 1997). It is known that the former Soviet Union experimented with aerosolized EBOV and MBGV (Alibek and Handelman, 1999; Miller *et al*., 2001). Despite the risks that filoviruses pose as threat agents, and the fact that the inhalation route is the most likely

portal of entry, there is a paucity of information regarding the capability of filoviruses to colonize the lower respiratory tract, and thereby breach the barrier function of the lungs, with resultant systemic viremia. Lethal aerosol exposure of nonhuman primates to EBOV has been reported (Johnson *at al*., 1995; P'yankov *et al*. 1995). Additionally, Bazhutin et al. (1992) compared the influence of the method of experimental infection with MBGV on the course of illness in African green monkeys. The authors showed a reduced lethality with aerosol exposure to MBGV but were unable to determine whether or not the survival differences were due to the alternative methods of infection. None of these aerogenic filoviral studies have characterized the release and/or role of any response mediators nor have they provided specific details regarding any dysregulation of normal host immune responses. A number of studies with other RNA viruses have shown that vaccines developed to protect against parenteral infections do not always protect against aerosol challenge (Jahrling *et al*., 1984; Pratt *et al*., 1998). This inconsistency is likely due to the fact that different pathways of virus spread are associated with varied host immune responses. Future efforts will be needed to identify the critical pathogenic mechanisms of aerosol EBOV exposures and determine whether or not there are different pathogenetic mechanisms associated with different routes of exposure. Knowledge of the specific mechanisms used by EBOV to regulate inflammatory processes in aerosol-acquired infections will be important for designing rational vaccines and will augment efforts to develop therapeutic modalities to combat EBOV infections.

Undoubtedly, the primary cellular targets of EBOV in primates are cells of the mononuclear phagocyte system (Geisbert *et al*., 1992; Stroher *et al*., 2001; Hensley *et al*.,

2002). Neither lymphocyte depletion nor lymphopenia is caused by EBOV infection of lymphocytes (Geisbert *et al*., 1992; Geisbert *et al*., 2000) and fibrin thrombi/hemorrhages associated with EBOV do not appear to be the result of direct infection-induced cytolysis of endothelial cells. In summary, the paradigm that we propose for EBOV pathogenesis in nonhuman primates (Figure 2), based on results presented in this thesis, is as follows: EBOV spreads from the initial infection site via monocytes/macrophages and dendritic cells to regional lymph nodes, likely via lymphatics, and to the liver and spleen via blood. At these sites, EBOV infects tissue macrophages (including Kupffer cells), dendritic cells and fibroblastic reticular cells. EBOV activates killer antigen-presenting cells (e.g., dendritic cells) early in the course of infection by upregulating expression of TRAIL. Such overexpression of TRAIL, which is sustained over the course of disease by overexpression of IFN-α, participates in T lymphocyte deletion via bystander apoptosis, lymphopenia, and establishment of virus-induced immunosuppression. Concomitantly, EBOV-infected monocytes/macrophages release various soluble factors including proinflammatory cytokines such as MIP-1α and MCP-1 that recruit additional macrophages to areas of infection making more target cells available for viral exploitation, and further amplifying an already dysregulated host response. As disease progresses, increased levels of oxygen free radicals (e.g., nitric oxide), released by EBOV-infected macrophages at inflammatory sites, trigger apoptosis of bystander NK cells, thwarting the innate immune response and leaving the host little time to mount an adaptive response. Left unchecked, extensive viral replication leads to increased levels of additional proinflammatory cytokines, notably IL-6, which triggers the coagulation cascade likely through upregulation of tissue factor on monocytes/macrophages.

Activation of the coagulation cascade, in turn, activates the fibrinogenic and fibrinolytic pathways leading to DIC. Inhibitors of the clotting system, particularly protein C, are consumed at a rate that exceeds synthesis by liver parenchymal cells, many of which by this point may have been rendered dysfunctional by the viral assault. Impairment of the coagulation system results in rapid progression of DIC, hemorrhagic shock, multiple organ failure, and finally death of the host.

This sequence of morphologic, cytologic, virologic, serologic, and inflammatory change following EBOV infection creates a useful model in the study of experimentally induced EBOV HF and the sequence of pathogenetic events identified should provide new targets for rational prophylactic and chemotherapeutic interventions. Because of massive synergism and redundancy in the pathways of inflammation associated with hemorrhagic shock, it is likely that combined or appropriate sequential targeting of the above-listed pathways will be more effective than targeting a single pathway.

Figure 2. Paradigm showing key cellular events in EBOV pathogenesis in primates. EBOV infection of monocytes/macrophages appears to be central to much of the observed pathology. EBOV infection induces monocytes/macrophages to release a variety of soluble factors that likely trigger a host of downstream events including bystander apoptosis of lymphocytes, activation of the coagulation cascade, and disruption of the vascular endothelium. The end result is loss of homeostasis and dysregulation of the host immune response.

Figure 2

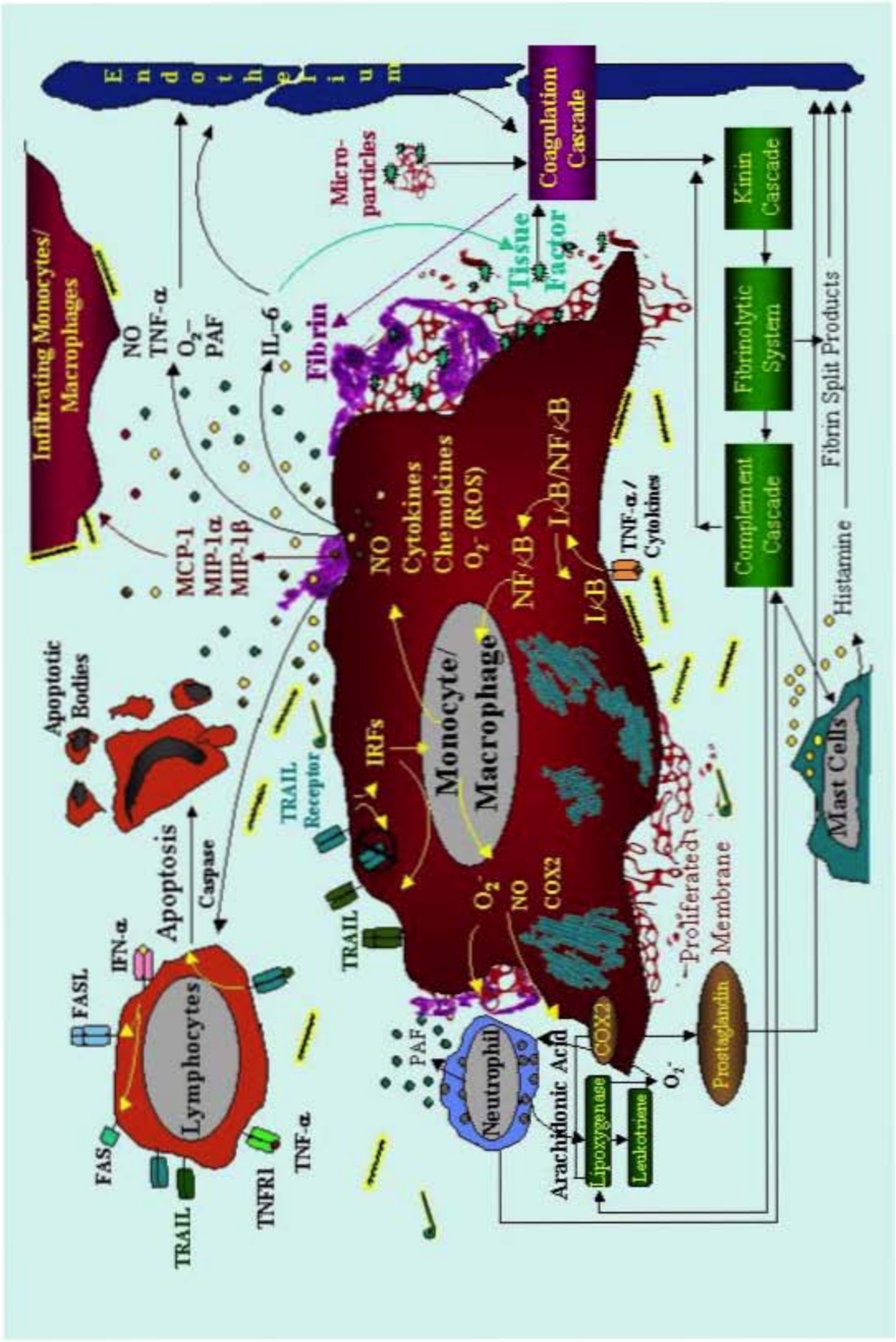
Endothelium
Infiltrating Monocytes/ Macrophages
NO
TNF-α
O2–
PAF
IL-6
Micro-particles
Coagulation Cascade
Tissue Factor
Fibrin
Kinin Cascade
Fibrinolytic System
Complement Cascade
Fibrin Split Products
Histamine
Mast Cells
MCP-1
MIP-1α
MIP-1β
NO
Cytokines
Chemokines
O2- (ROS)
NFκB
IκB/NFκB
IκB
TNF-α / Cytokines
Monocyte/ Macrophage
IRFs
TRAIL Receptor
Apoptotic Bodies
Apoptosis
Caspase
FASL
IFN-α
Lymphocytes
FAS
TRAIL
TNFR1
TNF-α
TRAIL
O2-
NO
COX2
Proliferated Membrane
PAF
Neutrophil
Arachidonic Acid
COX2
Lipoxygenase
Leukotriene
O2-
Prostaglandin

REFERENCES

Alibek, K., and S. Handelman. Biohazard: The Chilling True Story of the Largest Covert Biological Weapons Program in the World. Told From the Inside by the Man Who Ran It. Random House, New York, NY.

Baize, S., E.M. Leroy, M.-C. Georges-Courbot, M. Capron, J. Lansoud-Soukate, P. Debre, S.P. Fisher-Hoch, J.B. McCormick, and A.J. Georges. 1999. Defective humoral responses and extensive intravascular apoptosis are associated with fatal outcome in Ebola virus-infected patients. Nature Med. 5: 423-426.

Baize, S., E.M. Leroy, A.J. Georges, M.-C. Georges-Courbot, M. Capron, I. Bedjabaga, J. Lansoud-Soukate, and E. Mavoungou. 2002. Inflammatory responses in Ebola virus-infected patients. Clin. Exp. Immunol. 128:163-168.

Baskerville, A., S.P. Fisher-Hoch, G.H. Neild, and A.B. Dowsett. 1985. Ultrastructural pathology of experimental Ebola haemorrhagic fever virus infection. J. Pathol. 147:199-209.

Baumann, H., and J. Gauldie. 1994. The acute phase response. Immunol. Today. 15:74-89.

Bazhutin, N.B., E.F. Belanov, V.A. Spiridonov, A.V. Voitenko, N.A. Krivenchuk, S.A. Krotov, N.I. Omel'chenko, A.Iu. Tereshchenko, and V.V. Khomichev. 1992. The effect of the methods for producing an experimental Marburg virus infection on the characteristics of the course of the disease in green monkeys. Vopr. Virusol. 37:153-156.

Bernard, G.R., J.L. Vincent, P.F. Laterre, S.P. LaRosa, J.F. Dhainaut, A. Lopez-Rodriguez, J.S. Steingrub, G.E. Garber, J.D. Helterbrand, E.W. Ely, et al. 2001. Efficacy and safety of recombinant human activated protein C for severe sepsis. N. Engl. J. Med. 344:699-709.

Bidere N, and A. Senik. 2001. Caspase-independent apoptotic pathways in T lymphocytes: a minireview. Apoptosis. 6:371-5.

Bokarewa, M.I., J.H. Morissey, and A. Tarkowski. 2002. Tissue factor as a proinflammatory agent. Arthritis Res. 4:190-195.

Borisevich, I.V., V.V. Mikhailov, V.P. Krasnyanskii, V.N. Gradoboev, Ye.V. Lebedinskaya, N.V. Potryvaeva, and G.D. Timan'kova. 1995. Creation and study of immunoglobulin to Ebola fever. Vopr. Virusol. 40:270-273.

Bowen, E.T.W., G. Lloyd, W.J. Harris, G.S. Platt, A. Baskerville, and E.E. Vella. 1977. Viral haemorrhagic fever in southern Sudan and northern Zaire. Lancet. 1:571-573.

Bowen, E.T.W., G.S. Platt, D.I.H. Simpson, L.B. McArdell, and R.T. Raymond. 1978. Ebola haemorrhagic fever: experimental infection of monkeys. Trans. R. Soc. Trop. Med. Hyg. 72: 188-191.

Bowen, E.T.W., G.S. Platt, G. Lloyd, R.T. Raymond, and D.I.H. Simpson. 1980. A comparative study of strains of Ebola virus isolated from southern Sudan and northern Zaire in 1976. J. Med. Virol. 6:129-138.

Bray, M., K. Davis, T. Geisbert, C. Schmaljohn, and J. Huggins. 1998. A mouse model for evaluation of prophylaxis and therapy of Ebola hemorrhagic fever. J. Infect. Dis. 178: 651-661.

Bray, M., S. Hatfill, L. Hensley, and J.W. Huggins. 2001. Haematological, biochemical and coagulation changes in mice, guinea-pigs and monkeys infected with a mouse-adapted variant of Ebola Zaire virus. J. Comp. Pathol. 125:243-253.

Breman, J.G., P. Piot, K.M. Johnson, M.K. White, M. Mbuyi, P. Sureau, D.L. Heymann, S. van Nieuwenhove, J.B. McCormick, J.P. Ruppol, V. Kintoki, M. Isaacson, G. van der Groen, P.A. Webb, and K. Ngvete. 1978. The epidemiology of Ebola haemorrhagic fever in Zaire, 1976, p. 103-124. *In* S.R. Pattyn (ed.), Ebola Virus Haemorrhagic Fever. Elsevier/North-Holland, Amsterdam.

Carr, C., G.S. Bild, A.C. Chang, G.T. Peer, M.O. Palmier, R.B. Frazier, M.E. Gustafson, T.C. Wun, A.A. Creasey, L.B. Hinshaw, et al. 1994. Recombinant E. coli-derived tissue factor pathway inhibitor reduces coagulopathic and lethal effects in the baboon gram-negative model of septic shock. Circ. Shock. 44:126-37.

Centers for Disease Control and Prevention. 2001. Outbreak of Ebola hemorrhagic fever Uganda, August 2000-January 2001. MMWR Morb. Mortal. Wkly. Rep. 50:73-77.

Chan, S.Y., M.C. Ma, and M.A. Goldsmith. 2000. Differential induction of cellular detachment by envelope glycoproteins of Marburg and Ebola (Zaire) viruses. J. Gen. Virol. 81:2155-2159.

Chepurnov, A.A., I.V. Chernukhin, V.A. Ternovoi, N.M. Kudoyarova, N.M. Makhova, M.Sh. Azaev, and M.P. Smolina. 1995. Attempts to obtain a vaccine against Ebola fever. Vopr. Virusol. 40:257-260.

Chepurnov, A.A., Y.P. Chuev, O.V. P'yankov, and I.V. Efimova. 1995. Effects of some physical and chemical factors of inactivation of Ebola virus. Vopr. Virusol. 40:74-76.

Connolly, B.M., K.E. Steele, K.J. Davis, T.W. Geisbert, W.M. Kell, N.K. Jaax, and P.B. Jahrling. 1999. Pathogenesis of experimental Ebola virus infection in guinea pigs. J. Infect. Dis. Suppl. 179:S203-S217.

Davis, K.J., A.O. Anderson, T.W. Geisbert, K.E. Steele, J.B. Geisbert, P. Vogel, B.M. Connolly, J.W. Huggins, P.B. Jahrling, and N.K. Jaax. 1997. Pathology of experimental Ebola virus infection in African green monkeys. Arch. Pathol. Lab. Med. 121:805-819.

Dietrich, M., H.H. Schumacher, D. Peters, and J. Knobloch. 1978. Human pathology of Ebola (Maridi) virus infection in the Sudan, p. 37-42, In S.R. Pattyn (ed.), Ebola Virus Haemorrhagic Fever. Elsevier/North-Holland, Amsterdam.

Dowell, S.F., R. Mukunu, T.G. Ksiazek, A.S. Khan, P.E. Rollin, and C.J. Peters. 1999. Transmission of Ebola hemorrhagic fever: a study of risk factors in family members, Kikwit, Democratic Republic of the Congo, 1995. J. Infect. Dis. Suppl. 179:S87-S91.

Drake, T.A., J. Cheng, A. Chang, and F.B. Taylor, Jr. 1993. Expression of tissue factor, thrombomodulin, and E-selectin in baboons with lethal *escherichia coli* sepsis. Am. J. Pathol. 142:1458-1470.

Eitzen, E.M. 1997. Use of biological weapons, p. 437-450. *In* Medical Aspects of Chemical and Biological Warfare, Textbook of Military Medicine. Part 1. Warfare, Weaponry, and Casualty. Office of the Surgeon General at TMM Publications, Washington D.C.

Ellis, D.S., D.I.H. Simpson, D.P. Francis, J. Knobloch, E.T. Bowen, P. Lolik, and I.M. Deng. 1978. Ultrastructure of Ebola virus particles in human liver. J. Clin. Pathol. 31:201-208.

Feldmann, H., and M.P. Kiley. 1999. Classification, structure, and replication of filoviruses. Curr. Top. Microbiol. Immunol. 235:1-22.

Fisher-Hoch, S.P., G.S. Platt, G. Lloyd, D.I. Simpson, G.H. Neild, and A.J. Barrett. 1983. Haematological and biochemical monitoring of Ebola infection in rhesus monkeys: implications for patient management. Lancet. 2:1055-1058.

Fisher-Hoch, S.P., G.S. Platt, G.H. Neild, T. Southee, A. Baskerville, R.T. Raymond, G. Lloyd, and D.I.H. Simpson. 1985. Pathophysiology of shock and hemorrhage in a fulminating viral infection (Ebola). J. Infect. Dis. 152:887-894.

Fisher-Hoch, S.P., L.T. Brammer, S.G. Trappier, L.C. Hutwagner, B.B. Farrar, S.L. Ruo, B.G. Brown, L.M. Hermann, G.I. Perez-Oronoz, C.S. Goldsmith, M.A. Hanes, and J.B. McCormick. 1992. Pathogenic potential of filoviruses: role of geographic origin of primate host and virus strain. J. Infect. Dis. 166:753-763.

Formenty, P., C. Boesch, M. Wyers, C. Steiner, F. Donati, F. Dind, F. Walker, and B. Le Guenno. 1999. Ebola virus outbreak among wild chimpanzees living in a rain forest of Côte d'Ivoire. J. Infect. Dis. Suppl. 179:S120-S126.

Geisbert, T.W., and P.B. Jahrling. 1995. Differentiation of filoviruses by electron microscopy. Virus Res. 39:129-150.

Geisbert, T.W., P.B. Jahrling, M.A. Hanes, and P.M. Zack. 1992. Association of Ebola related Reston virus particles and antigen with tissue lesions of monkeys imported to the United States. J. Comp. Pathol. 106:137-152.

Geisbert, T.W., L.E. Hensley, T.R. Gibb, K.E. Steele, N.K. Jaax, and P.B. Jahrling. 2000. Apoptosis induced in vitro and in vivo during infection by Ebola and Marburg viruses. Lab. Invest. 80:171-186.

Geisbert, T.W., L.E. Hensley, J.B. Geisbert, and P.B. Jahrling. 2002. Evidence against an important role for infectivity-enhancing antibodies in Ebola virus infections. Virology. 293:15-19.

Geisbert, T.W., P. Pushko, K. Anderson, J. Smith, K.J. Davis, and P.B. Jahrling. 2002. Evaluation in nonhuman primates of vaccines against Ebola virus. Emerg. Infect. Dis. 8:503-507.

Georges-Courbot, M.C., A. Sanchez, C.Y. Lu, S. Baize, E. Leroy, J. Lansout-Soukate, C. Tevi-Benissan, A.J. Georges, S.G. Trappier, S.R. Zaki, R. Swanepoel, P.A. Leman, P.E. Rollin, C.J. Peters, S.T. Nichol, and T.G. Ksiazek. 1997. Isolation and phylogenetic characterization of Ebola viruses causing different outbreaks in Gabon. Emerg. Infect. Dis. 3:59-62.

Grignani, G., and A. Maiolo. 2000. Cytokines and hemostasis. Haematologica. 85:967-972 .

Harcourt, B.H., A. Sanchez, and M.K. Offerman. 1998. Ebola virus inhibits induction of genes by double-stranded RNA in endothelial cells. Virology. 252:179-188.

Hensley, L.E., H.A. Young, P.B. Jahrling, and T.W. Geisbert. 2002. Proinflammatory response during Ebola virus infection of primate models: possible involvement of the tumor necrosis factor receptor superfamily. Immunol. Lett. 80:169-179.

Hotchkiss, R.S., K.C. Chang, P.E. Swanson, K.W. Tinsley, J.J. Hui, P. Klender, S. Xanthoudakis, S. Roy, C. Black, E. Grimm, R. Aspiotis, Y. Han, D.W. Nicholson,

and I.E. Karl. 2000. Caspase inhibitors improve survival in sepsis: a critical role of the lymphocyte. Nat. Immunol. 1:496-501.

Isaacson, M., P. Sureau, G. Courteille, and S.R. Pattyn. 1978. Clinical aspects of Ebola virus disease at the Ngaliema hospital, Kinshasa, Zaire, 1976, p. 15-20. *In* S.R. Pattyn (ed.), Ebola Virus Haemorrhagic Fever. Elsevier/North-Holland, Amsterdam.

Jaax, N.K., K.J. Davis, T.W. Geisbert, P. Vogel, G.P. Jaax, M. Topper, and P.B. Jahrling. 1996. Lethal experimental infection of rhesus monkeys with Ebola-Zaire (Mayinga) virus by the oral and conjunctival route of exposure. Arch. Pathol. Lab. Med. 120:140-155.

Jaax, N., P. Jahrling, T. Geisbert, J. Geisbert, K. Steele, K. McKee, D. Nagley, E. Johnson, G. Jaax, and C. Peters. 1995. Transmission of Ebola virus (Zaire strain) to uninfected control monkeys in a biocontainment laboratory. Lancet. 346:1669-1671.

Jahrling P.B., and E.H. Stephenson. 1984. Protective efficacies of live attenuated and formaldehyde-inactivated Venezuelan equine encephalitis virus vaccines against aerosol challenge in hamsters. J. Clin. Microbiol. 19:429-431.

Jahrling, P.B., T.W. Geisbert, D.W. Dalgard, E.D. Johnson, T.G. Ksiazek, W.C. Hall, and C.J. Peters. 1990. Preliminary report: isolation of Ebola virus from monkeys imported to USA. Lancet. 335:502-505.

Jahrling, P.B., J. Geisbert, J.R. Swearengen, G.P. Jaax, T. Lewis, J.W. Huggins, J.J. Schmidt, J.W. LeDuc, and C.J. Peters. 1996a. Passive immunization of Ebola virus-

infected cynomolgus monkeys with immunoglobulin from hyperimmune horses. Arch. Virol. Suppl. 11:135-140.

Jahrling, P.B., T.W. Geisbert, N.K. Jaax, M.A. Hanes, T.G. Ksiazek, and C.J. Peters. 1996b. Experimental infection of cynomolgus macaques with Ebola-Reston filoviruses from the 1989-1990 U.S. epizootic. Arch. Virol. Suppl. 11:115-134.

Jahrling, P.B. 1997. Viral Hemorrhagic Fevers, p. 591-602. *In* Medical Aspects of Chemical and Biological Warfare, Textbook of Military Medicine. Part 1. Warfare, Weaponry, and Casualty. Office of the Surgeon General at TMM Publications, Washington, D.C.

Jahrling, P.B., T.W. Geisbert, J.B. Geisbert, J.R. Swearengen, M. Bray, N.K. Jaax, J.W. Huggins, J.W. LeDuc, and C.J. Peters. 1999. Evaluation of immune globulin and recombinant Interferon-α2b for treatment of experimental Ebola virus infections. J. Infect. Dis. Suppl. 179:S224-S234.

Johnson, E., N. Jaax, J. White, and P. Jahrling. 1995. Lethal experimental infections of rhesus monkeys by aerosolized Ebola virus. Int. J. Exp. Pathol. 76:227-236.

Johnson, K.M., J.V. Lange, P.A. Webb, and F.A. Murphy. 1977. Isolation and partial characterization of a new virus causing acute haemorrhagic fever in Zaire. Lancet. 1:569-571.

Kayagaki, N., N. Yamaguchi, M. Nakayama, H. Eto, K. Okumura, and H. Yagita. 1999. Type I interferons (IFNs) regulate tumor necrosis factor-related apoptosis-inducing ligand (TRAIL) expression on human T cells: a novel mechanism for the antitumor effects of type I INFs. J. Exp. Med. 189:1451-1460.

Khan, A.S., K. Tshioko, D.L. Heymann, B. Le Guenno, P. Nabreth, B. Kerstiens, Y. Fleerackers, P.H. Kilmarx, G.R. Rodier, O. Nkuku, P.E. Rollin, A. Sanchez, S.R. Zaki, R. Swanepoel, O. Tomori, S.T. Nichol, C.J. Peters, J.J. Muyembe-Tamfum, and T.G. Ksiazek. 1999. The reemergence of Ebola hemorrhagic fever, Democratic Republic of the Congo, 1995. J. Infect. Dis. Suppl. 179:S76-S86.

Kruse M, O. Rosorius, F. Kratzer, G. Stelz, C. Kuhnt, G. Schuler, J. Hauber, and A. Steinkasserer. 2000. Mature dendritic cells infected with herpes simplex virus type 1 exhibited inhibited T-cell stimulatory capacity. 74:7127-7136.

Ksiazek, T.G., P.E. Rollin, A.J. Williams, D.S. Bressler, M.L. Martin, R. Swanepoel, F.J. Burt, P.A. Leman, A.S. Khan, A.K. Rowe, R. Mukunu, A. Sanchez, and C.J. Peters. 1999. Clinical virology of Ebola hemorrhagic fever (EHF): virus, virus antigen, and IgG and IgM antibody findings among EHF patients in Kikwit, Democratic Republic of the Congo, 1995. J. Infect. Dis. Suppl. 179:S177-87.

Kudoyarova-Zubavichene, N.M., N.N. Sergeyev, A.A. Chepurnov, and S.V. Netesov. 1999. Preparation and use of hyperimmune serum for prophylaxis and therapy of Ebola virus infections. J. Infect. Dis. Suppl. 179:S218-S223.

Laroux, F.S., D.J. Lefer, S. Kawachi, R. Scalia, A.S. Cockrell, L. Gray, H. Van der Heyde, J.M. Hoffman, and M.B. Grisham. 2000. Role of nitric oxide in the regulation of acute and chronic inflammation. Antioxid. Redox. Signal. 2:391-396.

Le Guenno, B., P. Formenty, M. Wyers, P. Gounon, F. Walker, and C. Boesch. 1995. Isolation and partial characterization of a new strain of Ebola virus. Lancet. 345:1271-1274.

Leirs, H., J.N. Mills, J.W. Krebs, J.E. Childs, D. Akaibe, N. Woollen, G. Ludwig, C.J. Peters, and T.G. Ksiazek. 1999. Search for the Ebola virus reservoir in Kikwit, Democratic Republic of the Congo: reflections on a vertebrate collection. J. Infect. Dis. Suppl. 179:S155-63.

Levi, M., E. de Jonge, T. van der Poll, and H. ten Cate. 1999. Disseminated intravascular coagulation. Thromb. Haemost. 82:695-705.

Levi M, E. de Jonge, T. van der Poll, and H. ten Cate. 2001. Advances in the understanding of the pathogenetic pathways of disseminated intravascular coagulation result in more insight in the clinical picture and better management strategies. Semin Thromb. Hemost. 27:569-75.

Mammen, E.F. 2000. Disseminated intravascular coagulation (DIC). Clin. Lab. Sci. 13:239-245.

Mantovani, A., F. Bussolino, and E. Dejana. 1992. Cytokine regulation of endothelial cell function. FASEB J. 6:2591-2599.

Markin, V.A., V.V. Mikhailov, V.P. Krasnyanskii, I.V. Borisevich, and I.V. Firsova. 1997. Development of emergency prophylaxis and treatment of Ebola fever. Vopr. Virusol. 42:31-34.

Maruyama, T., M.J. Buchmeier, P.W.H.I. Parren, and D.R. Burton. 1998. Ebola virus, neutrophils, and antibody specificity. Science. 282:845.

Mikhailov, V.V., I.V. Borisevich, N.K. Chernikova, N.V. Potryvaeva, and V.P. Krasnyanskii. 1994. An evaluation of the possibility of Ebola fever specific prophylaxis in baboons (Papio hamadryas). Vopr. Virusol. 39:82-84.

Miller, J., S. Engelberg, and W.J. Broad. 2001. Germs: Biological Weapons and America's Secret War. Simon & Schuster, Waterville, Me.

Murphy, F.A. 1978. Pathology of Ebola virus infection, p. 43-60. *In* S.R. Pattyn (ed.), Ebola Virus Haemorrhagic Fever. Elsevier/North-Holland, Amsterdam.

Neumann, F.-J., I. Ott, N. Marx, T. Luther, S. Kenngott, M. Gawaz, M. Kotzsch, and A. Schomig. 1997. Effect of human recombinant interleukin-6 and interleukin-8 on monocyte procoagulant activity. Arterioscler. Thromb. Vasc. Biol. 17:3399-3405.

Nieuwland, R., R.J. Berckmans, S. McGregor, A.N. Boing, F.P. Romijn, R.G. Westendorp, C.E. Hack, and A. Sturk. 2000. Cellular origin and procoagulant properties of microparticles in meningococcal sepsis. Blood. 95:930-935.

Osterud, B. and E. Bjorklid. 2001. The tissue factor pathway in disseminated intravascular coagulation. Semin. Thromb. Hemost. 27:605-617.

Parren, P.W.H.I., T.W. Geisbert, T. Maruyama, P.B. Jahrling, and D.R. Burton. 2002. Pre- and Post-exposure prophylaxis of Ebola virus infection in an animal model by passive transfer of a neutralizing human antibody. J. Virol. 76:6408-6412.

Peters, C.J., and J.W. LeDuc. 1999. An introduction to Ebola virus: the virus and the disease. J. Infect. Dis. Suppl. 179:ix-xvi.

Podak, E.R. 1999. How to induce voluntary suicide: the need for dipeptidyl peptidase I. Proc. Natl. Acad. Sci. USA. 96:8312-8314.

Pratt, W.D., Gibbs, P., Pitt, M.L., and Schmaljohn, A.L. 1998. Use of telemetry to assess vaccine-induced protection against parenteral and aerosol infections of Venezuelan equine encephalitis virus in non-human primates. Vaccine. 16:1056-1064.

P'yankov, O.V., A.N. Sergeev, O.G. P'yankova, and A.A. Chepurnov. 1995. Experimental Ebola fever in macaca rhesus. Vopr. Virusol. 40:113-115.

Raftery, M.J., M. Schwab, S.M. Eibert, Y. Samstag, H. Walczak, and G. Schonrich G. 2001. Targeting the function of mature dendritic cells by human cytomegalovirus: a multilayered viral defense strategy. Immunity. 15:997-1009.

Rassadkin, Y.N., A.A. Gradgdantseva, and S.V. Lutchko. 2000. Comparative sensitivity to the lowest monkeys species to Ebola virus. In: Initiatives for Proliferation Prevention. International Science and Technology Center, Ministry of Science and Technologies of Russia, and North Atlantic Treaty Organization, eds. 2nd Session: Emerging and Reemerging Infectious Diseases – Basic Research. Advanced Research Workshop. Assessment of Sponsored Biological Research in Russia for the New Millenium, September 2-4, Novosibirsk, Novosibirsk Region, Russia.

Rodriguez, L.L., A. De Roo, Y. Guimard, S.G. Trappier, A. Sanchez, D. Bressler, A.J. Williams, A.K. Rowe, J. Bertolli, A.S. Khan, T.G. Ksiazek, C.J. Peters, and S.T. Nichol. 1999. Persistence and genetic stability of Ebola virus during the outbreak in Kikwit, Democratic Republic of the Congo, 1995. J. Infect. Dis. Suppl. 179:S170-S176.

Rowe, A.K., J. Bertolli, A.S. Khan, R. Mukunu, J.J. Muyembe-Tamfum, D. Bressler, A.J. Williams, C.J. Peters, L. Rodriguez, H. Feldmann, S.T. Nichol, P.E. Rollin, and T.G. Ksiazek. 1999. Clinical, virologic, and immunologic follow-up of convalescent Ebola hemorrhagic fever patients and their household contacts, Kikwit, Democratic Republic of the Congo. J. Infect. Dis. Suppl. 179:S28-S35.

Ryabchikova, E., L. Kolesnikova, M. Smolina, V. Tkachev, L. Pereboeva, A. Grazhdantseva, and Y. Rassadkin. 1996. Ebola virus infection of guinea pigs: presumable role of granulomatous infection in pathogenesis. Arch. Virol. 141:909-921.

Ryabchikova, E.I., L.V. Kolesnikova, and S.V. Luchko. 1999a. An analysis of features of pathogenesis in two animal models of Ebola virus infection. J. Infect. Dis. Suppl. 179:S199-S202.

Ryabchikova, E.I., L.V. Kolesnikova, and S.V. Netesov. 1999b. Animal pathology of filoviral infections. Curr. Top. Microbiol. Immunol. 235:145-173.

Sabatier, F., V. Roux, F. Anfosso, L. Camoin, J. Sampol, and F. Dignat-George. 2002. Interaction of endothelial microparticles with monocytic cells in vitro induces tissue factor-dependent procoagulant activity. Blood. 99:3962-3970.

Sanchez, A., M.P. Kiley, B.P. Holloway, and D.D. Auperin. 1993. Sequence analysis of the Ebola virus genome: organization, genetic elements, and comparison with the genome of Marburg virus. Virus Res. 29:215-240.

Sanchez, A., S.G. Trappier, B.W.J. Mahy, C.J. Peters, and S.T. Nichol. 1996. The virion glycoprotein of Ebola viruses are encoded in two open reading frames and are expressed through transcriptional editing. Proc. Natl. Acad. Sci. USA. 93:3602-3607.

Sanchez, A., Z.Y. Yang, L. Xu, G.J. Nabel, T. Crews, and C.J. Peters. 1998. Biochemical analysis of the secreted and virion glycoproteins of Ebola virus. J. Virol. 72:6422-6447.

Sanchez, A., T.G. Ksiazek, P.E. Rollin, M.E. Miranda, S.G. Trappier, A.S. Khan, C.J. Peters, and S.T. Nichol. 1999. Detection and molecular characterization of Ebola viruses causing disease in human and nonhuman primates. J. Infect. Dis. Suppl. 179:S164-169.

Sanchez, A., A.S. Khan, S.R. Zaki, G.J. Nabel, T.G. Ksiazek, and C.J. Peters. 2001. Filoviridae: Marburg and Ebola viruses. In: Fields Virology. D.M. Knipe, P.M. Howley, eds. Lippincott Williams & Wilkins, Philadelphia, pp 1279-1304.

Semeraro, N., and M. Colucci. 1997. Tissue factor in health and disease. Thromb. Haemost. 78:759-764.

Sevilla, N., Kunz, S., Holz, A., Lewicki, H., Homann, D., Yamada, H., Campbell, K.P., J.C. de la Torre, and M.B. Oldstone. 2000. Immunosuppression and resultant viral persistence by specific viral targeting of dendritic cells. J. Exp. Med. 192:1249-1260.

Stroher, U., E. West, H. Bugany, H.D. Klenk, H.J. Schnittler, and H. Feldmann. 2001. Infection and activation of monocytes by Marburg and Ebola viruses. J. Virol. 75:11025-33.

Sui, J., and W.A. Marasco. 2002. Evidence against Ebola virus sGP binding to human neutrophils by a specific receptor. Virology. 303:9-14.

Sullivan, N.J., A. Sanchez, P.E. Rollin, Z.-Y. Yang, and G.J. Nabel. 2000. Development of a preventative vaccine for Ebola virus infection in primates. Nature. 408:605-609.

Takabayashi, A., Y. Kawai, S. Iwata , M. Kanai, R. Denno, K. Kawada, K. Obama, and Y. Taki. 2000. Nitric oxide induces a decrease in the mitochondrial membrane

potential of peripheral blood lymphocytes, especially in natural killer cells. Antioxid. Redox. Signal. 2:673-680.

Takada, A., S. Watanabe, K. Okazaki, H. Kida, and Y. Kawaoka. 2001. Infectivity-enhancing antibodies to Ebola virus glycoprotein. J. Virol. 75:2324 2330.

Taylor, F.B., Jr., A. Chang, W. Ruf , J.H. Morrissey, L. Hinshaw, R. Catlett, K. Blick, and T.S. Edgington. 1991. Lethal E. coli septic shock is prevented by blocking tissue factor with monoclonal antibody. Circ. Shock. 33:127-34.

Villinger, F., P.E. Rollin, S.S. Brar, N.F. Chikkala, J. Winter, J.B. Sundstrom, S.R. Zaki, R. Swanepoel, A.A. Ansari, and C.J. Peters. 1999. Markedly elevated levels of interferon (IFN)-α, IFN-γ, interleukin (IL)-2, IL-10, and tumor necrosis factor-α associated with fatal Ebola virus infection. J. Infect. Dis. Suppl. 179:S188-S191.

Volchkov, V.E., S. Becker, V.A. Volchkova, V.A. Ternovoj, A.N. Kotov, S.V. Netesov, and H.-D. Klenk. 1995. GP mRNA of Ebola virus is edited by the Ebola virus polymerase and by T7 and vaccinia virus polymerases. Virology. 214:421-430.

Volchkov, V.E., H. Feldmann, V.A. Volchkova, and H.-D. Klenk. 1998a. Processing of the Ebola virus glycoprotein by the proprotein convertase furin. Proc. Natl. Acad. Sci. USA. 95:5762-5767.

Volchkov, V.E., V.A. Volchkova, W. Slenczka, H.-D. Klenk, and H. Feldmann. 1998b. Release of viral glycoproteins during Ebola virus infection. Virology. 245:110-119.

Volchkov, V.E., V.A. Volchkova, E. Muhlberger, L.V. Kolesnikova, M. Weik, O. Dolnik, and H.-D. Klenk. 2001. Recovery of infectious Ebola virus from complementary DNA: RNA editing of the GP gene and viral cytotoxicity. Science. 291:1965-1969.

WHO. 1978a. Ebola haemorrhagic fever in Sudan, 1976. Report of an international study team. Bull. World Health Organ. 56:247-270.

WHO. 1978b. Ebola haemorrhagic fever in Zaire, 1976. Report of an international commission. Bull. World Health Organ. 56:271-293.

Worrall, N.K., K. Chang, W.S. LeJeune, T.P. Misko, P.M. Sullivan, T.B. Ferguson, Jr., and J.R. Williamson. 1997. TNF-alpha causes reversible in vivo systemic vascular barrier dysfunction via NO-dependent and -independent mechanisms. Am. J. Physiol. 273:H2565-2574.

Wyers, M., P. Formenty, Y. Cherel, L. Guigand, B. Fernandez, C. Boesch, and B. Le Guenno. 1999. Histopathological and immunohistochemical studies of lesions associated with Ebola virus in a naturally infected chimpanzee. J. Infect. Dis. Suppl. 179:S54-S59.

Yang, Z., R. Delgado, L. Xu, R.F. Todd, E.G. Nabel, A. Sanchez, and G.J. Nabel. 1998. Distinct cellular interactions of secreted and transmembrane Ebola virus glycoproteins. Science. 279:1034-1037.

Yang, Z-Y., H.J. Duckers, N.J. Sullivan, A. Sanchez, E.G. Nabel, and G.J. Nabel. 2000. Identification of the Ebola virus glycoprotein as the main viral determinant of vascular cell cytotoxicity and injury. Nature Med. 6:886-889.

Zaki, S.R., and C.S. Goldsmith. 1999. Pathologic features of filovirus infections in humans. Curr. Top. Microbiol. Immunol. 235:97-116.

Zaki, S.R., W.J. Shieh, P.W. Greer, C.S. Goldsmith, T. Ferebee, J. Katshitshi, F.K. Tshioko, M.A. Bwaka, R. Swanepoel, P. Calain, A.S. Khan, E. Lloyd, P.E. Rollin, T.G. Ksiazek, and C.J. Peters. 1999. A novel immunohistochemical assay for the

detection of Ebola virus in skin: implications for diagnosis, spread, and surveillance of Ebola hemorrhagic fever. J. Infec. Dis. Suppl. 179:S36-S47.

Zimmermann, K.C., C. Bonzon, and D.R. Green. 2001. The machinery of programmed cell death. Pharmacol. Ther. 92:57-70.